UNIVERSITY OF CALIFORNIA
RIVERSIDE

A Functional Study of Arabidopsis ARGONAUTE10 in Floral Determinacy and Small RNA Pathways

A Dissertation submitted in partial satisfaction
of the requirements for the degree of

Doctor of Philosophy

in

Plant Biology

by

Lijuan Ji

March 2012

Dissertation committee:

Dr. Xuemei Chen, Chairperson
Dr. Patricia Springer
Dr. Harley Smith

The Dissertation of Lijuan Ji is approved:

Committee Chairperson

University of California, Riverside

Acknowledgements

I am sincerely grateful to the many people who made this dissertation possible.

Foremost, I owe my deepest gratitude to my advisor Dr. Xuemei Chen. She has provided consistent encouragement, sound advice, and invaluable ideas throughout my Ph.D training. Moreover, she has always been patient with me, especially during tough times in my graduate study. I appreciate all her contributions of time, intellect, and funding to make me productive and motivated. I am also enlightened by her excellence as a woman biologist.

I heartily thank the rest of my dissertation committee: Dr. Patricia Springer and Dr. Harley Smith, for their helpful comments and suggestions. My sincere thanks also go to three other faculty who were in my qualify examination committee, Dr. Shouwei Ding, Dr. Thomas Eulgem and Dr. Venugopala Gonehal Reddy, for their time and insightful questions. It's a pleasure to thank the many people who have taught me so far, especially the professors at UCR and my undergraduate teachers at China Agricultural University, for their teaching efforts and kind assistance to my applications, and so on. In particular, I am grateful to Dr. Weihua Wu and Dr. Zhizhong Gong for opening the door of biology research to me.

I am indebted to my fellow colleagues in the Chen lab for providing a stimulating and fun environment. I am especially grateful to Dr. Xigang Liu and Dr. Shengben Li for their day-to-day discussions, suggestions and assistance.

Other members have also shared friendship, good advice and collaborations in the past five and a half years. I am especially grateful to Theresa Dinh, for her company along the Ph.D pursuit and for all the fun we have shared.

I would like to thank the professors whom I have collaborated with: Dr. Jinbiao Ma at University of Alabama at Birmingham, Dr. Guiliang Tang at University of Kentucky, Dr. Xiaofeng Cao at Institute of Genetics and Developmental Biology, Chinese Academy of Sciences and Dr. Blake Meyers at University of Delaware. Dr. Jinbiao Ma offered me a precious opportunity to be involved in the investigation of the mechanisms underlying HEN1 activity. Dr. Guiliang Tang's handy help expedited the resubmission of my first manuscript. Without Dr. Xiaofeng Cao's anti-AGO1 antibodies, the biochemical assays would not have been as convenient. Her group also generated some genetic materials for the study reported in Chapter I of my dissertation. I appreciate Dr. Blake Meyers for his assistance in the bioinformatic analysis of the next generation sequencing data. Jixian Zhai, a talented graduate student in his group, made significant contributions to the bioinformatic analyses and beyond. I also appreciate the local expertise of the Genomics Core Facility in the Institute of Integrative Genome Biology (IIGB) at UCR. In particular, I would also like to acknowledge Dr. Glenn Hicks and Dr. John Weger for sharing their expert knowledge.

The text of Chapter I of this dissertation, in full, is a reprint with minor edits of the material as appeared in the March 2011 issue of *PLoS Genetics*. Dr.

Xuemei Chen, Dr. Guiliang Tang and Dr. Xiaofeng Cao directed and supervised the research that formed the basis for this part of the dissertation. Dr. Xigang Liu and Thanh Theresa Dinh provided technical expertise. Dr. Jun Yan, Dr.Wenming Wang, Rae Eden Yumul, Dr. Yun Ju Kim, Dr. Jun Liu, Dr. Xia Cui, Dr. Binglian Zheng, Dr. Manu Agarwal, Dr. Chunyan Liu provided molecular or genetics reagents for the research.

I am grateful to the staff members in the Department of Botany and Plant Sciences at UCR, for assisting me in many different ways. Jasmine Mejia, Rob Lennox, and Henry Gutierriz deserve special mention. I am also grateful to the advisors in International Education Center and Career Center for their advice and assistance.

My memory for the 2005 summer lectures in Peking University on the advances in plant biology is always vivid. The experience asserted my plan to pursue a Ph.D. in the U.S.A., and empowered me to overcome many difficulties during the application process. Thus, I would like to thank the organizers and speakers for the summer lectures. Through the training at UCR, I gained critical and creative thinking skills and experienced how scientific research is conducted. More importantly, I have developed a strong desire to improve myself in many aspects and to accept new challenges. It’s an honor for me to thank Dr. Natasha Raikhel, a well-established scientist who made untiring efforts to provide advice for young scientists about career development.

My time at UCR was made enjoyable thanks to the many friends that I

share my life with. I am grateful to all the friends and former roommates, for the cheerful get-togethers and the memorable trips to the mountains, beaches and other places of interests. My personal life was also enriched by the motivational seminar in Vancouver and all the fellows who accompanied me afterwards.

I would like to thank my family and relatives for all their love and care in my life. My brother, Ruilong Ji, has been particularly supportive. Most importantly, I wish to thank my parents for the life they have gifted me. They have been supporting me spiritually and financially to their best throughout my pursuits in life. Lastly, I appreciate my loving husband Lei Jing from the bottom of my heart for all the faithful support and encouragement during the final stages of my graduate study.

ABSTRACT OF THE DISSERTATION

A Functional Study of Arabidopsis ARGONAUTE10 in Floral Determinacy and Small RNA Pathways

by

Lijuan Ji

Doctor of Philosophy, Graduate Program in Plant Biology
University of California, Riverside, March 2012
Dr. Xuemei Chen, Chairperson

microRNAs (miRNAs) play regulatory roles in various developmental processes including stem cell maintenance and differentiation, which are central to animal and plant development. miRNAs function within a miRNA-protein complex termed RNA Induced Silencing Complex (RISC). In plants, miRNAs and the core protein components of RISC, argonaute proteins, have been shown to regulate the maintenance of stem cells. In *Arabidopsis*, the maintenance of floral stem cell fate is controlled both spatially and temporally. One aim of my Ph.D. thesis research was to uncover the mechanisms that underlie the programmed termination of floral stem cell maintenance. My studies show that miR165/166 and the argonaute protein that it associates with *in vivo*, AGO10, are both involved in the regulation of floral stem cells. This work is reported in Chapter I of

the dissertation. One intriguing observation made during my studies was that AGO10 represses the levels of miR165/166 *in vivo*, which is contrary to the expectation that argonaute proteins stabilize their associated miRNAs and implies the existence of a currently unknown mechanism regulating miRNA homeostasis. My research towards elucidating this regulatory mechanism is reported in Chapter II. I have accumulated evidence that AGO10 decreases the stability of miR165/166. Taken together, my dissertation research has demonstrated that regulation of miRNA stability through a specialized argonaute protein is critical to the regulation of stem cells in plant development.

Table of Contents

1. INTRODUCTION: METABOLISM AND FUNCTION OF SMALL RNAS AND FLORAL DETERMINACY 1
ABSTRACT 1
miRNA BIOGENESIS IN PLANTS 3
REGULATION OF PLANT miRNA BIOGENESIS 5
ARGONAUTE PROTEINS MEDIATE THE ACTIVITIES OF miRNAS 6
Functions of the Arabidopsis AGO1 clade 7
Functions of the Arabidopsis AGO2 clade 11
Functions of the Arabidopsis AGO4 clade 11
SMALL RNA STABILIZATION BY METHYLATION 12
Plant miRNAs and siRNAs are methylated by HEN1 12
Animal piRNAs and fly siRNAs are methylated by HEN1 homologs 15
Damaged bacterial RNAs are methylated by HEN1 in vitro 17
REMOVAL OF UNMETHYLATED SMALL RNAS IN *HEN1* MUTANTS 18
3' Uridylation of unmethylated small RNAs 18
3'-5' exonucleolytic degradation of small RNAs 20
ADDITIONAL FACTORS THAT INFLUENCE SMALL RNA STABILITY 21
Target mRNAs mediate the degradation or stabilization of small RNAs 21
3' nucleotide addition affects the stability of small RNAs 25
cis elements and trans factors affect small RNAs stability 27
FLORAL DETERMINACY 31
FIGURES 36
TABLES 39
REFERENCE 41

2. CHAPTER I: *ARGONAUTE10* AND *ARGONAUTE1* REGULATE THE TERMINATION OF FLORAL STEM CELLS THROUGH TWO MICRORNAS IN *ARABIDOPSIS* 54
ABSTRACT 54
INTRODUCTION 55
RESULTS 59
AGO10 promotes floral determinacy 59
AGO10 terminates floral stem cells through repression of WUS expression 63
AGO1 is also required for floral stem cell termination 65
AGO10 acts partly through miR172 to promote floral determinacy 66
AGO10 is associated with miRNAs in vivo 69
AGO10 has "slicer" activity 69
miR165/166 and its targets, the HD-Zip genes, are crucial players in floral determinacy 71
DISCUSSION 74
AGO10 and AGO1 have similar small RNA binding specificities but can act differently on miRNAs in vivo 74
Floral stem cell termination versus differentiation 76
HD-Zip genes, targets of miR165/166, are crucial for the temporal program of floral stem cells 77

AGO10 and AGO1 promote floral stem cell termination via similar and different mechanisms ... *78*
SAM and floral meristems – differences in stem cell maintenance ... *79*
MATERIALS AND METHODS ... 80
Plant strains and EMS mutagenesis ... *80*
Construction of amiR165/166 ... *81*
RNA extraction and real-time RT-PCR ... *82*
Small RNA northern blotting ... *83*
Immunoprecipitation ... *83*
In vitro transcription and RNA cleavage assay ... *84*
Protein extraction and western blotting ... *84*
FIGURES ... 86
SUPPLEMENTAL MATERIALS ... 96
REFERENCES ... 108

3. CHAPTER II: ARGONAUTE10 ACCELERATES THE DECAY RATE OF ASSOCIATED MIR165/166 ... 113
ABSTRACT ... 113
INTRODUCTION ... 114
RESULTS ... 115
AGO10 doesn't affect MIR165/166 transcription or pri-miR165/166 processing ... *115*
Evidence that miR165/166 is prone to degradation ... *117*
3' modifications of miR165/166 in ago10 mutants ... *119*
3' modifications of miR165/166 in 35S::YFP-AGO10 ... *119*
AGO10 accelerates the decay of associated miR165/166 ... *123*
Identify the pathway required for AGO10-associated miR165/166 degradation ... *126*
DISCUSSION ... 127
Argonaute proteins affect small RNA stability differently ... *127*
Small RNA tailing and truncation happen after RISC loading ... *129*
Functional specificity of AGO10 in land plants ... *130*
MATERIALS AND METHODS ... 132
Plant Materials ... *132*
Plasmid construction and plant transformation ... *132*
RNA extraction and analysis ... *133*
Protein purification and biochemical analysis ... *133*
Bioinformatic analysis of miRNAs ... *135*
Phylogenetic analysis ... *135*
FIGURES ... 136
SUPPLEMENTAL MATERIALS ... 144
TABLES ... 149
REFERENCES ... 150

4. CONCLUSIONS AND PERSPECTIVES ... 154
REFERENCES ... 157

5. APPENDIX A: SIDE PROJECTS AND CONSTRUCTS ... 158

6. APPENDIX B: SIDE PROJECTS AND PROTOCOLS ... 178
REFERENCES ... 178

List of Figures

FIGURE 1.1 2'-O-METHYLATION OF SMALL RNAS BY HEN1 36
FIGURE 1.2 HEN1 PROTECTS SMALL RNAS FROM URIDYLATION AND 3'-TO-5' DEGRADATION..... 37
FIGURE 1.3 MECHANISMS INFLUENCING SMALL RNA STABILITY..... 38
FIGURE 2.1 HEN6 (AGO10-12) AND HEN7 (AG-10) MUTATIONS ENHANCE HUA1 HUA2 86
FIGURE 2.2 AGO10 AND AGO1 ENHANCE FLORAL DETERMINACY..... 88
FIGURE 2.3 EXPRESSION PATTERNS OF AGO10, AG AND WUS IN FLORAL MERISTEMS 90
FIGURE 2.4 GENETIC INTERACTIONS BETWEEN AGO10 AND MERISTEM REGULATORS 91
FIGURE 2.5 AGO10 IS ASSOCIATED WITH MIRNAS IN VIVO AND IS CATALYTICALLY ACTIVE AS A "SLICER" IN VITRO..... 93
FIGURE 2.6 A MODEL OF AGO1 AND AGO10 IN FLORAL STEM CELL REGULATION 95
FIGURE 2.7 DIAGRAMS OF AG, AGO10 AND PHV GENES AND MULTIPLE SEQUENCE ALIGNMENTS OF ARABIDOPSIS AGO PROTEINS..... 96
FIGURE 2.8 THE ACCUMULATION OF MIRNAS, TA-SIRNAS AND THEIR TARGET MRNAS IN AGO10 MUTANTS 98
FIGURE 2.9 FLORAL PHENOTYPES OF VARIOUS GENOTYPES..... 100
FIGURE 2.10 AGO10 DOES NOT BIND MIR390..... 102
FIGURE 2.11 THE EXPRESSION OF ZPR3 IN WILD TYPE (LER) AND AGO10-13 AS DETERMINED BY REAL-TIME RT-PCR..... 102
FIGURE 2.12 A DIAGRAM OF AMIR165/166..... 103
FIGURE 3.1 ACCUMULATION OF PRI-/PRE-MIR165/166 IN WILD TYPE (LER) AND THE PNH-2 MUTANT .. 136
FIGURE 3.2 MIR165/166 IS PREFERENTIALLY TRUNCATED AND TAILED IN HEN1 MUTANTS 137
FIGURE 3.3 DEGRADATION OF MIR165/166 IS REDUCED IN AGO10 MUTANTS..... 139
FIGURE 3.4 CHARACTERIZATION OF 35S::YFP-AGO10 PLANTS 140
FIGURE 3.5 DEGRADATION OF MIR165/166 IN 35S::YFP-AGO10..... 142
FIGURE 3.6 DECAY OF AGO-ASSOCIATED MIR165/166..... 143
FIGURE 3.7 EXAMINATION OF PRI-/PRE-MIR165/166 IN AGO10 MUTANTS..... 144
FIGURE 3.8 TAILING AND TRUNCATION OF SEVERAL MIRNA* STRANDS IN HEN1 MUTANTS 145
FIGURE 3.9 RT-PCR EXAMINING THE LEVELS OF AGO10 MRNA IN COL AND 35S::YFP-AGO10 PLANTS 146
FIGURE 3.10 RELATIVE ABUNDANCE OF NON-INTACT SPECIES OF MIRNAS IN COL, 35S::YFP-AGO10 AND IP 147
FIGURE 3.11 PHYLOGENY OF AGO1 AND AGO10 IN LAND PLANTS 148
FIGURE 5.1 ARABIDOPSIS HEN1 SEQUENCE AND PREDICTED NLS, NES 160

List of Tables

TABLE 1.1 HEN1 HOMOLOGS THAT METHYLATE SMALL RNAS 39
TABLE 1.2 NUCLEOTIDYLTRANSFERASES AFFECTING MATURE SMALL RNAS 40
TABLE 2.1 FLORAL ORGAN COUNTS IN VARIOUS GENOTYPES 104
TABLE 2.2 SEQUENCES OF OLIGOS USED IN THE STUDY 105
TABLE 3.1 SEQUENCES OF OLIGOS USED IN THE STUDY 149
TABLE 5.1 160
TABLE 5.2 162
TABLE 5.3 162
TABLE 5.4 163
TABLE 5.5 165
TABLE 5.6 165
TABLE 5.7 166
TABLE 5.8 167
TABLE 5.9 167
TABLE 5.10 168
TABLE 5.11 169
TABLE 5.12 170
TABLE 5.13 171
TABLE 5.14 171
TABLE 5.15 172
TABLE 5.16 173
TABLE 5.17 175
TABLE 5.18 176

1. Introduction: metabolism and function of small RNAs and floral determinacy

Abstract

As sequence-specific guides in RNA silencing in all eukaryotes, small RNAs play important and diverse roles in many biological processes. In plants, microRNAs (miRNAs) have been shown to regulate the activity of stem cells, which is central to many developmental processes. The biogenesis of miRNAs, which is subject to regulation, includes the transcription of *MIR* genes, several steps of processing and final maturation in RNA Induced Silencing Complexes (RISCs). The functions of small RNAs are mediated by argonaute proteins, the core components of RISCs. Aberrant reduction or elevation in the levels of small RNAs is associated with many developmental and physiological defects. The *in vivo* levels of small RNAs are precisely regulated through modulating the rates of their biogenesis and turnover. 2'-*O*-methylation on the 3' terminal ribose is a major mechanism that increases the stability of small RNAs. Loss of 3' methylation unveiled the existence of a 3'-to-5' exonuclease activity and a 3' nucleotide addition activity that act on small RNAs. Other mechanisms impacting small RNA stability include influences from complementary sequences and RNA binding proteins.

RNA silencing, a universal mechanism to regulate gene expression in eukaryotes, plays important roles in diverse biological processes, such as development, stress responses, immunity and genome stability [1]. Different types of small RNAs of 21 to 32 nucleotides (nt) are the key components in distinct RNA silencing pathways. Small RNAs are classified into three major types, microRNAs (miRNAs), small-interfering RNAs (siRNAs) and Piwi-interacting RNAs (piRNAs) based on differences in their precursors, biogenesis and protein partners [1,2]. miRNAs are produced from miRNA gene transcripts that form stem-loop structures (reviewed in [3,4]). Mature miRNAs are usually 21-24 nt long and are generated through the processing of the precursors by RNaseIII type enzymes (Drosha and Dicer in animals; DICER-LIKE or DCL in plants) [3,4]. miRNAs, targeting endogenous genes for mRNA cleavage, decay and/or translational repression, are of particular importance as regulators of developmental processes in plants and animals [3,4]. siRNAs are derived from double-stranded RNA (dsRNA) precursors generated from sense and antisense transcription, transcription of inverted repeat elements, viral replication intermediates, or RNA-DEPENDENT RNA POLYMERASE (RDR) activity that converts single-stranded RNAs into dsRNAs [3,5]. siRNAs are 21-24 nt long and their biogenesis also requires the endonuclease activity of Dicer or DCL [3,5,6]. siRNAs repress the expression of transposable elements and transgenes, and cleave viral mRNAs [5,6]. piRNAs, found specifically in animals, are usually 24-32 nt long and processed from presumably single-stranded RNA precursors in a

Dicer-independent manner (reviewed in [2,7]). Their biogenesis is composed of a primary processing pathway and a ping-pong amplification pathway. In some cell types, the generation of piRNAs relies on primary processing pathway solely, while in other cell types, both pathways are employed for piRNA biogenesis [7]. piRNAs are derived from transposable elements (TEs), intergenic regions, and certain genes. piRNAs derived from TEs guide the DNA methylation of homologous genomic loci to cause transcriptional silencing [7]. While miRNAs and siRNAs are bound by the argonaute sub-clade of argonaute proteins, piRNAs associate specifically with the Piwi sub-clade of argonaute proteins [7].

miRNA biogenesis in plants

miRNAs and siRNAs are the prevailing types of small RNAs in plants [8]. miRNAs are generated from *MIR* genes encoded in the genome (reviewed in [9]). A *MIR* gene is transcribed by RNA Polymerase II (Pol II) to generate a precursor called pri-miRNA [10]. pri-miRNAs are capped and polyadenylated as other Pol II transcripts and are able to form imperfect stem-loop structures flanked by single-stranded extensions [11]. The precursor is processed to release the stem-loop structure (pre-miRNA) by the RNase III enzyme Dicer-Like1 or DCL1 [11]. The dicing by DCL1 generates a two-nucleotide 3’ overhang and a 5’ phosphate group. Then, DCL1 further cleaves the pre-miRNA to form an RNA duplex with 3’ overhangs and 5’ phosphate groups [9,11].

miRNA biogenesis requires more protein factors in addition to DCL1. In *Arabidopsis*, the *DAWDLE* (*DDL*) gene encodes a Forkhead-associated domain

(FHA) protein that interacts with DCL1 and binds to RNAs [12]. The level of pri-miRNAs is decreased in *ddl* mutants despite unchanged *MIR* gene transcription, indicating that DDL stabilizes the pri-miRNAs [12]. The functions of DDL are probably not limited to miRNA biogenesis given its broad RNA binding specificity [12]. The *ddl* mutant shows pleiotropic developmental defects, and has reduced levels of trans-acting siRNAs (ta-siRNAs) and several endogenous siRNAs [12]. The human ortholog of DDL, Smad nuclear-interacting protein1 (SNIP1), is also involved in miRNA biogenesis through interacting with Drosha (the RNase III enzyme needed for pri-to-pre-miRNA conversion), but not with Dicer (the human homolog of DCL1 needed for pre-miRNA processing) [12,13].

HYPONASTIC LEAVES1 (HYL1), SERRATE (SE), ABH1/CBP80 and CBP20 are required for the processing of pri-miRNAs in that more pri-miRNAs accumulate but less miRNAs are produced in these mutants [14-17]. HYL1 and SE, a double-stranded RNA-binding protein and a C2H2-zinc finger protein, respectively, interact with DCL1 in the nuclear D-bodies [14,15]. *ABH1/CBP80* and *CBP20* encode subunits of the nuclear cap-binding complex (CBC) [16,17]. In addition to defects in pri-miRNA processing, weak *se* alleles and *abh1/cbp80* and *cbp20* mutants exhibit general mRNA splicing defects [17].

Small RNA duplexes, including miRNA duplexes and all kinds of siRNA duplexes, are methylated by the small RNA methyltransferase HUA ENHANCER1 (HEN1) in plants [18]. Methyl groups are deposited on the 2’ OH of the 3’ terminal nucleotides of both strands for small RNA stabilization [19]. In

animals, pre-miRNAs are exported from the nucleus to the cytoplasm by exportin-5 [20,21]. HASTY, the plant homolog of exportin-5, is also required for miRNA accumulation even though its exact cargos are unidentified yet [22]. The accumulation of a set of miRNAs is not affected in *hasty* mutants [22], suggesting that they are exported through an unidentified HASTY-independent mechanism.

Regulation of plant miRNA biogenesis

The biogenesis of miRNAs can be regulated at different levels. The promoters of *MIR* genes contain conserved stress response elements, tissue-specific regulatory elements and known transcription factor binding sites [23]. Moreover, Mediator, a conserved multi-subunit complex promoting Pol II transcription in eukaryotes, is also required for miRNA biogenesis by recruiting Pol II to *MIR* gene promoters [24]. Indeed, the expression patterns of *MIR* genes are often temporally and/or spatially dynamic (reviewed in [25]).

Arabidopsis DCL1 is targeted by miR162 [26], implying that the global production of miRNAs is subject to feedback regulation. In addition, regulation of individual miRNAs during their biogenesis is likely responsible for the observed differences between precursor and mature miRNA levels [27], though no regulators have been identified. The presence of 24 nt species from some miRNA loci, especially those that produce non-conserved miRNAs, implicates that DCL3 is also involved in miRNA processing in certain circumstances [28,29]. Thus, the production of 21 nt versus 24 nt miRNAs could be determined by the relative abundance of DCL1 and DCL3 [28]. Moreover, it' s unclear whether the

generation of miRNA variants showing heterogeneity at their 5’ or 3’ termini from conserved miRNA loci in plants is also a regulated process [30,31].

Argonaute proteins mediate the activities of miRNAs

Argonaute (AGO) proteins, the catalytic component of RISC, were identified as major protein partners of small RNAs and effectors of RNA silencing [32]. Argonaute proteins are large, with a molecular weight above 100 kDa, and contain four structural domains: N-terminal, Piwi-Argonaute-Zwille (PAZ), MID and PIWI domains [33]. The PAZ domain forms a binding module for the 2 nt 3’ overhang of a small RNA duplex [33]. The MID domain contains a highly basic pocket binding the 5’ phosphate of small RNAs [34-36]. The PIWI domain is structurally similar to RNase H and exerts an endonuclease activity to cleave target RNAs [34-36]. Many AGO proteins have conserved DDH residues forming the catalytic triad within the PIWI domain [8,36]. However, the DDH residues are not the sole determinants for the *in vivo* mode of action of AGO proteins. Post-translational modifications and protein interactions possibly impact the activity of AGO proteins (reviewed in [37]).

One strand of the miRNA duplex associates with AGO proteins and accumulates *in vivo*. The opposite strand, usually named as miRNA*, is degraded during or after RISC assembly (reviewed in [9]). Plant RISCs can be assembled using *in vitro* translated AGO1 and synthesized siRNA or miRNA duplexes with the help of Heat Shock Protein 90 (HSP90) [38]. Interestingly, the removal of the passenger strand from a siRNA duplex requires the endonuclease

activity of AGO1, which cleaves the star strand, while the removal of the star strand from a miRNA duplex does not [38]. The *Arabidopsis* genome encodes 10 *AGO* genes, suggesting they are highly diversified and specialized [8]. Molecular and phylogenetic studies show that *AGO1*, *AGO10* and *AGO5* form one clade, and *AGO1* and *AGO10* mainly function in miRNA pathways [8,39]. *AGO2*, *AGO3* and *AGO7* form a second clade with some evidence supporting their function in plant immunity [8]. *AGO4*, *AGO6* and *AGO9* act in RNA-directed DNA methylation (RdDM) and heterochromatin silencing [40]. The three, together with *AGO8*, a possible pseudo gene, form a third clade [8,41]. Small RNAs are selectively sorted into particular AGO proteins in a 5' nucleotide-dependent manner [42,43]. For instance, AGO1 preferentially associates with small RNAs with a uridine at their 5’ termini, a feature for most miRNAs in *Arabidopsis* [42]. Small RNAs with an adenosine at their 5’ termini are overrepresented in AGO2, AGO4, AGO6 and AGO9 immunoprecipitations (IPs) [40,42,43]. AGO5 prefers small RNA with a cytosine at their 5’ ends [42,43]. The activity of small RNAs is strongly affected by the associated AGO proteins. The functions of individual AGO proteins will be further discussed in the following section with an emphasis on those that act in miRNA pathways.

Functions of the *Arabidopsis* AGO1 clade

Most miRNAs are loaded into AGO1, the founding member of the *Arabidopsis* AGO family [8]. The target RNAs contain miRNA binding sites with a high degree of complementarity that enable AGO1 cleavage at the position

opposite to the nucleotides 10 and 11 of the miRNA strand [44]. The 5′ and 3′ cleavage products are degraded from the newly generated 3′ and 5′ ends through the exosome (a multi-protein complex with 3′-to-5′ exonuclease activity), and the 5′-to-3′ exonuclease XRN4, respectively [45,46]. *Arabidopsis ago1* mutants have increased accumulation of miRNA target mRNAs [47]. In *ago1* null alleles, the accumulation of many miRNAs is reduced, implicating that miRNAs are less stable in the absence of AGO1 [47]. Being a critical regulator in plant development and stress responses, *AGO1* itself is targeted by miR168 to enable feedback regulation on global miRNA activities. Transgenic plants expressing miR168-resistant *AGO1* exhibit pleiotropic developmental defects [47].

An elite example of the function of AGO1 and associated miRNAs in development is the repression of *HD-Zip III* genes by miR165/166. In *Arabidopsis,* miR165/166 is a conserved miRNA family encoded by 9 loci in the genome [48]. The mature miR165/166 is present in the abaxial domain of leaf primorida and restricts the expression of *HD-Zip III* genes to the adaxial side through the universally expressed AGO1 [49-51]. Meanwhile, accumulation of miR166/165 also depends on AGO1 [49]. miR165/166 and *HD-Zip III* genes have been shown to function in the establishment of lateral organ polarity, the development of vascular tissues and the regulation of meristem activities [49-51]. A recent study shows that intercellular movement of miR165/166 is required for the specification of xylem cells in the root [52].

In addition to target cleavage, AGO1 down-regulates miRNA targets

through translational repression [53]. In plants, translational repression was initially reported for some miRNAs, such as miR172 and miR156/157 [54-56]. A later study suggests that translation repression may be more common than previously anticipated. In the hypomorphic *ago1-27* mutant, the accumulation of miRNA target transcripts is mildly affected, while the level of target proteins is substantially increased [53]. Consistently, a portion of miRNAs and AGO1 were shown to associate with polysomes possibly in a miRNA target mRNA dependent manner in *Arabidopsis* [57]. However, the relative contribution of translational repression and mRNA cleavage to miRNA activities remains unknown at present.

AGO1, in association with miR173, is required for the production of trans-acting siRNAs (ta-siRNAs) from *TAS1* and *TAS2* loci [58]. Through an unknown mechanism, the unique length (22 nt) of miR173 renders the target transcripts capable of trans-acting siRNA (tasiRNA) biogenesis after AGO1 cleavage [59]. In addition, the generation of ta-siRNAs involves RNA-DEPENDENT RNA POLYMERASE6 (RDR6), DCL4, and SUPPRESSOR OF GENE SILENCING3 (SGS3) [58]. Together with miR828, which is also 22 nt long, AGO1 initiates the biogenesis of ta-siRNAs from the *TAS4* locus [31]. The ta-siRNAs are associated with AGO1 for function [44]. AGO1 is also involved in Virus Induced Gene Silencing (VIGS) and the silencing of transgenes [44,60]. Hypomorphic *ago1* mutants accumulate higher level of viral RNAs, and are more susceptible to a series of pathogens, such as Cucumber mosaic virus (CMV) and viral suppressor protein (VSR) -defective turnip crinkle virus (TCV) [61,62]. Moreover, AGO1 was

found to bind viral siRNAs in the infected plants [63].

AGO10 was initially identified to play regulatory roles in Shoot Apical Meristem (SAM) maintenance and other developmental processes [64,65]. Being most closely related to *AGO1*, *AGO10* has overlapping and distinct roles with *AGO1* [66]. *AGO10* is a negative regulator of *AGO1* in that loss of *AGO10* led to an increase in AGO1 protein levels in hypomorphic *ago1* alleles [66]. Although the two are expressed in distinct patterns, promoter swapping and domain swapping experiments show that their functional specificity is mostly determined by the protein sequences, instead of expression domains [66]. AGO10 was shown to function in small RNA pathways through repressing the translation of some miRNA targets [53]. My thesis research and a more recent report demonstrate that AGO10 regulates the SAMs and floral meristems through miR165/166 [39]. Zhu *et al*. reported that AGO10 associates with miRNAs with a strong preference for miR165/166. AGO10 sequesters miR165/166 at the SAM to prevent the miRNA from acting through AGO1. Moreover, the catalytic activity of AGO10 is not required for its function in SAM development [67].

AGO5 is preferentially localized to the sperm cell cytoplasm in mature pollen and growing pollen tubes [68]. Therefore, AGO5 is likely to play some regulatory roles in male gamete development. Consistently, a number of potential novel miRNAs and variants of known miRNAs were identified in the male gamete [68].

Functions of the *Arabidopsis* AGO2 clade

Many pieces of evidence support a role of AGO2 in plant immunity against different pathogens. AGO2 is highly induced by the bacterial pathogen *Pseudomonas syringae* pv. Tomato (Pst) [69]. It has been demonstrated that AGO2 mediates the activity of miR393b* in the repression of a Golgi-localized SNARE gene [69]. Moreover, AGO2 functions in the restriction of Potato virus X (PVX) and in the defense against Cucumber mosaic virus (CMV-D2b) [60,70]. In addition, infection of *ago2* mutants with TCV and CMV resulted in more severe symptoms [71].

AGO7 specifically interacts with miR390 and acts in the biogenesis of ta-siRNAs from the *TAS3* loci [72]. miR390 guides AGO7 to interact with two binding sites in the *TAS3* transcripts to trigger the generation of ta-siRNAs [72]. Intriguingly, the initiation of ta-siRNA biogenesis requires cleavage at one of the two sites [72]. The increased accumulation of viral RNAs in a null *ago7* mutant suggests that AGO7 also functions in antiviral defense [62].

Functions of the *Arabidopsis* AGO4 clade

The closely related AGO4, AGO6, and AGO9 proteins are implicated in RNA-directed DNA methylation [40]. The 24 nt siRNAs associated with those AGOs are generated by a pathway involving RNA Polymerase IV (Pol IV), RDR2 and DCL3 [6,73]. However, the three AGOs have distinct preferences for siRNAs from different heterochromatin loci due to their different expression patterns and unidentified factors [40]. The ectopic expression of AGO6 or AGO9 under the

promoter of *AGO4* does not fully complement the loss of asymmetric DNA methylation in the *ago4* mutant background [40].

Small RNA stabilization by methylation

Precise and faithful regulation of small RNA levels is critical for diverse biological processes in various organisms. The stability of small RNAs contributes to their steady-state levels and impacts target gene expression. 3' Methylation was found to be a major stabilization mechanism employed by miRNAs and siRNAs in plants, piRNAs in animals and siRNAs in *Drosophila* [18,74-78]. HUA ENHANCER 1 (HEN1) was first identified in *Arabidopsis* as a small RNA methyltransferase that methylates miRNA and siRNA duplexes [18,19]. HEN1 homologs were found to methylate small RNAs in other plants, piRNAs in animals and Ago2-associated small RNAs in *Drosophila* [74-78]. In general, 2'-*O*-methylation serves as a protective mechanism against 3'-to-5' degradation and 3' uridylation of small RNAs [18,76,79].

Plant miRNAs and siRNAs are methylated by HEN1

In plants, the biogenesis of small RNAs, including miRNAs and all types of siRNAs, involves 2'-*O*-methylation at their 3' termini [18]. The requirement for methylation was uncovered through the isolation of *Arabidopsis hen1* mutants. miRNAs and siRNAs are methylated at their 3' termini in wild type *Arabidopsis*, but not in *hen1* mutants [18] (Figure 1.1A). In *hen1* mutants, miRNAs show reduced abundance and heterogeneity in sizes [18,79], the latter of which was reflected by a ladder of bands when total RNAs were resolved on high-resolution

acrylamide gels and hybridized with a probe for any miRNA species. Because primer extension studies demonstrated that the heterogeneous species have identical 5' ends [79], the ladder of signals probably represented heterogeneity at the 3' ends. Indeed, when particular miRNAs were cloned and sequenced from wild type and a *hen1* mutant, it became clear that miRNAs tended to acquire an oligonucleotide tail enriched for U residues [79]. The process of tailing miRNAs with uridine as the preferential nucleotides will be referred to as uridylation. miRNAs also become truncated from their 3' ends in the *hen1* mutant, and truncated miRNAs can also be uridylated [79]. Interestingly, miR173 and miR173* are not affected equally by the *hen1* mutation such that miR173* is rarely uridylated in the *hen1* mutant *in vivo* [79]. This observation suggests that uridylation happens after RISC assembly instead of on the small RNA duplexes. The uridylation of the unmethylated small RNAs perhaps leads to the 3'-to-5' degradation of the small RNAs, but this still needs to be confirmed genetically or biochemically. WAVY LEAF1 (WAF1), a HEN1 ortholog in rice, is also essential for the stabilization of small RNAs. The accumulation of miRNAs and trans-acting siRNAs is greatly reduced in *waf1* mutants [80].

Phylogenetic studies showed that the N-terminal three-fourth of *Arabidopsis* HEN1 is conserved only among the plant homologs, and the C-terminal domain, which constitutes approximately one-fourth of HEN1 and contains a recognizable S-adenosyl methionine (AdoMet)-binding motif [18], is conserved among many bacterial, fungal, and metazoan homologs [81] (Table

1.1). Bioinformatics analysis revealed that the methyltransferase catalytic domain of HEN1 is closely related to small molecule methyltransferases [81]. *In vitro* activity assays showed that recombinant *Arabidopsis* HEN1 acts on 21-24 nt small RNA duplexes and deposits a methyl group onto the 2' OH of the 3' terminal nucleotides of each strand [19]. The 2 nt overhang of the duplex and the 2' and 3' OH of the 3' nucleotide are two important features in the substrates of *Arabidopsis* HEN1 [19].

The mechanism of substrate recognition and methylation by HEN1 was revealed by the crystal structure of full-length HEN1 from *Arabidopsis* in complex with a 22 nt small RNA duplex. *Arabidopsis* HEN1 binds to the small RNA duplex substrate as a monomer [82]. The plant specific N-terminal part of HEN1 contains two double-stranded RNA-binding domains (dsRBD1 and dsRBD2) and an LCD domain containing a La motif [81,82]. Both dsRBDs are involved in the recognition of the substrates, and the substrate length specificity is determined by the distance between the methyltransferase (MTase) domain and the LCD, each interacting with one end of the small RNA duplex. HEN1 methylates the 2' OH of the 3' terminal nucleotide in a Mg^{2+}-dependent manner [82]. Kinetic studies illustrated that HEN1 is highly catalytically efficient in the absence of any supplementary proteins. The enzyme modifies individual strands in succession to complete the methylation of the duplex [83]. Since the C-terminal part of HEN1 (residues 666–942) efficiently modifies small RNA duplexes *in vitro* but exhibits

weaker affinities for both small RNA duplexes and AdoMet (the methyl donor), the function of the N-terminal part is to stabilize the catalytic complex [83].

Small RNA methylation by HEN1 in plants could be modulated *in vivo*. Small RNA methylation is interfered by several RNA silencing suppressors from plant viruses, such as the *Beet yellows virus* 21 kDa protein (p21), the *Tomato bushy stunt virus* 19 kDa protein (p19) and the *Turnip mosaic virus* silencing suppressor, P1/HC-Pro [84-86]. Interestingly, miRNA methylation defects in the weak *hen1-2* mutant can be partially suppressed by mutations in the endogenous 24 nt siRNA biogenesis pathway. The suppression suggests that siRNAs compete with miRNAs for methylation when HEN1 function is compromised in *Arabidopsis* [87]. In addition, differences in phenotypic severity of the same *hen1* lesion in Col versus L*er* ecotypes implicate the existence of a negative modifier of HEN1 activity or small RNA activity in the Columbia background [87].

Animal piRNAs and fly siRNAs are methylated by HEN1 homologs

piRNAs are expressed in animal germlines and guide Piwi proteins to silence TEs (reviewed in [7]). piRNAs and *Drosophila* Ago2-associated siRNAs are 2'-*O*-methylated at their 3' termini by HEN1 homologs in the animal kingdom [74-78,88] (Figure 1.1B, C). Animal Hen1 are less than half the size of the plant HEN1 proteins: they lack the plant specific N-terminal part [74-78,88]. Most animal Hen1 proteins have a similar expression pattern as the Piwi proteins [75,76,78]. For example, mouse Hen1 is expressed specifically in testis as

piRNAs and Piwi proteins. Recombinant mouse Hen1 methylates single-stranded piRNAs *in vitro* [74,75].

Zebrafish Hen1 is expressed in both female and male germ lines, but is essential only for oocyte development and dispensable for testis development. Hen1 protein is localized to nuage, a germ cell-specific structure where Ziwi (one of the Piwi proteins in zebrafish) is localized [76]. In the testes of *hen1* mutants, piRNAs become either uridylated or adenylated with a higher uridylation frequency on piRNAs targeting RNA-based TEs. Correspondingly, the retrotransposon-derived piRNAs are reduced in abundance and the retrotransposons are mildly de-repressed in *hen1* mutants. Therefore, Hen1-mediated methylation stabilizes piRNAs for transposon silencing in ovary and testis [76].

piRNAs and Ago2-associated siRNAs in *Drosophila* are 2'-*O*-methylated at their 3' termini [77,78]. Kuniaki Saito *et al.* showed that loss of Pimet (piRNA methyltransferase), the HEN1 homolog in *Drosophila*, results in loss of 2'-*O*-methylation of piRNAs. Recombinant Pimet methylates single-stranded small RNA oligos *in vitro* and physically interacts with the Piwi protein [78]. The HEN1 homolog in *Drosophila* was named DmHen1 by Horwich *et al* [77]. DmHen1 methylates the 3' termini of Piwi-associated piRNAs and Ago2-associated siRNAs, but not Ago1-associated miRNAs. Without DmHen1, the length and abundance of piRNAs are decreased, and the levels of piRNA targets are elevated. Horwich *et al*. further showed that methylation occurs on the single-

stranded siRNAs in association with Ago2 [77], which is also likely to be the case for piRNAs *in vivo*.

A HEN1 homolog is also identified in the ciliated protozoan *Tetrahymena thermophila*, which contains 12 Piwi proteins, but no Ago proteins [88]. *Tetrahymena thermophila* scnRNAs are 28-29 nt long, expressed during sexual reproduction, and bind specifically to the Piwi protein Twi1p [89]. Hen1p (the *Tetrahymena* HEN1 homolog) and Twi1p are co-expressed and physically interact *in vitro* [88]. Loss of Hen1p causes a reduction in the abundance and length of scnRNAs, defects in programmed DNA elimination, and inefficient production of sexual progeny. Recombinant Hen1p methylates single-stranded scnRNAs *in vitro*. Therefore, Hen1p-mediated 2'-*O*-methylation stabilizes scnRNAs and ensures DNA elimination in *Tetrahymena* [88].

Damaged bacterial RNAs are methylated by HEN1 *in vitro*

Bacterial Hen1 is encoded by a two-gene operon that also encodes polynucleotide kinase-phosphatase (Pnkp), an RNA repair enzyme [90,91]. Bacterial Hen1 methylates the 3' terminal nucleotide of the 5' fragment of a broken tRNA in a Mn^{2+} dependent manner to protect it against further damage by a transesterifying endonuclease; then the Pnkp in the Hen1-Pnkp complex repairs the RNA substrate by end healing and sealing [91,92]. The bacterial Hen1 MTase domain contains a core fold shared by other RNA and DNA MTases as well as motifs unique to bacterial Hen1 homologs. The interaction between bacterial Hen1 and their RNA substrates is likely similar to that of their

eukaryotic counterparts [91].

Removal of unmethylated small RNAs in *hen1* mutants

Loss of HEN1 activity causes reduced accumulation of naturally methylated small RNAs, and studies of *hen1* mutants revealed previously unknown mechanisms that degrade small RNAs. These studies suggest that 3' uridylation and 3'-to-5' exonucleolytic degradation are two major mechanisms that turnover unmethylated small RNAs.

3' Uridylation of unmethylated small RNAs

Methylation protects plant small RNAs, animal piRNAs and fly Ago2-associated siRNAs against 3' nucleotide addition and 3'-to-5' exonucleolytic degradation [18,76,79,88,93]. In *Arabidopsis*, 3' uridylation has been proposed to stimulate the degradation of small RNAs [79] (Figure 1.2A). However, the putative nucleotidyltransferase(s) has not been identified in *Arabidopsis* such that the role of uridylation in miRNA turnover has not been genetically evaluated. Instead, the characterization of a *Chlamodymonas reinhardtii* mutant (*Mut-68*) has shed light on the mechanisms of uridylation and degradation of unmethylated miRNAs and siRNAs.

In the alga *Chlamydomonas reinhardtii*, siRNAs and miRNAs are 2'-*O*-methylated at their 3' termini as in angiosperms [94]. MUT68, a terminal nucleotidyltransferase, was initially shown to add adenines to the 5' cleavage fragments from mRNAs targeted by RISCs to lead to their efficient decay [45]. MUT68 cooperates with the cytoplasmic exosome to degrade RISC-generated 5'

RNA cleavage products [45], but cooperates with the peripheral exosome subunit RRP6 to degrade small RNAs [95]. In a *Mut-68* mutant and an *RRP6* depletion line, the levels of a subset of miRNAs and siRNAs are elevated. MUT68 plays a role in the uridylation of the 3' ends of small RNAs *in vivo* and stimulates their degradation by RRP6 *in vitro*. MUT68 and RRP6 were unable to use a 2'-*O*-methylated miR912 oligonucleotide as a substrate *in vitro*, indicating that MUT68 may only act on unmethylated siRNA and miRNAs [95]. However, it's not clear if MUT68 and RRP6 compose the downstream pathway degrading unmethylated small RNAs in *hen1*, since it has not been tested yet whether *MUT68* loss of function or *RRP6* depletion suppresses the molecular defects associated with HEN1 loss of function.

In a zebrafish *hen1* mutant, both adenylation and uridylation of piRNAs increase significantly [76]. The A- or U-tails are usually only one or two bases long, whereas plant miRNAs acquire a tail of 1-7 nt in a *hen1* mutant. The length difference implicates that the zebrafish nucleotidyltransferase or the exonuclease differs in efficiency or processivity from their counterparts in plants. However, neither enzyme has been identified yet. Moreover, uridylation, but not adenylation, discriminates the piRNAs targeting RNA- and DNA-based TEs and is associated with piRNA destabilization, most likely through a 3'-to-5' exonucleolytic activity. The fact that piRNAs targeting RNA-based TEs tend to be uridylated in *hen1* suggests that the uridylation activity on piRNAs is possibly triggered by interactions with the target RNAs [76] (Figure 1.2).

In *Drosophila*, 2'-*O*-methylation of Ago2-associated endo-siRNAs also protects the siRNAs from 3' tailing and trimming. In the absence of Hen1 activities, endo-siRNAs generally become 3' truncated and/or acquire a 3' tail. The most abundant nucleotide added is uridine, followed by adenine. Long tails are rare but are nearly always uridine tails [93] (Figure 1.2).

In summary, 2'-*O*-methylation of small RNAs by HEN1 protects the small RNAs from uridine addition at the 3' termini, which probably stimulates a 3'-to-5' exonucleolytic activity to degrade the tagged small RNAs. However, it's still mysterious what the nucleotidyltransferases modifying the small RNAs are in most organisms (Table 1.2). Once these enzymes are identified, it would be interesting to determine whether they impact small RNA metabolism under the normal condition when HEN1 function is present.

3'-5' exonucleolytic degradation of small RNAs

The discovery of a small RNA 3' truncation activity in *Arabidopsis hen1* mutants prompted a search for the 3'-to-5' exonuclease responsible for this activity. A family of 3'-to-5' exoribonucleases named *SMALL RNA DEGRADING NUCLEASE* (*SDN*) was found to turnover mature miRNAs and siRNAs in *Arabidopsis* [96]. *In vitro* assays showed that SDN1 acts specifically on single-stranded small RNA oligonucleotides that are longer than 8 nt, and is deterred but not completely inhibited by the 2'-*O*-methyl modification on the 3' termini of small RNAs [96]. There are 4 closely related SDN family exoribonucleases sharing overlapping functions in *Arabidopsis*; only simultaneous knockdown of

multiple *SDN* genes results in elevated miRNA levels *in vivo* and pleiotropic developmental defects [96]. Interestingly, the efficiency for SDN1 to degrade U-tailed miR173 is lower than that for miR173 *in vitro*, which suggests that SDN1 may not be the enzyme that degrades the uridylated small RNAs in the absence of HEN1 activity [96]. Are the SDN proteins responsible for the 3' truncation of small RNAs in *hen1* mutants? This has yet to be evaluated by knocking down multiple *SDN* genes in *hen1* mutants and observing the status of miRNA 3' truncation in this background. Another pressing question is whether the SDNs degrade small RNAs released from RISCs or small RNAs bound by argonaute proteins *in vivo*. If SDNs can degrade argonaute-bound small RNAs, how do they access the small RNA 3' end that is anchored in the PAZ domain of the argonaute protein? The *SDN* homologs are universally present in eukaryotes, but whether they exert similar functions is currently unknown [96].

Additional factors that influence small RNA stability

Most animal miRNAs do not adopt methylation as a mechanism of stabilization. The mechanisms underlying the turnover of naturally unmethylated small RNAs include cis-acting elements, target transcripts or target mimic transcripts, and trans-acting proteins that modulate the accessibility of small RNAs to the degradation machinery.

Target mRNAs mediate the degradation or stabilization of small RNAs

In *Drosophila*, miRNAs typically associate with Ago1 to repress the translation, and/or cause the decay, of their target mRNAs, whereas siRNAs

guide Ago2 to destroy viral and transposon RNAs. miRNAs are complementary to their targets only at the seed sequence region, with few additional base pairs tethering the two RNAs together. The abundance of the corresponding miRNAs decreases when transgenes containing one or more highly complementary sites were introduced [93]. Extensive base-pairing between Ago1-associated miRNAs and their target mRNAs triggers miRNA 3' extension and 3'-to-5' trimming that could result from the activities of a terminal nucleotidyltransferase and a 3'-to-5' exonuclease, respectively. Therefore, the partial complementarity between animal miRNAs and their targets avoids highly-complementary-target-induced 3' tailing and 3' truncation [93]. In fact, structural studies on an archea (*Thermus thermophilus*) argonaute in complex with the guide sequence and the target strands of varying lengths show that the presence of a long, but not a short, stretch of sequence complementarity between the guide and the target induces the 3' end of the guide to be dislodged from the PAZ domain [97]. This presumably would allow a nucleotidyltransferase or an exonuclease to access the 3' end of the small RNA. The nucleotidyltransferase and the exonuclease are likely to be the same ones that act upon Ago2-bound, unmethylated siRNAs in the *hen1* mutant [93]. In fact, tailing and truncation of siRNAs in the *hen1* mutant may also be induced by their endogenous target mRNAs, which are highly complementary to the siRNAs.

Target complementarity also affects small RNA stability in human cells. Synthetic, chemically modified target RNA analogs, "antagomirs", cause the

sequence-specific 3' trimming and tailing of their complementary miRNAs *in vivo* [93]. Moreover, trimming of miRNAs in a HeLa cell cytoplasmic extract was recapitulated by supplying *in vitro* transcribed target mRNAs containing fully complementary sites to miRNAs [93]. These results suggest that target-dependent small RNA tailing and trimming is conserved between flies and mammals. A recent kinetic analysis of miR-233 with and without the supplement of targets in human cells shows that target regulation increased the decay of miRNAs. Furthermore, the decay of miR-233 in cells co-expressing a perfectly complementary target was at least two times faster than that in cells co-expressing a target with mismatches [98]. Deep sequencing unveiled that the frequency of miR-233 with 3' mono-uridylation was consistently increasing during decay, suggesting that the addition of a uridine may be a destabilizing modification [98]. The level of miR-233 with one or two adenine added to its 3' end was also elevated in the cells co-expressing a target with mismatches. However, the frequency of these variants did not change during decay [98].

Target-mediated degradation of miRNAs is likely also conserved in plants. In *Arabidopsis*, miR399 is regulated by *IPS1* (*INDUCED BY PHOSPHATE STARVATION1*), which encodes a non-coding RNA containing a short motif highly complementary to miR399 [99]. The *IPS1* sequence contains a three-nucleotide insertion at the cleavage site, which prevents endonucleolytic cleavage of *IPS1* transcripts by miR399 RISC, resulting in the sequestration of miR399 and reduction of miR399 activity [99]. Based on this principle, artificial

target mimics have become a popular tool to down-regulate miRNA activity for functional studies in *Arabidopsis* [100,101]. Todesco *et al*. generated a large set of artificial target mimics for *Arabidopsis* miRNAs. In all target mimic lines they examined, the levels of the corresponding miRNAs were decreased, suggesting that unproductive interaction of miRISC with a decoy target affects miRNA stability, even though such an effect was not observed in the interaction between *IPS1* and miR399 [101].

In contrast to the effects caused by aberrant target mRNAs described above, the presence of wild type target mRNAs appears to mediate the stabilization of miRNAs in *C. elegans*. XRN-2 was found to affect miRNA homeostasis in *C. elegans* by promoting the dislodging of miRNAs from RISC and degrading the free miRNAs through its 5'-to-3' exoribonucleolytic activity [102]. miRNAs are efficiently released from the RISC complex and degraded by XRN-2 in a *C. elegans* larval lysate. However, both of the release and the degradation of miRNAs can be blocked by adding miRNA target mRNAs. *In vivo*, the steady-state miRNA levels are increased in the presence of target mRNAs [102]. However, it's currently unknown how the dislodging of miRNAs from RISC by XRN-2 is achieved or how target mRNAs stabilize miRISCs. It is also not known whether the XRN-2-dependent turnover and target mRNA-mediated stabilization of miRNAs also exist in other organisms. The plant homologs of XRN-2 are involved in miRNA biogenesis in that they degrade the non-miRNA fragments as by-products of pri-miRNA processing, but do not affect mature

miRNA levels [103].

In summary, target mRNAs can serve as an additional layer of regulation for miRNA activity and turnover. This can potentially be exploited for therapeutic intervention on miRNA expression.

3' nucleotide addition affects the stability of small RNAs

3' nucleotide addition of small RNAs has been observed on a global scale in high throughput sequencing studies [104-106]. A recent study showed that 3' nucleotide addition to miRNAs is a common physiological posttranscriptional event that exhibits selectivity for specific miRNAs ranging from *C. elegans* to humans [106]. The modifications are predominantly mono-adenylation and mono-uridylation across different tissue types, disease states, and developmental stages [106]. Multiple enzymes, including MTPAP, PAPD4, PAPD5, ZCCHC6, ZCCHC11, and TUT1, were found to govern the 3' nucleotide addition in a miRNA-specific manner [106]. 3' nucleotide addition can influence miRNA stability and function, depending on the specific miRNAs examined. For example, uridylation of miR-233 was increased during miRNA decay [98]. Mature miR-122 was shown to be adenylated by the RNA nucleotidyltransferase PAPD4/GLD-2 in humans and mice, resulting in an increase in the stability of the miRNA [107]. PAPD4/ GLD-2 was identified as a regulatory cytoplasmic poly(A) polymerase that controls germline progression through meiosis in *C. elegans* [108]. Considering the low *in vitro* specificity of PAPD4/GLD-2, either some specificity factors recruit PAPD4/GLD-2 to the 3' terminus of miR-122 or a

broader set of miRNAs is regulated by PAPD4/GLD-2 through adenylation *in vivo*.

In *C. elegans*, uridylation of siRNAs is not a widespread phenomenon, but is largely restricted to RNAi pathways involving CSR-1, an argonaute that is not involved in regulating mRNA levels [109]. A nucleotidyltransferase CDE-1 uridylates the siRNAs in the CSR-1 pathway, and loss of CDE-1 activity leads to an increase in the levels of CSR-1 siRNAs. As a result, these siRNAs are fed into other RNAi pathways. This is accompanied by defects in chromosome segregation, much like those observed in *csr-1* mutants [109]. Thus, CDE-1 restricts siRNAs produced from specific loci to CSR-1, thereby playing a role in keeping the diverse RNAi pathways in *C. elegans* distinct and functionally separated from each other [110]. Therefore, the 3' uridylation of CSR-1 associated siRNAs, which are naturally unmethylated [111], regulates the accumulation of these siRNAs by destabilizing them.

Adenylation was observed for both full length and truncated miRNAs in *Populus trichocarpa* [112]. One to seven adenines could be observed on miRNA 3' termini in *Populus*. An *in vitro* decay assay showed that replacement of the 3' nucleotide with an adenine residue resulted in slower miRNA degradation in *P. trichocarpa* extracts [112].

These observations imply that 3' nucleotide addition, predominantly uridylation and adenylation, is a widespread modification on small RNAs. The investigation of the biological functions of small RNA 3' nucleotide addition is still

at an early stage. When studied, the 3' nucleotide addition promotes, reduces or exerts no effects on small RNA decay depending on the specific miRNAs and siRNAs being investigated. Uridylation and adenylation on other RNAs occur competitively, and a single adenylation prevents further oligo-uridylation [113]. It hasn't been tested whether this is true for the miRNAs and siRNAs.

cis elements and *trans* factors affect small RNAs stability

The stability of some specific miRNAs is regulated by *cis* elements in the mature miRNAs. Most miRNAs in animals appear to be stable, with the exception of a few miRNAs. In particular, miR-382, a miRNA that contributes to HIV-1 latency in resting $CD4^+$ T lymphocytes, is unstable in cells [114,115]. In a cell-free system, the differential stabilities of miRNAs were recapitulated with *in vitro*-processed mature miRNAs derived from pre-miRNAs. Bail *et al* showed that the 3' terminal seven nucleotides were necessary for the low stability of miR-382 in the cell-free system [114]. They did not test whether these nucleotides were sufficient to impart instability to other stable miRNAs. miR-382 decay was primarily due to the exosome with a more modest contribution by Xrn1 and no detectable contribution by Xrn2 [114].

Almost half of the human miRNA genes are arranged in clusters in the genome. It was demonstrated that individual members are uniformly expressed in most clusters, but differentially expressed in some clusters in several human leukemia cell lines [116], suggesting possible posttranscriptional control. miR-200c and miR-141, differing by 5 nucleotides and encoded by the miR-200c_141

cluster, show varied relative abundances in different cell lines [117]. Strikingly, cell detachment induced the decay of miR-141 but not miR-200c. A sequence motif (UGUCU) was identified to be necessary for the destabilization of miR-141 by cell detachment. Several other miRNAs, miR-200a, miR-429 and miR-34a, which also contain this motif, were also destabilized upon cell detachment. But the motif wasn't able to render let-7 unstable [117].

A point mutation in *let-7* reduced the accumulation of the mature miRNA and derepressed its targets [102]. Both effects as well as the additional developmental defects were suppressed by the depletion of a 5'-3' exonuclease, XRN-2 [102]. This suggests that the sequence of let-7 influences its stability. Examination of the half-lives of brain-enriched miRNAs showed that the percent of AU or UA dinucleotides in several miRNAs is correlated with their instability. The motifs were hypothesized to be analogous to the mRNA AU-rich element that confers mRNA instability [118]. PMI Alzheimer's disease (AD)-affected human brain temporal lobe neocortex was found to exhibit significant up-regulation of a few miRNAs, which was not observed in the same brain regions affected with amyotrophic lateral sclerosis (ALS), Parkinson's disease or schizophrenia [118]. Thus, it appeared that both elements within the miRNAs and cellular states could affect miRNA stability.

Components of the RISC or RISC-associated factors may influence the stability of small RNAs. Most endogenous miRNAs are in RISCs, and only a very small proportion is free in cells [119]. But 2'-*O*-methyl antagomirs that are

complementary to miRNAs are able to dissociate the targeted miRNAs from the RISC complex, causing the loss of protection of the miRNAs by RISC [119]. The antagomir-induced miRNA degradation may be similar to highly-complementary-target mRNA-mediated miRNA degradation, and the two may share common mechanisms, such as the displacement of the miRNAs from RISCs. In the mouse, Argonaute proteins promote mature miRNA accumulation posttranscriptionally, in that overexpession of Argonaute genes elevates the levels of miRNAs and *Ago2* knockout reduces the levels of miRNAs. Expression of Argonaute is positively correlated with mature miRNA levels [120]. Moreover, half-lives of multiple endogenous miRNAs are correlated with the cellular Ago2 levels [121]. Similar stabilization effects of miRNAs by Ago proteins were observed in *Arabidopsis*. Loss of function of AGO1, the major miRNA effector in *Arabidopsis*, results in reduced levels of most miRNAs [47]. *Arabidopsis* AGO2 is highly induced by the bacterial pathogen *Pseudomonas syringae*. Meanwhile, the accumulation of several miRNA star strands that are bound by AGO2 is also elevated [69].

Other proteins also posttranscriptionally regulate small RNA stability, such as Translin, a nucleic acid-binding protein that is known to bind several mRNAs, a noncoding RNA and miR-122a in germ cells of mouse testis [122]. The binding of Translin to miR-122a increases its *in vivo* stability, suggesting that miRNA stability can be regulated by the association with RNA binding proteins [122]. It is not known how Translin affects miR-122a stability. It is conceivable that proteins

can affect small RNA stability by stabilizing or destabilizing RISCs to influence the accessibility of the small RNA degradation machinery to small RNAs.

The levels of small RNAs, determined by the rates of biogenesis and turnover, are crucial for their regulation on target gene expression. Either reduction or elevation in small RNA levels results in pleiotropic developmental defects in *Arabidopsis*, as illustrated by the phenotypes of plants with *hen1* mutations or *SDN* depletion [18,96]. In *C. elegans*, when the excess siRNAs from the CSR-1 pathway are fed into other RNAi pathways, chromosome segregation is disrupted [110]. Understanding the mechanisms regulating small RNA stability will benefit our utilization of RNAi. For example, the stability of fork-siRNAs (a type of siRNAs with designed mismatches in the duplexes to enhance asymmetry in Ago loading) was significantly improved by methylating the nuclease sensitive sites. As a result, the duration of the gene silencing activity of the modified fork-siRNAs doubled that of the unmethylated analogs [123]. Modulation of miR-382 stability could potentially impact the control of HIV-1 latency [115], which is major barrier for the eradication of the virus in patients on suppressive highly active antiretroviral therapy (reviewed in [124]). Moreover, novel therapeutic applications could be devised based on the knowledge of highly-complementary-target-mediated miRNA instability to target miRNAs whose overexpression is associated with human disorders. The stability of individual miRNAs can be altered after we learn how the specificity of miRNA turnover or stabilization is achieved. A recent report showed that plant miRNAs

can be obtained by animals through food intake. Strikingly, the plant miR168 could even repress the expression of human/mouse low-density lipoprotein receptor adapter protein 1 (LDLRAP1) across kingdom [125]. Although this finding raised safety issues about transgenic foods, it also enlightens scientists on the production and the delivery of miRNAs into patients for therapeutic purposes.

Floral determinacy

Stem cells are a group of pluripotent cells that produce daughter cells for organogenesis while maintaining their undifferentiated property. In plants, the stem cells are retained post-embryonically in the meristems located at the tips of shoots, roots, and flowers [126,127]. In *Arabidopsis*, *WUSCHEL* (*WUS*), which is restrictively expressed in a small niche, called the organization center, beneath the stem cells, is an essential regulator for the maintenance of stem cells [128]. Stem cells at the shoot apical and root apical meristems maintain their property throughout the life of a plant. These vegetative meristems are indeterminate [129]. In contrast, the floral meristems are determinate such that the stem cells are differentiated at a certain developmental time point [130]. *Arabidopsis* flowers are composed of four whorls of floral organs with a fixed number. The floral meristem is terminated after the generation of the carpel primordia [130].

Floral determinacy is a genetically programmed and temporally regulated process, which is interwoven with the differentiation of floral organs. In *Arabidopsis*, the ABC classes of homeotic genes specify the four types of floral

organs (reviewed in [131]). The A class genes, *APETALA1* (*AP1*) and *APETALA2* (*AP2*), are primarily expressed in the first and second whorls and are involved in the specification of sepals and petals [131]. The B class genes, *APETALA3* (*AP3*) and *PISTILLATA* (*PI*) that are expressed in the second and third whorls, specify petals with the A class genes and specify stamens with the C class gene *AGAMOUS* (*AG*) [131]. *AG* is expressed in the third and fourth whorls and specifies reproductive organs, namely stamens and carpels [131]. In *Arabidopsis*, *AG* acts as the key regulator to terminate the stem cells in floral meristems. The floral stem cell fate is determined by the activities of *WUS* and *AG*. *WUS* maintains stem cell activity at early stages of flower development and activates *AG* expression at floral stage 3 [132,133]. The *wus-1* flowers terminate precociously in a central stamen. In contrast, *ag-1* flowers generate numerous sepals and petals in a reiterative manner. It has been shown that *AG* is necessary to terminate the floral meristem through repressing *WUS* expression [132,133].

Additional factors regulate floral determinacy through *AG*-dependent or *AG*-independent pathways. One of the *AG*-independent regulators is the C2H2 zinc finger protein SUPERMAN (SUP), which negatively regulates stem cell activity at floral stages 3 and 4 [134]. *sup* mutations enhance the floral determinacy defects of null *ag* mutants, suggesting that *SUP* and *AG* act in parallel, although *WUS* acts at downstream of *SUP* as well as *AG* [135]. *SUP* likely controls floral stem cells through the B class genes [136].

A number of regulators have been found to act in an *AG*-dependent manner in the termination of floral stem cells. *KNUCKLEs* (*KNU*), encoding a putative zinc finger protein and transcription repressor, was identified as a direct target of AG in the repression of *WUS* at floral meristems [137]. Although *AG* is induced at stage 3, the shutdown of *WUS* expression is not completed until stage 6 due to the delay of *KNU* expression by repressive chromatin as marked by H3K27me3 [137]. Thus, the epigenetic marks serve as a timing mechanism for the termination of *WUS* expression. *AG* represses *WUS* expression through other mechanisms too. A YABBY transcription factor, CRABS CLAW (CRC) might act downstream from *AG* and B class genes [138]. *CRC* is expressed in the carpels and nectaries [138]. *crc* mutants show defects in carpel and nectary development, and enhance the determinacy defects of *ag-1/+* plants [139]. *ULTRAPETALA1* (*ULT1*) prevents the formation of extra primary floral organs and of supernumerary carpel whorls [140,141]. *REBELOTE* (*RBL*), *SQUINT* (*SQN*), and *ULT1* act synergistically with *CRC* and with each other in floral determinacy [135]. *RBL, SQN* and *ULT1* likely regulate the expression of *AG* though different mechanisms, since their predicted molecular activities differ [135,142]. One of the A class genes, *AP2*, is targeted by miR172 in the inner two whorls of *Arabidopsis* flower. It's been shown that miR172-resistant *AP2* promotes stem cell activity through *WUS* in both an AG-dependent and an AG-independent manner [143].

As important regulator of plant growth and development, the plant

hormone cytokinin affects the size and activity of meristems [144]. Double mutants of *Cytokinin oxidase/dehydrogenase 3* (*CKX3*) and *CKX5* show prolonged stem cell activity and expanded stem cell niche. Consistently, *CKX3* has a similar expression pattern as *WUS* [144]. Furthermore, a mutation in *ARABIDOPSIS HISTIDINE PHOSPHOTRANSFER PROTEIN 6*, a negative regulator of cytokinin signaling expressed at the meristem flanks, further prolonged stem cell activity [144]. Auxin, another plant hormone regulating many aspects of plant growth and development, also regulates flower development. High concentration of auxin induces the growth at the tips of developing floral organ primordia [145]. However, how auxin transport and signaling are related to floral determinacy is currently not well understood.

Clearly, the termination of floral stem cells is a temporally precisely controlled process regulated by diverse mechanisms. The punctilious signaling network itself implies the importance of terminating floral stem cells timely, which is a key issue for plant reproduction. Alteration of the temporal program of floral stem cells is deleterious to the generation of progeny. Precocious termination would affect organogenesis of reproductive organs, while delayed termination disrupts the proper development of ovules, resulting in reduced seed yield. Further investigations will likely provide new insights into the temporal control of stem cell activities in the floral meristems, enlightening us on the regulation of cell fate and differentiation.

My Ph.D. research began with the goal of dissecting the temporal program of stem cell termination. Through a genetic screen, we identified *AGO10*, which is most closely related to *AGO1* (the major effecter of miRNAs in *Arabidopsis*), as a factor that promotes the termination of floral stem cells. The role of *AGO10* in floral determinacy implicates the functions of miRNAs and their targets in this process. Our study demonstrated that *AGO10* acts through *WUS* to terminate the floral stem cells. Moreover, we show that the function of AGO10 is realized through miR172 and miR165/166. We established miR165/166 and their targets, type III *HD-Zip* genes, as critical regulators of floral determinacy in *Arabidopsis*. These studies are summarized in Chapter I of my disseration. Strikingly, AGO10 terminates the floral stem cells by repressing the levels of miR165/166 instead of mediating their activities *in vivo*. In contrast, AGO1 mediates the activities of miR165/166 and stabilizes the mature miRNAs through physical association. The studies reported in Chapter II of my dissertation aim to understand how AGO10 down-regulates the accumulation of miR165/166 despite its similar biochemical activities and biological functions with AGO1. Our data show that *AGO10* doesn't affect the transcription of *MIR165/166* genes or the processing of miR165/166 precursors. Therefore, we proposed and tested the hypothesis that AGO10-associated miR165/166 is less stable than AGO1-associated miR165/166. We obtained molecular genetic evidence supporting a role of AGO10 in enhancing the decay of miR165/166. I am performing biochemical and genetic analyses to further confirm this hypothesis and to uncover how AGO10 enhances the decay

of miR165/166. My studies will likely unveil a new function of AGO proteins in eukaryotes and shed light on mechanisms of stem cell regulation.

Figures

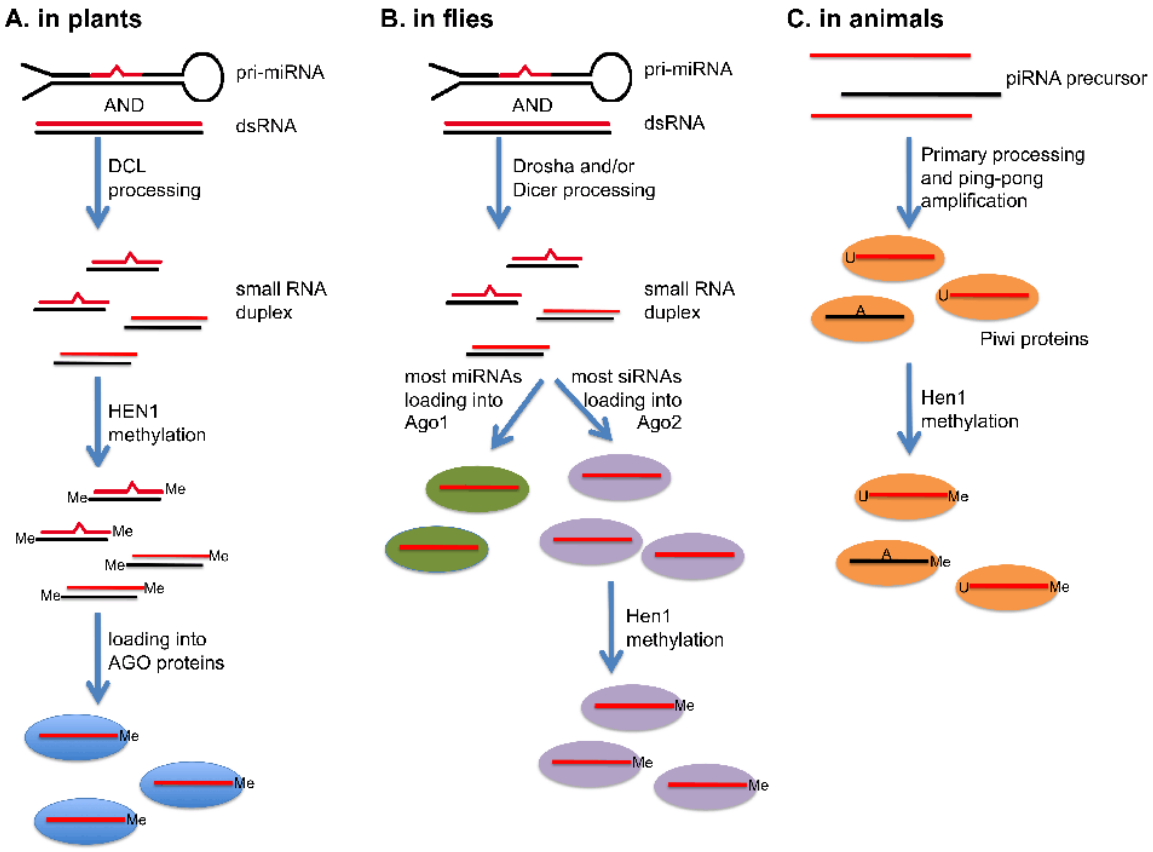

Figure 1.1 2'-O-methylation of small RNAs by HEN1

(A) Plant HEN1 methylates the 3' termini of both strands of small RNA duplexes. (B) *Drosophila* Hen1 methylates Ago2-associated siRNAs, but not Ago1-associated miRNAs. (C) Animal Hen1 methylates piRNAs in germ cells.

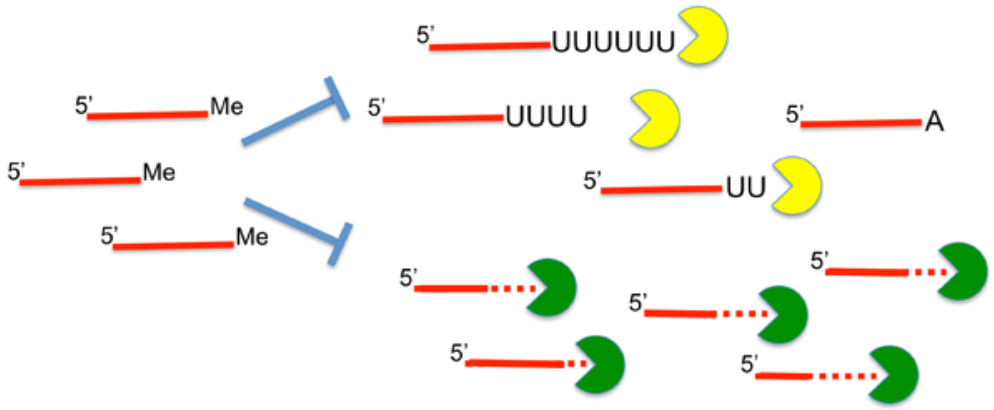

Figure 1.2 HEN1 protects small RNAs from uridylation and 3'-to-5' degradation

Methylation protects small RNAs from 3' tailing and truncation that lead to the degradation of the small RNAs.

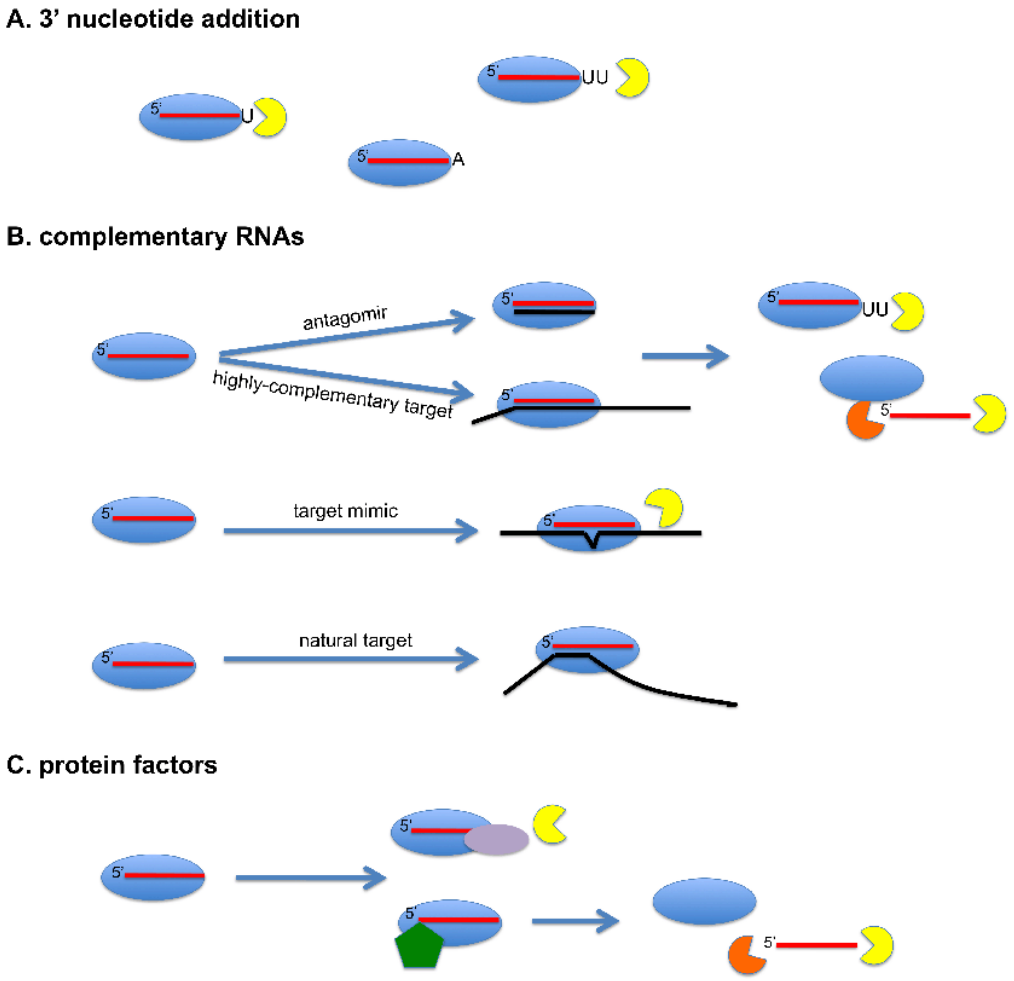

Figure 1.3 Mechanisms influencing small RNA stability

(A) 3' nucleotide addition affects the stability of small RNAs. While U-tails probably lead to small RNA degradation, 3' adenylation may have a protective role against degradation or have no effects on the stability of small RNAs. (B) Target transcripts can either enhance or suppress the degradation of the corresponding small RNAs in different situations. (C) Protein factors can stabilize or destabilize RISCs to influence the accessibility of nucleases to small RNAs.

Tables

Table 1.1 HEN1 homologs that methylate small RNAs

Name	Organism	Substrates	Mutant phenotypes
HEN1	*Arabidopsis*	Small RNA duplexes	Reduction of small RNA abundance; Pleiotropic developmental defects
WAF1	Rice		Reduction of small RNA abundance; Seedling lethality and pleiotropic defects
mHen1	Mouse	piRNAs	
DmHen1/ Pimet	*Drosophila*	piRNAs, Ago2-assoicated small RNAs	Decrease of piRNA length and abundance; Derepression of piRNA targets; Trimming and tailing of Ago2-associated siRNAs
Hen1	Zebrafish	piRNAs	Defects in oocyte development; Uridylation, adenylation of piRNAs; Decrease of piRNA abundance; Transposon derepression
Hen1p	*Tetrahymena thermophila*	scnRNAs	Reduction of scnRNA length and abundance; Defects in programmed DNA elimination and production of sexual progeny

Table 1.2 Nucleotidyltransferases affecting mature small RNAs

name	Organism	substrates	Activity	Potential effects
CDE-1	*C. elegans*	siRNAs from the CSR-1 pathway	uridylation	Destabilization
MTPAP, PAPD4, PAPD5, ZCCHC6, ZCCHC11, and TUT1,	Humans	miRNAs	uridylation and adenylation	Regulation of miRNA stability and/or activity
MUT68	*Chlamydomonas reinhardtii*	miRNAs and siRNAs	uridylation	Destabilization
Unknown	*Populus trichocarpa*	miRNA	adenylation	Stabilization
Unknown	Zebrafish	Unmethylated piRNAs	uridylation and adenylation	Regulation of piRNA stability
Unknown	*Arabidopsis*	Unmethylated small RNAs	predominantly uridylation	Destabilization

Reference

1. Ambros V, Chen X (2007) The regulation of genes and genomes by small RNAs. Development 134: 1635-1641.

2. Suh N, Blelloch R (2011) Small RNAs in early mammalian development: from gametes to gastrulation. Development 138: 1653-1661.

3. Kim VN (2005) Small RNAs: classification, biogenesis, and function. Mol Cell 19: 1-15.

4. Voinnet O (2009) Origin, biogenesis, and activity of plant microRNAs. Cell 136: 669-687.

5. Zhang H, Zhu JK (2011) RNA-directed DNA methylation. Curr Opin Plant Biol 14: 142-147.

6. Xie Z, Johansen LK, Gustafson AM, Kasschau KD, Lellis AD, et al. (2004) Genetic and functional diversification of small RNA pathways in plants. PLoS Biol 2: E104.

7. Siomi MC, Sato K, Pezic D, Aravin AA (2011) PIWI-interacting small RNAs: the vanguard of genome defence. Nat Rev Mol Cell Biol 12: 246-258.

8. Vaucheret H (2008) Plant ARGONAUTES. Trends Plant Sci 13: 350-358.

9. Chen X (2005) MicroRNA biogenesis and function in plants. FEBS Lett 579: 5923-5931.

10. Lee Y, Kim M, Han J, Yeom KH, Lee S, et al. (2004) MicroRNA genes are transcribed by RNA polymerase II. EMBO J 23: 4051-4060.

11. Kurihara Y, Watanabe Y (2004) Arabidopsis micro-RNA biogenesis through Dicer-like 1 protein functions. Proc Natl Acad Sci U S A 101: 12753-12758.

12. Yu B, Bi L, Zheng B, Ji L, Chevalier D, et al. (2008) The FHA domain proteins DAWDLE in Arabidopsis and SNIP1 in humans act in small RNA biogenesis. Proc Natl Acad Sci U S A 105: 10073-10078.

13. Lee Y, Ahn C, Han J, Choi H, Kim J, et al. (2003) The nuclear RNase III Drosha initiates microRNA processing. Nature 425: 415-419.

14. Kurihara Y, Takashi Y, Watanabe Y (2006) The interaction between DCL1 and HYL1 is important for efficient and precise processing of pri-miRNA in plant microRNA biogenesis. RNA 12: 206-212.

15. Fang Y, Spector DL (2007) Identification of nuclear dicing bodies containing proteins for microRNA biogenesis in living Arabidopsis plants. Curr Biol 17: 818-823.

16. Gregory BD, O'Malley RC, Lister R, Urich MA, Tonti-Filippini J, et al. (2008) A link between RNA metabolism and silencing affecting Arabidopsis development. Dev Cell 14: 854-866.

17. Laubinger S, Sachsenberg T, Zeller G, Busch W, Lohmann JU, et al. (2008) Dual roles of the nuclear cap-binding complex and SERRATE in pre-mRNA splicing and microRNA processing in Arabidopsis thaliana. Proc Natl Acad Sci U S A 105: 8795-8800.

18. Yu B, Yang Z, Li J, Minakhina S, Yang M, et al. (2005) Methylation as a crucial step in plant microRNA biogenesis. Science 307: 932-935.

19. Yang Z, Ebright YW, Yu B, Chen X (2006) HEN1 recognizes 21-24 nt small RNA duplexes and deposits a methyl group onto the 2' OH of the 3' terminal nucleotide. Nucleic Acids Res 34: 667-675.

20. Yi R, Qin Y, Macara IG, Cullen BR (2003) Exportin-5 mediates the nuclear export of pre-microRNAs and short hairpin RNAs. Genes Dev 17: 3011-3016.

21. Lund E, Guttinger S, Calado A, Dahlberg JE, Kutay U (2004) Nuclear export of microRNA precursors. Science 303: 95-98.

22. Park MY, Wu G, Gonzalez-Sulser A, Vaucheret H, Poethig RS (2005) Nuclear processing and export of microRNAs in Arabidopsis. Proc Natl Acad Sci U S A 102: 3691-3696.

23. Megraw M, Baev V, Rusinov V, Jensen ST, Kalantidis K, et al. (2006) MicroRNA promoter element discovery in Arabidopsis. RNA 12: 1612-1619.

24. Kim YJ, Zheng B, Yu Y, Won SY, Mo B, et al. (2011) The role of Mediator in small and long noncoding RNA production in Arabidopsis thaliana. EMBO J 30: 814-822.

25. Xie Z, Khanna K, Ruan S (2010) Expression of microRNAs and its regulation in plants. Semin Cell Dev Biol 21: 790-797.

26. Xie Z, Kasschau KD, Carrington JC (2003) Negative feedback regulation of Dicer-Like1 in Arabidopsis by microRNA-guided mRNA degradation. Curr Biol 13: 784-789.

27. Nogueira FT, Chitwood DH, Madi S, Ohtsu K, Schnable PS, et al. (2009) Regulation of small RNA accumulation in the maize shoot apex. PLoS Genet 5: e1000320.

28. Vazquez F, Blevins T, Ailhas J, Boller T, Meins F, Jr. (2008) Evolution of Arabidopsis MIR genes generates novel microRNA classes. Nucleic Acids Res 36: 6429-6438.

29. Wu L, Zhou H, Zhang Q, Zhang J, Ni F, et al. (2010) DNA methylation mediated by a microRNA pathway. Mol Cell 38: 465-475.

30. Ebhardt HA, Fedynak A, Fahlman RP (2010) Naturally occurring variations in sequence length creates microRNA isoforms that differ in argonaute effector complex specificity. Silence 1: 12.

31. Rajagopalan R, Vaucheret H, Trejo J, Bartel DP (2006) A diverse and evolutionarily fluid set of microRNAs in Arabidopsis thaliana. Genes Dev 20: 3407-3425.

32. Peters L, Meister G (2007) Argonaute proteins: mediators of RNA silencing. Mol Cell 26: 611-623.

33. Parker JS, Barford D (2006) Argonaute: A scaffold for the function of short regulatory RNAs. Trends Biochem Sci 31: 622-630.

34. Yuan YR, Pei Y, Ma JB, Kuryavyi V, Zhadina M, et al. (2005) Crystal structure of A. aeolicus argonaute, a site-specific DNA-guided endoribonuclease, provides insights into RISC-mediated mRNA cleavage. Mol Cell 19: 405-419.

35. Parker JS, Roe SM, Barford D (2005) Structural insights into mRNA recognition from a PIWI domain-siRNA guide complex. Nature 434: 663-666.

36. Boland A, Huntzinger E, Schmidt S, Izaurralde E, Weichenrieder O (2011) Crystal structure of the MID-PIWI lobe of a eukaryotic Argonaute protein. Proc Natl Acad Sci U S A 108: 10466-10471.

37. Johnston M, Hutvagner G (2011) Posttranslational modification of Argonautes and their role in small RNA-mediated gene regulation. Silence 2: 5.

38. Iki T, Yoshikawa M, Nishikiori M, Jaudal MC, Matsumoto-Yokoyama E, et al. (2010) In vitro assembly of plant RNA-induced silencing complexes facilitated by molecular chaperone HSP90. Mol Cell 39: 282-291.

39. Ji L, Liu X, Yan J, Wang W, Yumul RE, et al. (2011) ARGONAUTE10 and ARGONAUTE1 regulate the termination of floral stem cells through two microRNAs in Arabidopsis. PLoS Genet 7: e1001358.

40. Havecker ER, Wallbridge LM, Hardcastle TJ, Bush MS, Kelly KA, et al. (2010) The Arabidopsis RNA-directed DNA methylation argonautes functionally diverge based on their expression and interaction with target loci. Plant Cell 22: 321-334.

41. Mallory A, Vaucheret H (2010) Form, function, and regulation of ARGONAUTE proteins. Plant Cell 22: 3879-3889.

42. Mi S, Cai T, Hu Y, Chen Y, Hodges E, et al. (2008) Sorting of small RNAs into Arabidopsis argonaute complexes is directed by the 5' terminal nucleotide. Cell 133: 116-127.

43. Takeda A, Iwasaki S, Watanabe T, Utsumi M, Watanabe Y (2008) The mechanism selecting the guide strand from small RNA duplexes is different among argonaute proteins. Plant Cell Physiol 49: 493-500.

44. Baumberger N, Baulcombe DC (2005) Arabidopsis ARGONAUTE1 is an RNA Slicer that selectively recruits microRNAs and short interfering RNAs. Proc Natl Acad Sci U S A 102: 11928-11933.

45. Ibrahim F, Rohr J, Jeong WJ, Hesson J, Cerutti H (2006) Untemplated oligoadenylation promotes degradation of RISC-cleaved transcripts. Science 314: 1893.

46. Souret FF, Kastenmayer JP, Green PJ (2004) AtXRN4 degrades mRNA in Arabidopsis and its substrates include selected miRNA targets. Mol Cell 15: 173-183.

47. Vaucheret H, Vazquez F, Crete P, Bartel DP (2004) The action of ARGONAUTE1 in the miRNA pathway and its regulation by the miRNA pathway are crucial for plant development. Genes Dev 18: 1187-1197.

48. Reinhart BJ, Weinstein EG, Rhoades MW, Bartel B, Bartel DP (2002) MicroRNAs in plants. Genes Dev 16: 1616-1626.

49. Kidner CA, Martienssen RA (2004) Spatially restricted microRNA directs leaf polarity through ARGONAUTE1. Nature 428: 81-84.

50. Kim J, Jung JH, Reyes JL, Kim YS, Kim SY, et al. (2005) microRNA-directed cleavage of ATHB15 mRNA regulates vascular development in Arabidopsis inflorescence stems. Plant J 42: 84-94.

51. Jung JH, Park CM (2007) MIR166/165 genes exhibit dynamic expression patterns in regulating shoot apical meristem and floral development in Arabidopsis. Planta 225: 1327-1338.

52. Carlsbecker A, Lee JY, Roberts CJ, Dettmer J, Lehesranta S, et al. (2010) Cell signalling by microRNA165/6 directs gene dose-dependent root cell fate. Nature 465: 316-321.

53. Brodersen P, Sakvarelidze-Achard L, Bruun-Rasmussen M, Dunoyer P, Yamamoto YY, et al. (2008) Widespread translational inhibition by plant miRNAs and siRNAs. Science 320: 1185-1190.

54. Aukerman MJ, Sakai H (2003) Regulation of flowering time and floral organ identity by a MicroRNA and its APETALA2-like target genes. Plant Cell 15: 2730-2741.

55. Chen X (2004) A microRNA as a translational repressor of APETALA2 in Arabidopsis flower development. Science 303: 2022-2025.

56. Gandikota M, Birkenbihl RP, Hohmann S, Cardon GH, Saedler H, et al. (2007) The miRNA156/157 recognition element in the 3' UTR of the Arabidopsis SBP box gene SPL3 prevents early flowering by translational inhibition in seedlings. Plant J 49: 683-693.

57. Lanet E, Delannoy E, Sormani R, Floris M, Brodersen P, et al. (2009) Biochemical evidence for translational repression by Arabidopsis microRNAs. Plant Cell 21: 1762-1768.

58. Montgomery TA, Yoo SJ, Fahlgren N, Gilbert SD, Howell MD, et al. (2008) AGO1-miR173 complex initiates phased siRNA formation in plants. Proc Natl Acad Sci U S A 105: 20055-20062.

59. Cuperus JT, Carbonell A, Fahlgren N, Garcia-Ruiz H, Burke RT, et al. (2010) Unique functionality of 22-nt miRNAs in triggering RDR6-dependent siRNA biogenesis from target transcripts in Arabidopsis. Nat Struct Mol Biol 17: 997-1003.

60. Wang XB, Jovel J, Udomporn P, Wang Y, Wu Q, et al. (2011) The 21-nucleotide, but not 22-nucleotide, viral secondary small interfering RNAs direct potent antiviral defense by two cooperative argonautes in Arabidopsis thaliana. Plant Cell 23: 1625-1638.

61. Morel JB, Godon C, Mourrain P, Beclin C, Boutet S, et al. (2002) Fertile hypomorphic ARGONAUTE (ago1) mutants impaired in post-transcriptional gene silencing and virus resistance. Plant Cell 14: 629-639.

62. Qu F, Ye X, Morris TJ (2008) Arabidopsis DRB4, AGO1, AGO7, and RDR6 participate in a DCL4-initiated antiviral RNA silencing pathway negatively regulated by DCL1. Proc Natl Acad Sci U S A 105: 14732-14737.

63. Zhang X, Yuan YR, Pei Y, Lin SS, Tuschl T, et al. (2006) Cucumber mosaic virus-encoded 2b suppressor inhibits Arabidopsis Argonaute1 cleavage activity to counter plant defense. Genes Dev 20: 3255-3268.

64. Lynn K, Fernandez A, Aida M, Sedbrook J, Tasaka M, et al. (1999) The PINHEAD/ZWILLE gene acts pleiotropically in Arabidopsis development and has overlapping functions with the ARGONAUTE1 gene. Development 126: 469-481.

65. Moussian B, Schoof H, Haecker A, Jurgens G, Laux T (1998) Role of the ZWILLE gene in the regulation of central shoot meristem cell fate during Arabidopsis embryogenesis. EMBO J 17: 1799-1809.

66. Mallory AC, Hinze A, Tucker MR, Bouche N, Gasciolli V, et al. (2009) Redundant and specific roles of the ARGONAUTE proteins AGO1 and ZLL in development and small RNA-directed gene silencing. PLoS Genet 5: e1000646.

67. Zhu H, Hu F, Wang R, Zhou X, Sze SH, et al. (2011) Arabidopsis Argonaute10 specifically sequesters miR166/165 to regulate shoot apical meristem development. Cell 145: 242-256.

68. Borges F, Pereira PA, Slotkin RK, Martienssen RA, Becker JD (2011) MicroRNA activity in the Arabidopsis male germline. J Exp Bot 62: 1611-1620.

69. Zhang X, Zhao H, Gao S, Wang WC, Katiyar-Agarwal S, et al. (2011) Arabidopsis Argonaute 2 regulates innate immunity via miRNA393(*)-mediated silencing of a Golgi-localized SNARE gene, MEMB12. Mol Cell 42: 356-366.

70. Jaubert M, Bhattacharjee S, Mello AF, Perry KL, Moffett P (2011) ARGONAUTE2 mediates RNA-silencing antiviral defenses against Potato virus X in Arabidopsis. Plant Physiol 156: 1556-1564.

71. Harvey JJ, Lewsey MG, Patel K, Westwood J, Heimstadt S, et al. (2011) An antiviral defense role of AGO2 in plants. PLoS One 6: e14639.

72. Montgomery TA, Howell MD, Cuperus JT, Li D, Hansen JE, et al. (2008) Specificity of ARGONAUTE7-miR390 interaction and dual functionality in TAS3 trans-acting siRNA formation. Cell 133: 128-141.

73. Onodera Y, Haag JR, Ream T, Costa Nunes P, Pontes O, et al. (2005) Plant nuclear RNA polymerase IV mediates siRNA and DNA methylation-dependent heterochromatin formation. Cell 120: 613-622.

74. Kirino Y, Mourelatos Z (2007) 2'-O-methyl modification in mouse piRNAs and its methylase. Nucleic Acids Symp Ser (Oxf): 417-418.

75. Kirino Y, Mourelatos Z (2007) The mouse homolog of HEN1 is a potential methylase for Piwi-interacting RNAs. RNA 13: 1397-1401.

76. Kamminga LM, Luteijn MJ, den Broeder MJ, Redl S, Kaaij LJ, et al. (2010) Hen1 is required for oocyte development and piRNA stability in zebrafish. EMBO J 29: 3688-3700.

77. Horwich MD, Li C, Matranga C, Vagin V, Farley G, et al. (2007) The Drosophila RNA methyltransferase, DmHen1, modifies germline piRNAs and single-stranded siRNAs in RISC. Curr Biol 17: 1265-1272.

78. Saito K, Sakaguchi Y, Suzuki T, Suzuki T, Siomi H, et al. (2007) Pimet, the Drosophila homolog of HEN1, mediates 2'-O-methylation of Piwi-interacting RNAs at their 3' ends. Genes Dev 21: 1603-1608.

79. Li J, Yang Z, Yu B, Liu J, Chen X (2005) Methylation protects miRNAs and siRNAs from a 3'-end uridylation activity in Arabidopsis. Curr Biol 15: 1501-1507.

80. Abe M, Yoshikawa T, Nosaka M, Sakakibara H, Sato Y, et al. (2010) WAVY LEAF1, an ortholog of Arabidopsis HEN1, regulates shoot development by maintaining MicroRNA and trans-acting small interfering RNA accumulation in rice. Plant Physiol 154: 1335-1346.

81. Tkaczuk KL, Obarska A, Bujnicki JM (2006) Molecular phylogenetics and comparative modeling of HEN1, a methyltransferase involved in plant microRNA biogenesis. BMC Evol Biol 6: 6.

82. Huang Y, Ji L, Huang Q, Vassylyev DG, Chen X, et al. (2009) Structural insights into mechanisms of the small RNA methyltransferase HEN1. Nature 461: 823-827.

83. Vilkaitis G, Plotnikova A, Klimasauskas S (2010) Kinetic and functional analysis of the small RNA methyltransferase HEN1: the catalytic domain is essential for preferential modification of duplex RNA. RNA 16: 1935-1942.

84. Yu B, Chapman EJ, Yang Z, Carrington JC, Chen X (2006) Transgenically expressed viral RNA silencing suppressors interfere with microRNA methylation in Arabidopsis. FEBS Lett 580: 3117-3120.

85. Lozsa R, Csorba T, Lakatos L, Burgyan J (2008) Inhibition of 3' modification of small RNAs in virus-infected plants require spatial and temporal co-expression of small RNAs and viral silencing-suppressor proteins. Nucleic Acids Res 36: 4099-4107.

86. Jamous RM, Boonrod K, Fuellgrabe MW, Ali-Shtayeh MS, Krczal G, et al. (2011) The helper component-proteinase of the Zucchini yellow mosaic virus inhibits the Hua Enhancer 1 methyltransferase activity in vitro. J Gen Virol 92: 2222-2226.

87. Yu B, Bi L, Zhai J, Agarwal M, Li S, et al. (2010) siRNAs compete with miRNAs for methylation by HEN1 in Arabidopsis. Nucleic Acids Res 38: 5844-5850.

88. Kurth HM, Mochizuki K (2009) 2'-O-methylation stabilizes Piwi-associated small RNAs and ensures DNA elimination in Tetrahymena. RNA 15: 675-685.

89. Mochizuki K, Gorovsky MA (2004) Conjugation-specific small RNAs in Tetrahymena have predicted properties of scan (scn) RNAs involved in genome rearrangement. Genes Dev 18: 2068-2073.

90. Jain R, Shuman S (2010) Bacterial Hen1 is a 3' terminal RNA ribose 2'-O-methyltransferase component of a bacterial RNA repair cassette. RNA 16: 316-323.

91. Mui Chan C, Zhou C, Brunzelle JS, Huang RH (2009) Structural and biochemical insights into 2'-O-methylation at the 3'-terminal nucleotide of RNA by Hen1. Proc Natl Acad Sci U S A 106: 17699-17704.

92. Chan CM, Zhou C, Huang RH (2009) Reconstituting bacterial RNA repair and modification in vitro. Science 326: 247.

93. Ameres SL, Horwich MD, Hung JH, Xu J, Ghildiyal M, et al. (2010) Target RNA-directed trimming and tailing of small silencing RNAs. Science 328: 1534-1539.

94. Molnar A, Schwach F, Studholme DJ, Thuenemann EC, Baulcombe DC (2007) miRNAs control gene expression in the single-cell alga Chlamydomonas reinhardtii. Nature 447: 1126-1129.

95. Ibrahim F, Rymarquis LA, Kim EJ, Becker J, Balassa E, et al. (2010) Uridylation of mature miRNAs and siRNAs by the MUT68 nucleotidyltransferase promotes their degradation in Chlamydomonas. Proc Natl Acad Sci U S A 107: 3906-3911.

96. Ramachandran V, Chen X (2008) Degradation of microRNAs by a family of exoribonucleases in Arabidopsis. Science 321: 1490-1492.

97. Wang Y, Juranek S, Li H, Sheng G, Wardle GS, et al. (2009) Nucleation, propagation and cleavage of target RNAs in Ago silencing complexes. Nature 461: 754-761.

98. Baccarini A, Chauhan H, Gardner TJ, Jayaprakash AD, Sachidanandam R, et al. (2011) Kinetic analysis reveals the fate of a microRNA following target regulation in mammalian cells. Curr Biol 21: 369-376.

99. Franco-Zorrilla JM, Valli A, Todesco M, Mateos I, Puga MI, et al. (2007) Target mimicry provides a new mechanism for regulation of microRNA activity. Nat Genet 39: 1033-1037.

100. Rubio-Somoza I, Manavella PA (2011) Mimicry technology: suppressing small RNA activity in plants. Methods Mol Biol 732: 131-137.

101. Todesco M, Rubio-Somoza I, Paz-Ares J, Weigel D (2010) A collection of target mimics for comprehensive analysis of microRNA function in Arabidopsis thaliana. PLoS Genet 6: e1001031.

102. Chatterjee S, Grosshans H (2009) Active turnover modulates mature microRNA activity in Caenorhabditis elegans. Nature 461: 546-549.

103. Gy I, Gasciolli V, Lauressergues D, Morel JB, Gombert J, et al. (2007) Arabidopsis FIERY1, XRN2, and XRN3 are endogenous RNA silencing suppressors. Plant Cell 19: 3451-3461.

104. Ruby JG, Jan C, Player C, Axtell MJ, Lee W, et al. (2006) Large-scale sequencing reveals 21U-RNAs and additional microRNAs and endogenous siRNAs in C. elegans. Cell 127: 1193-1207.

105. Landgraf P, Rusu M, Sheridan R, Sewer A, Iovino N, et al. (2007) A mammalian microRNA expression atlas based on small RNA library sequencing. Cell 129: 1401-1414.

106. Wyman SK, Knouf EC, Parkin RK, Fritz BR, Lin DW, et al. (2011) Post-transcriptional generation of miRNA variants by multiple nucleotidyl transferases contributes to miRNA transcriptome complexity. Genome Res 21: 1450-1461.

107. Katoh T, Sakaguchi Y, Miyauchi K, Suzuki T, Kashiwabara S, et al. (2009) Selective stabilization of mammalian microRNAs by 3' adenylation mediated by the cytoplasmic poly(A) polymerase GLD-2. Genes Dev 23: 433-438.

108. Wang L, Eckmann CR, Kadyk LC, Wickens M, Kimble J (2002) A regulatory cytoplasmic poly(A) polymerase in Caenorhabditis elegans. Nature 419: 312-316.

109. Claycomb JM, Batista PJ, Pang KM, Gu W, Vasale JJ, et al. (2009) The Argonaute CSR-1 and its 22G-RNA cofactors are required for holocentric chromosome segregation. Cell 139: 123-134.

110. van Wolfswinkel JC, Claycomb JM, Batista PJ, Mello CC, Berezikov E, et al. (2009) CDE-1 affects chromosome segregation through uridylation of CSR-1-bound siRNAs. Cell 139: 135-148.

111. Gu W, Shirayama M, Conte D, Jr., Vasale J, Batista PJ, et al. (2009) Distinct argonaute-mediated 22G-RNA pathways direct genome surveillance in the C. elegans germline. Mol Cell 36: 231-244.

112. Lu S, Sun YH, Chiang VL (2009) Adenylation of plant miRNAs. Nucleic Acids Res 37: 1878-1885.

113. Chen Y, Sinha K, Perumal K, Reddy R (2000) Effect of 3' terminal adenylic acid residue on the uridylation of human small RNAs in vitro and in frog oocytes. RNA 6: 1277-1288.

114. Bail S, Swerdel M, Liu H, Jiao X, Goff LA, et al. (2010) Differential regulation of microRNA stability. RNA 16: 1032-1039.

115. Huang J, Wang F, Argyris E, Chen K, Liang Z, et al. (2007) Cellular microRNAs contribute to HIV-1 latency in resting primary CD4+ T lymphocytes. Nat Med 13: 1241-1247.

116. Yu J, Wang F, Yang GH, Wang FL, Ma YN, et al. (2006) Human microRNA clusters: genomic organization and expression profile in leukemia cell lines. Biochem Biophys Res Commun 349: 59-68.

117. Kim YK, Yeo J, Ha M, Kim B, Kim VN (2011) Cell Adhesion-Dependent Control of MicroRNA Decay. Mol Cell 43: 1005-1014.

118. Sethi P, Lukiw WJ (2009) Micro-RNA abundance and stability in human brain: specific alterations in Alzheimer's disease temporal lobe neocortex. Neurosci Lett 459: 100-104.

119. Tang F, Hajkova P, O'Carroll D, Lee C, Tarakhovsky A, et al. (2008) MicroRNAs are tightly associated with RNA-induced gene silencing complexes in vivo. Biochem Biophys Res Commun 372: 24-29.

120. Diederichs S, Haber DA (2007) Dual role for argonautes in microRNA processing and posttranscriptional regulation of microRNA expression. Cell 131: 1097-1108.

121. Winter J, Diederichs S (2011) Argonaute proteins regulate microRNA stability: Increased microRNA abundance by Argonaute proteins is due to microRNA stabilization. RNA Biol 8(6): 21941127.

122. Yu Z, Hecht NB (2008) The DNA/RNA-binding protein, translin, binds microRNA122a and increases its in vivo stability. J Androl 29: 572-579.

123. Petrova Kruglova NS, Meschaninova MI, Venyaminova AG, Zenkova MA, Vlassov VV, et al. (2010) 2'-O-methyl-modified anti-MDR1 fork-siRNA duplexes exhibiting high nuclease resistance and prolonged silencing activity. Oligonucleotides 20: 297-308.

124. Zhou J, Rossi JJ (2011) Current progress in the development of RNAi-based therapeutics for HIV-1. Gene Ther 18: 1134-1138.

125. Zhang L, Hou D, Chen X, Li D, Zhu L, et al. (2011) Exogenous plant MIR168a specifically targets mammalian LDLRAP1: evidence of cross-kingdom regulation by microRNA. Cell Res doi: 10.1038/cr.2011.158

126. Weigel D, Jurgens G (2002) Stem cells that make stems. Nature 415: 751-754.

127. Laux T (2003) The stem cell concept in plants: a matter of debate. Cell 113: 281-283.

128. Mayer KF, Schoof H, Haecker A, Lenhard M, Jurgens G, et al. (1998) Role of WUSCHEL in regulating stem cell fate in the Arabidopsis shoot meristem. Cell 95: 805-815.

129. Ha CM, Jun JH, Fletcher JC (2010) Shoot apical meristem form and function. Curr Top Dev Biol 91: 103-140.

130. Fletcher JC (2002) Shoot and floral meristem maintenance in arabidopsis. Annu Rev Plant Biol 53: 45-66.

131. Causier B, Schwarz-Sommer Z, Davies B (2010) Floral organ identity: 20 years of ABCs. Semin Cell Dev Biol 21: 73-79.

132. Lenhard M, Bohnert A, Jurgens G, Laux T (2001) Termination of stem cell maintenance in Arabidopsis floral meristems by interactions between WUSCHEL and AGAMOUS. Cell 105: 805-814.

133. Lohmann JU, Hong RL, Hobe M, Busch MA, Parcy F, et al. (2001) A molecular link between stem cell regulation and floral patterning in Arabidopsis. Cell 105: 793-803.

134. Sakai H, Medrano LJ, Meyerowitz EM (1995) Role of SUPERMAN in maintaining Arabidopsis floral whorl boundaries. Nature 378: 199-203.

135. Prunet N, Morel P, Thierry AM, Eshed Y, Bowman JL, et al. (2008) REBELOTE, SQUINT, and ULTRAPETALA1 function redundantly in the temporal regulation of floral meristem termination in Arabidopsis thaliana. Plant Cell 20: 901-919.

136. Sakai H, Krizek BA, Jacobsen SE, Meyerowitz EM (2000) Regulation of SUP expression identifies multiple regulators involved in arabidopsis floral meristem development. Plant Cell 12: 1607-1618.

137. Sun B, Xu Y, Ng KH, Ito T (2009) A timing mechanism for stem cell maintenance and differentiation in the Arabidopsis floral meristem. Genes Dev 23: 1791-1804.

138. Lee JY, Baum SF, Alvarez J, Patel A, Chitwood DH, et al. (2005) Activation of CRABS CLAW in the Nectaries and Carpels of Arabidopsis. Plant Cell 17: 25-36.

139. Alvarez J, Smyth DR (1999) CRABS CLAW and SPATULA, two Arabidopsis genes that control carpel development in parallel with AGAMOUS. Development 126: 2377-2386.

140. Fletcher JC (2001) The ULTRAPETALA gene controls shoot and floral meristem size in Arabidopsis. Development 128: 1323-1333.

141. Carles CC, Choffnes-Inada D, Reville K, Lertpiriyapong K, Fletcher JC (2005) ULTRAPETALA1 encodes a SAND domain putative transcriptional regulator that controls shoot and floral meristem activity in Arabidopsis. Development 132: 897-911.

142. Smith MR, Willmann MR, Wu G, Berardini TZ, Moller B, et al. (2009) Cyclophilin 40 is required for microRNA activity in Arabidopsis. Proc Natl Acad Sci U S A 106: 5424-5429.

143. Zhao L, Kim Y, Dinh TT, Chen X (2007) miR172 regulates stem cell fate and defines the inner boundary of APETALA3 and PISTILLATA expression domain in Arabidopsis floral meristems. Plant J 51: 840-849.

144. Bartrina I, Otto E, Strnad M, Werner T, Schmulling T (2011) Cytokinin regulates the activity of reproductive meristems, flower organ size, ovule formation, and thus seed yield in Arabidopsis thaliana. Plant Cell 23: 69-80.

145. Sundberg E, Ostergaard L (2009) Distinct and dynamic auxin activities during reproductive development. Cold Spring Harb Perspect Biol 1: a001628.

2. CHAPTER I: *ARGONAUTE10* and *ARGONAUTE1* Regulate the Termination of Floral Stem Cells through Two MicroRNAs in *Arabidopsis*

Abstract

Stem cells are crucial in morphogenesis in plants and animals. Much is known about the mechanisms that maintain stem cell fates or trigger their terminal differentiation. However, little is known about how developmental time impacts stem cell fates. Using *Arabidopsis* floral stem cells as a model, we show that stem cells can undergo precise temporal regulation governed by mechanisms that are distinct from, but integrated with, those that specify cell fates. We show that two microRNAs, miR172 and miR165/166, through targeting *APETALA2* and homeodomain-leucine zipper (HD-Zip) genes, respectively, regulate the temporal program of floral stem cells. In particular, we reveal a role of the HD-Zip genes, previously known to specify lateral organ polarity, in stem cell termination. Both reduction in HD-Zip expression by over expression of miR165/166 and mis-expression of HD-Zip genes by rendering them resistant to miR165/166 lead to prolonged floral stem cell activity, indicating that the expression of HD-Zip genes needs to be precisely controlled to achieve floral stem cell termination. We also show that both the ubiquitously expressed *ARGONAUTE1* (*AGO1*) gene and its homolog *AGO10*, which exhibits highly restricted spatial expression patterns, are required to maintain the correct

temporal program of floral stem cells. We provide evidence that AGO10, like AGO1, associates with miR172 and miR165/166 *in vivo* and exhibits “slicer” activity *in vitro*. Despite the common biological function and similar biochemical activities, *AGO1* and *AGO10* exert different effects on miR165/166 *in vivo*. This work establishes a network of microRNAs and transcription factors governing the temporal program of floral stem cells and sheds light on the relationships between different *AGO* genes, which tend to exist in gene families in multicellular organisms.

Introduction

Stem cells are key to morphogenesis in multicellular organisms and understanding the mechanisms governing their maintenance or termination is a major goal in developmental biology. In plants, small populations of pluripotent stem cells are found in meristems located at the tips of roots, shoots, or developing flowers. The stem cells in the shoot apical meristem (SAM) continuously provide new cells for organogenesis to give rise to the entire above-ground portion of the plant. The SAM generates leaf primordia during vegetative growth and, after floral transition, produces floral meristems on its flanks. *Arabidopsis* floral meristems produce four concentric whorls of floral organs of fixed numbers, namely four sepals, four petals, six stamens and two fused carpels. In contrast to the SAM, floral meristems are genetically programmed to terminate after the primordia of the female reproductive organs (carpels) are formed (reviewed in [1]). The termination of floral stem cells is temporally

precisely regulated to coincide with the formation of the female reproductive organs to ensure successful reproduction of plants. This property of floral stem cells, i.e. determinacy, offers an opportunity to understand the temporal regulation of stem cell maintenance.

A key factor in stem cell maintenance in plants is the *WUSCHEL* (*WUS*) gene encoding a homeodomain transcription factor. In both the SAM and floral meristems, *WUS* is expressed in a small group of cells named the organizing center (OC) located underneath the stem cells [2]. The OC signals to the overlying stem cells to maintain their “stemness”. In loss-of-function *wus* mutants, the stem cells in both the SAM and floral meristems terminate precociously. For example, flowers of the null *wus-1* mutant lack a full complement of floral organs and terminate in a central stamen. *WUS* expression commences as soon as the floral meristem is formed (at stage 1; stages according to [3]). By stage 6, when the carpel primordia are formed, *WUS* expression is shut off [4], and this temporally precise repression of *WUS* expression underlies the proper termination of floral stem cells.

The temporal regulation of *WUS* expression requires at least two transcription factors with opposing activities, AGAMOUS (AG) and APETALA2 (AP2), which are best known for their roles in the specification of reproductive and perianth organ identities, respectively, in flower development (reviewed in [5]). The MADS-domain protein AG promotes floral meristem termination by repressing *WUS* expression at stage 6 [6,7]. In an *ag* null mutant, such as *ag-1,*

WUS expression persists throughout flower development [6,7] and the floral meristems lose determinacy to result in a flowers-within-flower phenotype [8]. Flowers of the *ag-1 wus-1* double mutant resemble *wus-1* flowers, indicating that *AG* causes floral stem cell termination by repressing *WUS* expression [2]. While *AG* acts to terminate floral stem cells, *AP2*, an AP2-domain containing transcription factor gene [9] regulated by the microRNA (miRNA) miR172 [10,11], promotes stem cell maintenance. In plants that express the miR172-resistant *AP2* cDNA *AP2m3* [11] from the *AP2* promoter, flowers have numerous stamens that are continuously produced by indeterminate floral meristems [12]. *WUS* expression is prolonged in *AP2p::AP2m3* flowers, and the prolonged *WUS* expression underlies the indeterminate phenotype because *wus-1* is completely epistatic to *AP2m3* [12]. *AP2* is known to repress the transcription of *AG* in the outer two floral whorls [13]. De-repressed *AP2* in *AP2m3* plants causes a moderate reduction in *AG* mRNA levels in the center of the floral meristem and this partially underlies the stem cell termination defects of *AP2m3* flowers [12]. De-repressed *AP2* also compromises floral stem cell termination in an *AG*-independent manner, which is reflected by the stronger phenotypes of *AP2m3 ag-1* relative to *ag-1* [12].

Small RNAs of 21-24 nucleotides (nt) are sequence-specific guides in RNA silencing at the transcriptional and posttranscriptional levels in plants (reviewed in [14]). ARGONAUTE (AGO) proteins associate with small RNAs and serve as effectors in RNA silencing (reviewed in [15]). Different AGO proteins

associate with, and mediate the functions of, distinct types of small RNAs. Among the ten AGO proteins in *Arabidopsis*, AGO1, 2, 4, 5, 6, 7, and 9 have been shown to bind specific sets of endogenous small RNAs [16,17,18,19]. AGO1, the founding member of the family, binds most miRNAs, trans-acting siRNAs (tasi-RNAs), and transgene siRNAs and exhibits “slicer” activity, an endonucleolytic activity that precisely cleaves target mRNAs [20]. ZWILLE (ZLL)/PINHEAD (PNH), which will be hereafter referred to as AGO10 (unless specific alleles or constructs are referred to), is most related to AGO1 among the ten *Arabidopsis* AGO proteins [21]. While *AGO1* is ubiquitously expressed [22], *AGO10* expression is restricted to meristems, the vasculature, and adaxial sides of lateral organ primordia [23,24]. *AGO10* was initially identified as a factor required for SAM maintenance [23,24,25]. Null mutations in *AGO10* lead to the absence of a SAM with incomplete penetrance. Examination of several miRNA target genes at the mRNA and protein levels in *ago10* mutants implicated *AGO10* in miRNA-mediated translational repression [26,27]. However, the lack of knowledge of the small RNA binding and enzymatic properties of AGO10 has hindered the understanding of the molecular mechanisms of action of AGO10 in development and in RNA silencing, especially in relationship to AGO1.

In our previous studies, we found that four genes with potential roles in RNA metabolism, *HUA1*, *HUA2*, *HUA ENHANCER2* (*HEN2*), and *HEN4*, promote *AG* expression [28]. Loss-of-function mutations in any one gene do not sufficiently compromise *AG* expression or flower development, but double or

triple mutants have reduced *AG* expression and phenotypes indicative of partial loss-of-function of *AG*. In a genetic screen in the *hua1 hua2* background and in two separate genetic screens in backgrounds compromised for *AG* expression or function, we isolated *ago10* mutations with defects in floral stem cell termination. We also establish a role of *AGO1* in floral stem cell termination. Genetic evidence suggests that *AGO10* acts to terminate floral stem cells in part by facilitating miR172-mediated repression of *AP2*. We demonstrate the HD-Zip genes *PHABULOSA* (*PHB*) and *PHAVOLUTA* (*PHV*), targets of miR165/166, play a previously unknown yet crucial role in the proper termination of floral stem cells. Like AGO1, AGO10 associates with miR172 and miR165/166 *in vivo* and exhibits slicing activity *in vitro*. Intriguingly, AGO1 and AGO10 exert opposite effects on miR165/166 *in vivo*, yet both contribute to the termination of floral stem cells.

Results

AGO10 promotes floral determinacy

To identify genes with functions similar to those of *AG* in promoting stamen/carpel identities and terminating floral stem cells, we performed ethyl methanesulfonate (EMS) mutagenesis to screen for enhancers of the *hua1-1 hua2-1* double mutant, which will be hereafter referred to as *hua1 hua2*. *hua1 hua2* flowers are largely normal except that the gynoecia are enlarged at the apical end (Figure 2.1A). The floral phenotypes of *hua1 hua2* are sensitive to the dosage of functional *AG*. Combination of *ag-1/+* or *ag-4* with *hua1 hua2*

drastically enhances the homeotic and floral determinacy defects of *hua1 hua2* [29]. Accordingly, a genetic screen in the *hua1 hua2* background effectively identified genes that promote reproductive organ identity specification or floral determinacy [28,30,31,32,33]. Among the new mutations we isolated in this screen were *hua enhancer6* (*hen6*) and *hua enhancer7* (*hen7*), recessive alleles in two genes.

hen6 enhanced the floral phenotypes of *hua1 hua2* in terms of both reproductive organ identities and floral determinacy. While *hua1 hua2* flowers have stamens in the third whorl, petaloid stemens were observed in *hua1 hua2 hen6* flowers (Figure 2.1A,B; Figure 2.9H), indicating a defect in stamen identity specification. In addition, *hua1 hua2 hen6* gynoecia were much shorter than those of *hua1 hua2* and appeared bulged or heart-shaped (Figure 2.1B,D,E). Extra floral organs internal to the fourth whorl carpels were present in *hua1 hua2 hen6* but not in *hua1 hua2* gynoecia; these extra organs were generated from an indeterminate floral meristem as observed in longitudinal sections of flowers (Figure 2.1G,H; Table 2.1). *hen6* was mapped to the BAC MQD19 on chromosome 5, from which *AGO10* was selected as a candidate gene for sequencing. A C-to-T transition leading to the substitution of leucine (L) 674, which is highly conserved among all *Arabidopsis* AGO proteins, by phenylalanine (F) was found in *AGO10* (Figure 2.7A,B). The homeotic and floral determinacy defects of *hua1 hua2 hen6* were rescued by *AGO10* genomic DNA and the fully rescued plants appeared morphologically identical to *hua1 hua2* (Figure 2.1I).

Therefore, *hen6* was renamed *ago10-12*. While many previously isolated *ago10* alleles show SAM defects with incomplete penetrance, the *ago10-12* single mutant had no obvious SAM defects, suggesting that the L674F mutation does not completely compromise *AGO10* function.

hen7 strongly enhanced *hua1 hua2* such that *hua1 hua2 hen7* flowers resembled those of *ag* null mutants. Stamens were transformed to petals and the floral meristems failed to terminate (Figure 2.1A,C). Rough mapping showed that *hen7* was linked to *AG*, and sequencing of *AG* revealed a G-to-A mutation resulting in an E-to-K substitution at the 144th amino acid (Figure 2.7A). To show that *AG* could rescue the *hen7* mutant phenotypes, we utilized the fertile *hua1 hen7* double mutant. *hua1 hen7* flowers had no organ identity defects, but the gynoecia were heart-shaped with secondary floral organs inside the primary carpels (Figure 2.1F; Table 2.1). The floral determinacy defects of *hua1 hen7* flowers could be rescued by a *pAG::AG-GFP* construct (Figure 2.1F). Therefore, *hen7* is an *ag* allele, which we named *ag-10*. The *ag-10* single mutant flowers had a normal complement of floral organs as in wild type (Figure 2.2A); as such, it is the weakest *ag* allele known to date. Most siliques on an *ag-10* plant, however, can be distinguished from wild type by their curvature (Figure 2.2D). A small proportion of siliques were slightly bulged with additional organs inside (Figure 2.2D, Table 2.1). This contrasted with *hua1 ag-10* plants, in which all siliques were heart-shaped with internal floral organs inside (Table 2.1).

Therefore, *ag-10* was mildly defective in floral determinacy and this defect was drastically enhanced by *hua1*.

We performed another EMS screen in the *hua1 ag-10* background to identify mutants with enhanced floral determinacy defects. One mutant had a flowers-within-flower phenotype reminiscent of *ag* null mutants. After removal of the *hua1* mutation by crossing, the double mutant of *ag-10* and the enhancer mutation still exhibited strong floral determinacy defects; all siliques on the double mutant were severely bulged and ectopic flowers were present inside the primary carpels (Figure 2.2B,E; Table 2.1). Flowers of the double mutant did not exhibit any homeotic transformation and were fertile. We noticed that seedlings of the double mutant exhibited SAM defects at a low penetrance similar to *ago10* alleles. This, together with the mapping of the mutation to the top of chromosome 5, led us to suspect that the enhancer mutation was in *AGO10*. Sequencing *AGO10* from the double mutant identified a G-to-A mutation that introduced a premature stop codon at the end of the second exon of *AGO10* (Figure 2.7A). Introduction of a *pAGO10::AGO10-FLAG* construct into the double mutant fully rescued the floral determinacy defect (Figure 2.2C). Therefore, we named this mutation *ago10-13*. From longitudinal sections, it was clear that the floral meristems persisted well beyond stage 6 in all *ag-10 ago10-13* flowers but not in most *ag-10* flowers (Figure 2.2G,H), suggesting that *AGO10* is crucial for floral stem cell termination. Like other *ago10* alleles, the gynoecia and siliques of the *ago10-13* single mutant were shorter and wider than wild type (Figure 2.9A,B).

In an EMS screen in the *ag-10* background, we identified yet another *ago10* allele, *ago10-14*, which harbored a G-to-A mutation that changes the 731th amino acid from aspartic acid to asparagine (Figure 2.7A). Flowers of *ag-10 ago10-14* resembled those of *ag-10 ago10-13* in that the gynoecia were buldged (data not shown). The following genetic and molecular studies were performed mainly with *ago10-12* and *ago10-13* alleles.

Given that *ago10-12* enhanced *hua1 hua2* and both *ago10-13* and *ago10-14* enhanced *ag-10* in terms of floral determinacy, we conclude that *AGO10* promotes floral stem cell termination. Consistent with such a role, the YFP-ZLL fusion protein from the functional *pZLL::YFP-ZLL* transgene [38] was found in the center of stages 5-6 floral meristems by immunolocalization (Figure 2.3A). By stage 7, YFP-ZLL was found on the adaxial side of carpel primordia (Figure 2.3B).

AGO10 terminates floral stem cells through repression of _WUS_ expression

To investigate how *AGO10* regulates floral stem cells, we examined the genetic interactions between *ago10* alleles and mutations in key stem cell regulators. In *wus-1*, the floral meristems are terminated prematurely, resulting in incomplete flowers with four sepals, four petals, and typically a single stamen [2] (Figure 2.9E). *hua1 hua2 ago10-12 wus-1* flowers had identical phenotypes to those of *wus-1* in terms of floral determinacy (Figure 2.4A), indicating that *wus-1* was epistatic to *hua1 hua2 ago10-12*. Unlike *wus-1* (Figure 2.9E), the single stamen in *hua1 hua2 ago10-12 wus-1* was petaloid as in *hua1 hua2 ago10-12*

(Figure 2.4A), indicating that the homeotic transformation of stamens into petaloid stamens in *hua1 hua2 ago10-12* was independent of *WUS*. Similarly, *wus-1* was epistatic to *ag-10 ago10-13* in terms of floral determinacy (data not shown). Therefore, *AGO10* acts through *WUS* to regulate floral meristem activity. This conclusion was also supported by the prolonged expression of *WUS* in floral meristems caused by *ago10* mutations. Using *in situ* hybridization, we found that *WUS* expression in *hua1 hua2 ago10-12* flowers persisted well beyond floral stage 6, when *WUS* expression was terminated in *hua1 hua2* flowers (Figure 2.3E,F). Similarly, *WUS* expression was detected in very old *ag-10 ago10-13* but not *ag-10* flowers (Figure 2.3G,H).

CLV3 controls the spatial domain of *WUS* expression and the size of the stem cell domain [34]. *clv3-1* flowers contain extra floral organs of all types, particularly stamens and carpels, due to enlarged floral meristems [35]. The combination of *hua1 hua2 ago10-12* and *clv3-1* had a synergistic effect on floral determinacy. The gynoecia of the quadruple mutant generated a massive amount of stigmatic tissue bursting out of the primary carpels (Figure 2.9G). Similar phenotypes were observed for *ag-10 ago10-13 clv3-1* flowers (data not shown), implying that *AGO10* and *CLV3* act largely independently.

Since *AG* is crucial in the termination of floral stem cells, we evaluated the relationship between *AG* and *AGO10* through extensive genetic interaction studies. We first introduced the null *ag-1* allele into *hua1 hua2 ago10-12*. The quadruple mutant flowers were initially similar to *ag-1* flowers, but the meristems

continued to develop and appeared fasciated in old flowers (data not shown). Given that *ago10-12* was a weak allele, we next combined the stronger *ago10* alleles *pnh-1* [25] or *ago10-13* with *ag-1*. Most flowers of the *ag-1 pnh-1* and *ag-1 ago1-13* double mutants appeared more fasciated than *ag-1* flowers (Figure 2.4B,C; data not shown). The mild enhancement implies that *AGO10* acts through an *AG* pathway to repress *WUS* expression but that *AGO10* also has an *AG*-independent function in floral stem cell regulation. We conducted *in situ* hybridization to examine the patterns of *AG* expression in *ag-10* and *ag-10 ago10-13* flowers. As expected, *AG* transcripts were detected in the inner two whorls of *ag-10* and *ag-10 ago10-13* floral meristems (Figure 2.3C,D). Therefore, *ago10-13* did not affect the spatial domain of *AG* expression or lead to obvious changes in *AG* mRNA levels in floral meristems.

AGO1 is also required for floral stem cell termination

Since *AGO1* is most closely related to *AGO10* among the ten *Arabidopsis AGO* genes, we sought to determine whether *AGO1* is also required for floral stem cell termination. We introduced the partial loss-of-function *ago1-11* mutation [36] into *hua1 hua2* and *ag-10*. The infertile *ago1-11* flowers develop all four types of floral organs, although the organs are abnormal in morphology (Figure 2.2J; Figure 2.9C). In *hua1 hua2 ago1-11* flowers, either the gynoecia were severely bulged or the carpels were completely unfused with ectopic flowers developing internal to the primary carpels (Figure 2.2K). Similarly, indeterminate

phenotypes were observed in the *ag-10 ago1-11* double mutant (Figure 2.2L). Therefore, *AGO1*, like *AGO10*, is required for floral stem cell termination.

Genetic studies conducted by others as well as by ourselves show that *AGO1* and *AGO10* have overlapping functions in terminating floral meristems. First, it was previously shown that combining the strong *ago1-7* and *pnh-2* (an *ago10* allele) alleles resulted in embryo lethality [23]. But *ago1-7*/+ *pnh-2*/*pnh-2* and *ago1-7*/*ago1-7 pnh-2*/+ flowers showed an increase in the number of floral organs as well as ectopic growth of tissues inside the primary carpels (i.e., loss of floral determinacy). Second, we crossed the weak *ago1-11* allele with the strong *ago10-13* allele but also failed to obtain viable double mutants. The *ago1-11 ago10-13/+* plants were smaller than *ago1-11* in stature. Some inflorescences harbored flowers with filamentous floral organs and obviously enlarged floral meristems (Figure 2.9D). When carpels were formed, they were unfused and additional floral organs were observed inside the primary carpels (Figure 2.2I). In *ago10-13 ago1-11*/+ plants, gynoecia were bulged with additional floral organs inside (Figure 2.2F). In summary, both *ago1 ago10*/+ or *ago1*/+ *ago10* plants were more severe in floral determinacy defects than the corresponding single mutants. The dosage effects of *ago1* and *ago10* alleles indicate that the two genes have overlapping functions in floral stem cell termination.

AGO10 acts partly through miR172 to promote floral determinacy

miR172 negatively regulates *AP2* mainly through translational repression [10,11] to result in proper floral patterning including the termination of floral stem

cells [12] as well as stamen identity specification [30]. In the *hua1 hua2* background in which *AG* expression is reduced, loss of function in *HEN1*, a player in miRNA biogenesis [37], results in stamen-to-petal transformation. The homeotic transformation is mainly due to de-repressed *AP2* expression since the *ap2-2* mutation restores stamen identity to *hua1 hua2 hen1-1* flowers [30].

To determine whether *AGO10* acts through miR172 in floral patterning, we examined the genetic interactions between *ago10* and *ap2* mutations by generating *hua1 hua2 ago10-12 ap2-2* and *ag-10 ago10-13 ap2-2*. First, *ap2-2* suppressed the homeotic defects of *hua1 hua2 ago10-12* in that the third whorl petaloid stamens in the triple mutant were restored to stamens in the quadruple mutant (Figure 2.4D). While the third whorl organs in *hua1 hua2 ago10-12* had patches of cone-shaped cells reminiscent of petal epidermal cells (Figure 2.9I,J), the third whorl organs in *hua1 hua2 ago10-12 ap2-2* had epidermal cells with the shapes of interlocking puzzle pieces resembling anther epidermal cells (Figure 2.9K,L). This indicates that the homeotic transformation in *hua1 hua2 ago10-12* flowers is due to de-repressed *AP2* and that *AGO10* mediates the function of miR172 in repressing *AP2*. Second, *ap2-2* partially suppressed the floral determinacy defects of *hua1 hua2 ago10-12* and *ag-10 ago10-13* flowers. *ap2-2* did not affect the shapes of *hua1 hua2* or *ag-10* gynoecia ([29]; Figure 2.9M), but caused *hua1 hua2 ago10-12* and *ag-10 ago10-13* gynoecia to be less bulged (compare Figure 2.4D to Figure 2.1B and Figure 2.4E to Figure 2.2E), suggesting that the determinacy defects were not as severe as in *hua1 hua2 ago10-12* or

ag-10 ago10-13. To quantify this effect, we dissected gynoecia to observe the presence/absence of ectopic organs inside. Compared with *hua1 hua2 ago10-12* and *ag-10 ago10-13* plants that had ectopic floral organs in 91% and 100% of flowers, respectively, *ap2-2* reduced the percentage of flowers with internal organs to 41% and 86% in *hua1 hua2 ago10-12* and *ag-10 ago10-13*, respectively (Table 2.1). Although the suppression effect for the latter genotype was not large, we found that *ap2-2* completely suppressed the presence of an elongated gynophore in *ag-10 ago10-13* (Figure 2.9N-P). An elongated gynophore probably reflects a partial conversion of the floral meristem to an inflorescence meristem, hence, prolonged stem cell activity. Therefore, the floral stem cell defects of *ago10* mutants were partially rescued by *ap2-2*, indicating that *AP2* is likely de-repressed in *ago10* mutants and that the de-repression is partially responsible for the floral stem cell defects. This conclusion is consistent with the similar genetic behavior of *AP2m3* and *ago10* in that both enhanced *ag-1* ([12]; Figure 2.4B,C).

Despite the genetic evidence supporting de-repressed *AP2* expression in *ago10* mutants, we were unable to consistently detect an increase in AP2 protein levels in *ag-10 ago10-13* vs. *ag-10* or *ago10-13* vs. wild type by western blotting (data not shown). This is likely attributable to insufficient sensitivity of the assay in the detection of small differences. Since the levels of miR172 were not affected by *ago10-13* (Figure 2.8A), it is likely that miR172-mediated repression of *AP2* requires *AGO10*.

AGO10 is associated with miRNAs *in vivo*

Although our genetic evidence indicates that *AGO10* mediates the activities of miR172 and previous genetic studies implicate *AGO10* in mediating the translational repression of target mRNAs by multiple miRNAs [26], molecular evidence of AGO10 acting directly with miRNAs has been lacking. We sought to determine whether AGO10 was associated with miRNAs *in vivo*. We immunoprecipitated (IP) YFP-ZLL from inflorescences of *zll-1 pZLL::YFP-ZLL* plants [38] with anti-GFP antibodies. *pAG::AG-GFP* and L*er* (wild type) were used as a positive and a negative control, respectively, for the IP. Proteins of the expected sizes from the *pZLL::YFP-ZLL* and *pAG::AG-GFP* IP samples were detected by western blotting (Figure 2.5A). We also included *pAGO1::FLAG-AGO1* [20] and Col (a control for *pAGO1::FLAG-AGO1*) for comparison. We extracted RNAs from the IP samples and performed small RNA northern blotting to detect selected miRNAs and siRNAs. AGO10 bound miRNAs such as miR165/166, miR172, miR173, miR319 and miR168 (Figure 2.5B), but not miR390 (Figure 2.10), which specifically associates with AGO7 [18]. Northern blotting failed to detect signals for 24 nt endogenous siRNAs from several loci from the IP samples (data not shown). The AGO10-associated miRNAs are also known to be associated with AGO1 *in vivo* [17,20].

AGO10 has "slicer" activity

Because AGO10 contains the DDH catalytic residues that are critical for the "slicer" activity of AGO proteins, we decided to determine whether AGO10 is

catalytically active *in vitro*. We performed a “slicer” activity assay on the miR165/166 target *PHABULOSA* (*PHB*). A portion of the *PHB* transcript containing the miR165/166 binding site was generated through *in vitro* transcription and incubated with IP samples from *pAGO1::FLAG-AGO1* and *pZLL::YFP-ZLL* plants as well as the corresponding negative controls Col and *pAG::AG-GFP*, respectively. A miR165/166-resistant *PHB* transcript, *PHBm*, was also included as a negative control. The *PHB* transcript was cleaved into two fragments of expected sizes by both FLAG-AGO1 and YFP-ZLL but not by the corresponding control IPs (Figure 2.5C). As expected, the *PHBm* transcript failed to be cleaved by either FLAG-AGO1 or YFP-ZLL (Figure 2.5C). This shows that AGO10, like AGO1, can cause the cleavage of miRNA-targeted mRNAs.

Given that AGO10 has “slicer” activity, we next examined the levels of miRNA target mRNAs in *ago10* mutants. The levels of most examined miRNA-targeted mRNAs were not obviously different between *ago10-13* and wild type (Figure 2.8B), consistent with findings from a previous study [26]. A small elevation in the levels of *CUC1* mRNA, which is targeted by miR164, was consistently detected in *ago10-13* (Figure 2.8B). Interestingly, a small reduction in the levels of miR164 in *ago10* mutants was consistently observed (Figure 2.8A). The miR164-resistant *CUC1* transgene (*pCUC1::CUC1m-GFP*; [39]) did not enhance the determinacy defects of *ag-10* (data not shown), suggesting the *ag-10 ago10-13* floral determinacy defects were unlikely attributable to de-repressed *CUC1* expression. There are several explanations for the lack of

differences in miRNA target mRNA levels between *ago10* and wild type. First, changes are masked by the target mRNAs outside of the highly restricted expression domain of *AGO10*. Second, *AGO1* is sufficient to regulate most miRNA-targeted mRNAs at the transcript level, and AGO10 acts primarily through translational inhibition *in vivo*.

miR165/166 and its targets, the HD-Zip genes, are crucial players in floral determinacy

The fact that the *ap2-2* mutation failed to completely suppress *hua1 hua2 ago10-12* or *ag-10 ago10-13* suggests that *AGO10* regulates floral stem cell termination also through other miRNAs. Because AGO10 associates with miR165/166 and the HD-Zip genes *PHB*, *PHAVOLUTA* (*PHV*), and *REVOLUTA* (*REV*) targeted by this miRNA strongly influence the formation of the SAM [40], we tested whether proper regulation of *PHB* by miR165/166 was crucial for floral stem cell termination. We introduced the miR165/166-resistant form of *PHB*, *phd-1d* [49], into *ag-10*. Both *ag-10 phb-1d/+* and *ag-10 ago10-13/+ phb-1d/+*, but not *phb-1d/+* flowers had bulged gynoecia with internal floral organs inside (Figure 2.4F; Figure 2.9Q,R). Sections of *ag-10 phb-1d/+* flowers revealed indeterminate floral meristems inside the primary carpels (Figure 2.4H). In addition, in the genetic screen in the *ag-10* background, we isolated a semi-dominant *phv* allele, *phv-5d*, as an *ag-10* enhancer. The *ag-10 phv-5d* double mutant exhibited bulged siliques throughout the plant (Figure 2.4G) whereas most but not all siliques in *ag-10 phv-5d/+* plants were bulged (Figure 2.9O). *phv-5d* contained a G-to-A

mutation in the miR165/166 binding site (Figure 2.7A,C) and this lesion was identical to those of the previously characterized *phv-1d*, *-2d*, *-3d*, and *-4d* alleles [40]. Although the mutation resulted in a glycine-to-aspartic acid substitution, extensive studies of an identical mutation in *PHB* (*phb-3d*) showed that it was the disruption of miR165/166 targeting rather than the amino acid change that caused the developmental defects in *phb-3d* [41]. Collectively, these results demonstrate that miR165/166-mediated regulation of HD-Zip genes is necessary for floral stem cell termination.

Having shown that the repression of *PHB* and *PHV* by miR165/166 is important for floral stem cell termination, we sought to determine whether *ago1* or *ago10* mutations resulted in defects in miR165/166-mediated repression of HD-Zip genes. We first examined the accumulation of miR165/166 in *ago1-11*, *ago10-13*, *ago1-11*/+ *ago10-13*, and *ago1-11 ago10-13*/+ inflorescences. Intriguingly, miR165/166 levels were reduced in *ago1-11* but increased in *ago10-13* (Figure 2.5D). The increase in miR165/166 levels was consistently observed in all *ago10* alleles tested (*ago10-12*, *ago10-13*, and *pnh-1*; Figure 2.8A and data not shown), and was also previously observed in *ago10* seedlings [42].

Next, we examined the levels of HD-Zip mRNAs in L*er*, *ago1-11*, *ago10-13*, *ag-10*, and *ag-10 ago10-13* flowers by real-time RT-PCR. The levels of *PHB*, *PHV* and *CORONA* (*CNA*) mRNAs were reduced in *ago10* genotypes as compared to controls (Figure 2.5E,F), which correlated with the increased abundance of miR165/166. This indicated that *AGO1* was sufficient to control the

mRNA levels of the HD-Zip genes in the absence of *AGO10*. In *ago1-11*, in which miR165/166 levels were low, *PHB* and *PHV* mRNA levels were slightly higher than wild type (Figure 2.5E), consistent with AGO1 being the major slicer of *PHB* and *PHV in vivo*. Therefore, *ago1* and *ago10* mutations have opposite effects on miR165/166 accumulation and expression of the HD-Zip genes.

ago10 mutants were previously found to have increased levels of miR165/166 in seedlings and the increase in miR165/166 and the resulting decrease in HD-Zip expression were responsible for the SAM and leaf polarity defects of *ago10* mutants [42]. Therefore, it is possible that reduced HD-Zip expression caused by elevated levels of miR165/166 also underlies the floral determinacy defects of *ago10* mutants. However, it is possible that *AGO10* regulates the HD-Zip genes through translational repression since it is known to do so on other miRNA target genes [26]. If this were the case, the levels of HD-Zip proteins would be increased in *ago10-13* despite the reduction in the mRNA levels. The lack of antibodies against the HD-Zip proteins prevented us from directly determining the levels of HD-Zip proteins in *ago10* mutants. We used the mRNA levels of *LITTLE ZIPPER3* (*ZPR3*), which is a direct target of *PHB* [43], as a proxy for PHB protein levels. It was shown that *ZPR3* mRNA levels are reduced in HD-Zip loss-of-function mutants and increased in miRNA165/166-resistant HD-Zip mutants [43]. Real-time RT-PCR showed that *ZPR3* levels were severely reduced in *ago10-13* (Figure 2.11), suggesting that HD-Zip protein levels were low in *ago10-13*. Next, we investigated whether reduced HD-Zip

gene expression could result in loss of floral determinacy. *ag-10* plants were transformed with an artificial miR165/166 construct in which pre-miR165 and pre-miR166 were placed in tandem and driven by the 35S promoter. Among 64 primary transformants, 16 exhibited premature termination of the SAM, a phenotype reminiscent of *ago10* mutants (Figure 2.9T). A few of them couldn't survive to generate true leaves. 12 plants exhibited bulged gynoecia similar to *ag-10 ago10* and 4 plants had more severe floral determinacy defects in that the gynoecia were replaced by an internal flower (Figure 2.4I-L). This demonstrated that down-regulation of HD-Zip gene expression by over-expression of miR165/166 compromises floral determinacy.

Discussion

AGO10 and AGO1 have similar small RNA binding specificities but can act differently on miRNAs *in vivo*

Among the ten argonaute proteins in *Arabidopsis*, AGO10 is most similar in sequence to AGO1, the major miRNA effector. Genetic evidence indicates that *AGO10* and *AGO1* have redundant, overlapping, or even antagonistic functions in development and RNA silencing [23,27]. For several tested miRNA target genes, protein but not mRNA levels are elevated in *ago10* mutants, suggesting that AGO10 is necessary for miRNA-mediated translational repression of targets [26]. However, direct molecular evidence supporting AGO10 as a miRNA effector has been lacking, perhaps owing to the spatially highly restricted expression of *AGO10*, which makes it challenging to assay small RNA binding and cleavage

activities of AGO10. In this study, we provide direct evidence that AGO10 associates with miRNAs *in vivo* and possesses miRNA-directed cleavage activity *in vitro*. So far, three other *Arabidopsis* AGO proteins, AGO1, AGO4 and AGO7, have been shown to possess “slicer” activity [18,20,44]. AGO1 preferentially associates with most miRNAs, ta-siRNAs and transgene siRNAs and mediates target mRNA cleavage and translational inhibition [17,20,26]. AGO7 specifically binds and mediates the function of miR390 in ta-siRNA production through both cleavage and non-cleavage functions [18]. AGO4 binds 24 nt endogenous siRNAs and causes transcriptional silencing of target loci in either a slicer-dependent or slicer-independent manner [44]. From our limited examination of small RNAs bound by AGO10, it appears that AGO10 has similar small RNA binding specificities as AGO1 in that it binds all examined miRNAs except for miR390 and it does not bind 24 nt endogenous siRNAs.

Despite the similar small RNA binding specificities of the two proteins, mutations in the two genes can have different effects on miRNA accumulation and the expression of miRNA target genes. The abundance of many miRNAs is reduced in severe *ago1* mutants [45] but not affected in *ago10* null alleles ([26] and this study). While many miRNA target mRNAs are increased in abundance in *ago1* mutants [21], most assayed miRNA targets are not significantly affected in *ago10* mutants ([26] and this study). miR165/166 is an extreme example of the differential effects of *ago1* and *ago10* mutations. While miR165/166 levels are reduced in *ago1-11*, they are increased in *ago10* mutants. The targets of

miR165/166 are also affected in opposite directions in the two mutants – they are de-repressed in *ago1-11* and further repressed in *ago10*. This shows that AGO1 is the major slicer acting upon the HD-Zip mRNAs *in vivo*, although AGO10 has slicer activity *in vitro*. While the two argonaute proteins act differently on miR165/166, they both mediate the activities of miR172. Both *ago1-11* and *ago10* result in petaloid stamens in the *hua1 hua2* background, suggesting both *ago1* and *ago10* mutations lead to de-repression of *AP2*. Therefore, AGO1 and AGO10 mediate the activities of some miRNAs but also have different effects on others.

Floral stem cell termination versus differentiation

Floral stem cell termination is tightly coupled to the formation of carpel primordia in flower development. *AG*, which specifies carpel identities, also acts to terminate the floral stem cells. It may thus be presumed that the termination of floral stem cells is simply via differentiation of these cells into carpel cells. However, the fact that *ag-10 ago10-13* and *hua1 hua2 ago10-12* flowers have 4th whorl carpels but are indeterminate indicates that carpel identity specification and floral stem cell termination, although both directed by *AG*, are two separable processes. It is expected that factors acting downstream of *AG* in the two processes must be distinct. *KNUCKLES*, for example, is a target of *AG* that is only required for floral determinacy specification [46].

HD-Zip genes, targets of miR165/166, are crucial for the temporal program of floral stem cells

Our previous studies show that both miR172 and its target *AP2* regulate the temporal program of floral stem cells. Plants expressing miR172-resistant *AP2* cDNA have prolonged *WUS* expression and indeterminate floral meristems that produce numerous stamens [12]. In this study, we show that the HD-Zip genes, which are targets of miR165/166 and which are previously known for their role in the specification of adaxial identity in lateral organs, are also crucial factors in floral stem cell regulation. Over-expression of miR165/166 in the *ag-10* background results in indeterminate flowers. Consistent with this, the *phb phv cna* triple mutant was observed to have occasional flowers with enlarged gynoecia containing ectopic carpels inside [47]. On the other hand, *ag-10 phb-1d/+* and *ag-10 phv-5d* gynoecia are also indeterminate. Given the similar phenotypes of de-repressed *PHB* or *PHV* and loss of function in *PHB*, *PHV* and *CNA* in terms of floral determinacy, it is likely that either too much or too little HD-Zip activity is detrimental to the precise regulation of floral stem cells. Given that the HD-Zip genes promote adaxial identities of lateral organs, our findings raise the intriguing possibility that floral stem cell determination depends on correct polarity specification of the fourth whorl organs. This hypothesis will be tested in the future.

AGO10 and *AGO1* promote floral stem cell termination via similar and different mechanisms

The relationship between *AGO10* and *AGO1* varies depending on the developmental processes. During embryogenesis, *AGO10* and *AGO1* share overlapping functions in maintaining *STM* expression [23]. In the weak *zll-15* mutant background, increasing the dosage of *AGO1* suppressed the defects in embryonic stem cells, while reducing *AGO1* dosage enhanced the defects [27]. Our studies provide the molecular evidence supporting the overlapping biological roles of *AGO1* and *AGO10* by showing that they have similar small RNA binding specificities and that they both have “slicer” activity. A previous study also documented that *AGO10* antagonizes *AGO1* function. *ago10* mutations partially suppress the leaf margin serration phenotype of the hypomorphic *ago1-27* allele [27]. Moreover, defects in transgene PTGS and miRNA-mediated gene silencing in the hypomorphic *ago1* mutant are also restored by *ago10* mutations [27]. The elevated AGO1 protein levels in the double mutants reveal that *AGO10* is a negative regulator of *AGO1* at the translational level. By showing that AGO10 binds miR168, which targets *AGO1*, we provide the molecular evidence for the direct regulation of *AGO1* by *AGO10* through miR168.

Our studies support overlapping roles for *AGO10* and *AGO1* in the temporal regulation of floral stem cells but also reveal that the two proteins do so with both similar and different molecular mechanisms (Figure 2.6). It is well established that *AGO1* mediates the functions of miR172 and miR165/166 in

different aspects of plant development. It is likely that *AGO1* promotes floral stem cell termination by repressing *AP2* and HD-Zip expression. Consistent with this, de-repression of *AP2* or HD-Zip genes compromises floral stem cell termination. We show here that AGO10 also associates with these two miRNAs *in vivo*. Genetic evidence suggests that *AGO10* mediates the functions of miR172 in both stamen identity specification and floral determinacy. Therefore, *AGO10* reinforces the functions of *AGO1* in the regulation of *AP2*. Perhaps *AGO1* alone is not sufficient to mediate the functions of miR172 in floral meristems such that *AGO10*, which is specifically expressed in certain cells in the floral meristem, is necessary to act upon the same miRNA. Intriguingly, *AGO1* and *AGO10* exert opposite effects on miR165/166 accumulation and the expression of the HD-Zip genes. The increased miR165/166 levels and reduced expression of HD-Zip genes in *ago10* mutants suggest that *AGO10* promotes HD-Zip gene expression by repressing miR165/166 levels. How *AGO10* does so is currently unknown. Despite the opposite effects on HD-Zip expression, *AGO1* and *AGO10* both promote floral determinacy. This can be reconciled by the fact that both reduced expression and de-repression of HD-Zip genes compromise floral determinacy.

SAM and floral meristems – differences in stem cell maintenance

It has not escaped our attention that loss of function of *AGO10* results in opposite effects in stem cell regulation between the SAM and floral meristems. While *ago10* mutations lead to premature termination of stem cells in the SAM, they result in prolonged floral stem cell maintenance. A previous study found that

over expression of miR165/166 recapitulates the SAM defects of *ago10* mutants [42]. In this study, we show that over expression of miR165/166 recapitulates not only the SAM defects but also the floral stem cell defects of *ago10* mutants. Therefore, over accumulation of miR165/166 and reduced expression of the HD-Zip genes probably underlie the failure to maintain the SAM and to terminate the floral stem cells. How reduced expression of the HD-Zip genes leads to opposite effects in the two types of meristems is currently unknown.

Materials and methods

Plant strains and EMS mutagenesis

The plant strains used in this study are all in Landsberg *erecta* (L*er*) ecotype except for *ago1-36 pAGO1::FLAG-AGO1* [20], which is in the Columbia (Col) background. All plants were grown at 23°C under continuous light unless stated otherwise. z*ll-1 pZLL::YFP-ZLL* [38], *clv3-1* [35], *wus-1* [2], *ap2-2* [48], *phb-1d* [49], *hua1-1* [29], *hua2-1* [29], and *pnh-1* [25] were all previously characterized.

ag-10, *ago10-12*, *ago10-13*, *ago10-14* and *phv-5d* were isolated in this study. An EMS mutagenesis screen was carried out in the *hua1 hua2* background as described [30]. Single M2 families were screened and two independent mutants, *hua1 hua2 ago10-12* and *hua1 hua2 ag-10*, with heart-shaped gynoecia and *ag* null mutant-like phenotypes, respectively, were identified. The *ag-10* mutation was recovered from fertile siblings. The two lines were backcrossed to *hua1 hua2* three times to clean up the genetic

backgrounds. They were also crossed to either *hua1* or *hua2* to generate *hua1 ago10-12*, *hua2 ago10-12*, *hua1 ag-10* and *hua2 ag-10* double mutants. The *ago10-12* or *ag-10* single mutant was obtained by crossing *hua1 ago10-12* or *hua1 ag-10* to wild type. The *ago10-13* allele was isolated in a separate EMS mutagenesis screen in the *hua1 ag-10* background as a mutation that enhanced the floral determinacy phenotypes of *hua1 ago-10*. The mutant was backcrossed to *ag-10* three times to obtain the *ag-10 ago10-13* double mutant, with which most subsequent analysis were conducted. The *ago10-13* single mutant was obtained by crossing *ag-10 ago10-13* to L*er*. The *phv-5d* allele was isolated in an EMS mutagenesis screen in the *ag-10* background as an enhancer of its weak floral determinacy defects (see supplemental material for more information on this mutant).

Construction of amiR165/166

The amiR165/166 plasmid contains modified pre-miR165 and pre-miR166, each in a pre-miR168 backbone, inserted in tandem between the 2X *35S* promoter and the 35S terminator in a small-sized pOT2 vector. amiR165 and amiR166 construction was done by two rounds of PCR cloning using a proofreading Taq polymerase and two pairs of long primers (~60-100 nt) engineered to contain a SwaI and a PmeI site, respectively. The two pairs of primers (M0SL-at-miR165-SwaI-PR and M0SL-at-miR165-SwaI-PF or M4SL-at-miR166-PmeI-PR and M4SL-at-miR166-PmeI-PF) covered the entire artificial stem-loop sequences of miR165 or miR166 to minimize errors in the miR165

or166 duplex regions during the PCR reactions. First, primers (M0SL-at-miR165-SwaI-PR and M0SL-at-miR165-SwaI-PF) were used to amplify the pOT2 vector that contains the miR168 backbone. The PCR products were cleaved by SwaI and self-ligated to generate a plasmid that contains pre-miR165. Second, PCR was performed using this plasmid as the template with the primers M4SL-at-miR166-PmeI-PR and M4SL-at-miR166-PmeI-PF. The PCR products were cleaved by PmeI and self-ligated to generate a plasmid containing the tandem pre-miR165 and pre-miR166 sequences. Finally, the plasmid in pOT2 was amplified by a pair of primers (Origin-del-PacI-PF and Origin-del-PacI-PR) that contained PacI sites to delete the plasmid replication origin. The PCR products that contained the amiR165/166 and a chloramphenicol selection marker were introduced into a modified pFGC5941 binary vector through the unique PacI site. Recombinant binary plasmids were verified by DNA sequencing before being used for plant transformation.

RNA extraction and real-time RT-PCR

Total RNAs were extracted from inflorescences using TRI Reagent (Molecular Research Center, Cat# TR118) as per manufacturer's instructions. Contaminating DNA was removed by DNase I (Promega, Cat# M610A; Roche, Cat# 04716728001) digestion. cDNA was synthesized from 2 μg total RNAs using reverse transcriptase (Fermentas, Cat# EP0441) and an oligo-dT primer. Quantitative PCR was performed in triplicates on a Bio-Rad IQ cycler apparatus

with the iQ SYBR green supermix (Bio-Rad, Cat# 170-8882). The primers used are listed in Table 2.2.

Small RNA northern blotting

Northern blotting to detect small RNAs was performed as described [37,50]. 5'-end-labeled (^{32}P) antisense DNA oligonucleotides were used to detect miRNAs from total RNAs from inflorescences. 5'-end-labeled (^{32}P) antisense LNA oligonucleotides were used to detect miRNAs from AGO1 or AGO10 immunoprecipitation samples. The probe sequences are listed in Table 2.2.

Immunoprecipitation

FLAG-AGO1 immunoprecipitation was performed as described [20]. *ag-1 pAG::AG-GFP* and *zll-1 pZLL::YFP-ZLL* inflorescences were ground in liquid nitrogen and homogenized in an equal volume of extraction buffer (20 mM Tris HCl pH 7.5, 300 mM NaCl, 5 mM $MgCl_2$, 5 mM DTT, 1% (v/v) protease inhibitor cocktail (Roche, Cat# 11244800; 1 tablet was dissolved in 1 ml nuclease-free water)). The extracts were centrifuged for 10 min at 16,000g three times to pellet any debris. The lysates were then precleared with protein-A agarose (Thermo Scientific, Cat# 20333) for 1 hr. Anti-GFP antibodies (Clontech, Cat# 632460) were added to the samples at a 1:200 dilution and the samples were incubated on a rotating shaker for 2 hrs. Protein-A agarose was added at a 1:50 ratio and incubation was continued for another 2 hrs. The immune complexes were washed four times with 1.5 ml of extraction buffer supplied with 0.5% NP-40 and two times with RISC (RNA-induced silencing complex) buffer (40 mM Hepes pH

7.4, 100 mM KOAc, 5 mM MgOAc, 4 mM DTT). Finally, the immune complexes were resuspended into 100 µl RISC buffer.

In vitro transcription and RNA cleavage assay

The *PHB* and *PHBm* cDNAs were amplified by PCR with primers *PHBprobeF* and *PHBprobeR* (see Table 2.2 for sequence information) from the wild type *PHB* and the miR165/166-resistant *PHB G202G* [41] templates, respectively. The PCR products were cloned into pGEM-T Easy (Promega, Cat#A1360) and selected clones were sequenced to ensure the absence of unwanted mutations. The clones were linearized with *Spe*I (NEB, Cat# R0133L) and the linearized DNA was gel purified. *In vitro* transcription and RNA cleavage assays were carried out as described (Baumberger and Baulcombe, 2005). *In vitro* transcription was performed by incubating 800 ng DNA in a 25 µl reaction with T7 RNA polymerase (Promega, Cat# P2077) and α-P^{32}-UTP at 37°C for 1.5 hrs. Labeled *PHB* and *PHBm* probes were gel purified and dissolved in 50 µl nuclease-free water. 3 µl probes were used in a 25 µl cleavage reaction mix containing 20 µl AGO1 or AGO10 immune complexes in RISC buffer, 1 µl 25 mM ATP and 1 µl RNase inhibitor (Fermentas, Cat# EO0381). The reaction mix was incubated at 37°C for 1.5 hrs. The RNAs were resolved in an 8 M Urea/5% polyacrylamide gel and detected with a Typhoon Phosphoimager.

Protein extraction and western blotting

To extract proteins from plants, 25 mg inflorescence material was ground in liquid nitrogen and homogenized with 150 µl 1XSDS loading buffer supplied

with 0.5% (v/v) 2-mercaptoethanol and 1% (v/v) protease inhibitor cocktail mix. The extracts were boiled for 5 min, followed by centrifugation at 16,000 g at 4 °C for 5 min. 15 µl supernatant was resolved in a 10% SDS-PAGE gel. To assay the AGO1 or AGO10 immunoprecipitation samples, 8 µl immune complexes were boiled with an equal volume of 2XSDS loading buffer with 1% (v/v) 2-mercaptoethanol and 2% protease inhibitor cocktail mix. The proteins were resolved in a 7.5% SDS-PAGE gel and a monoclonal anti-GFP antibody (Abcam, Cat# ab3277) was used for immunodetection.

Figures

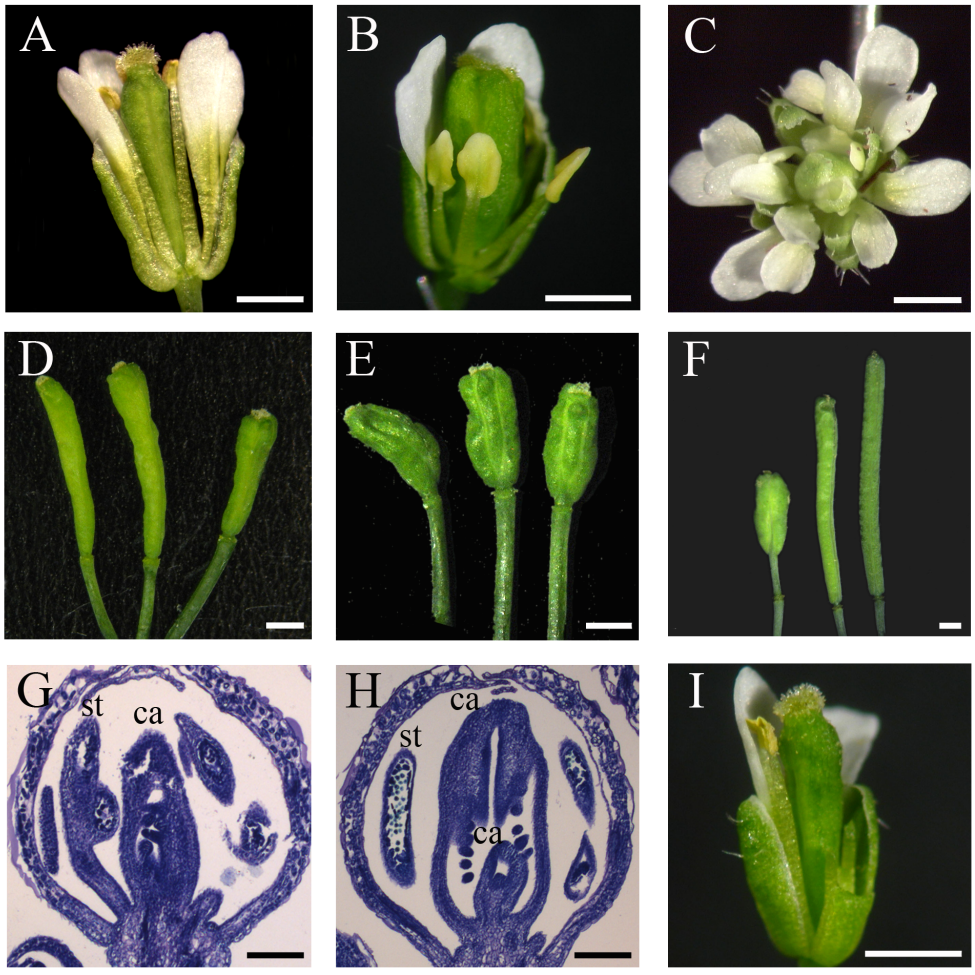

Figure 2.1 hen6 (ago10-12) and hen7 (ag-10) mutations enhance hua1 hua2 (A) A *hua1 hua2* flower with a gynoecium that was slightly enlarged at the top. (B) A *hua1 hua2 hen6* (or *hua1 hua2 ago10-12*) flower with petaloid stamens and a bulged gynoecium containing ectopic floral organs inside. (C) A *hua1 hua2 hen7* (or *hua1 hua2 ag-10*) flower that resembled that of an *ag* null mutant in that the third whorl stamens were transformed into petals and that the sepal-petal-petal pattern was reiterated. (D) Siliques of *hua1 hua2*. (E) Siliques of *hua1 hua2 ago10-12*. (F) A representative silique of *hua1 ag-10* (left), *hua1 ag-10* plants

carrying the *pAG::AG-GFP* transgene (middle), and L*er* (right). (G, H) Longitudinal sections of *hua1 hua2* and *hua1 hua2 ago10-12* stages 10-11 flowers. An ectopic floral meristem inside the fourth whorl carpels was present in *hua1 hua2 ago10-12* (H) but not *hua1 hua2* (G). (I) A *hua1 hua2 ago10-12* flower carrying *AGO10* genomic DNA, which rescued the floral determinacy and homeotic defects of *hua1 hua2 ago10-12*. Some outer whorl organs were removed to expose the gynoecia in (A), (B), and (I). Scale bars, 50 μm in (G), (H) and 1 mm in all other panels.

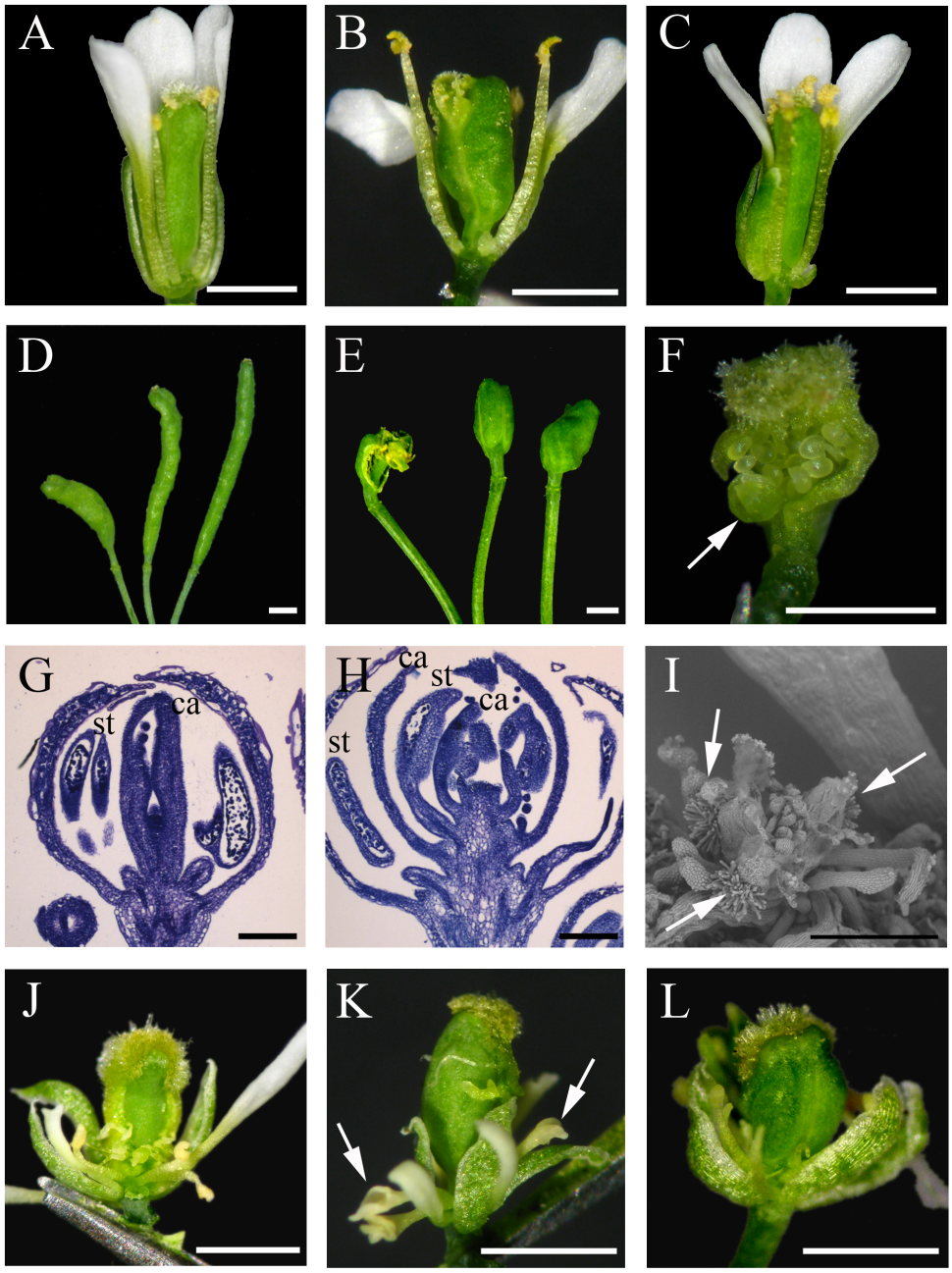

Figure 2.2 AGO10 and AGO1 enhance floral determinacy

*(*A) An *ag-10* flower; most *ag-10* flowers were similar to wild-type ones. (B) An *ag-10 ago10-13* flower; the gynoecia of *ag-10 ago10-13* flowers were bulged and contained ectopic floral organs internally. (C) A flower of *ag-10 ago10-13 pAGO10::AGO10-FLAG* showing that *AGO10* rescued the floral determinacy

defects of *ag-10 ago10-13*. (D) Representative siliques from *ag-10* plants. Most were similar to wild-type siliques, while some were constricted on one side but still long and thin. Bulged siliques with internal floral organs (represented by the one on the left) were observed at a low frequency (usually 1-2 flowers per plant). (E) Siliques from *ag-10 ago10-13* plants. 100% of the siliques on an *ag-10 ago10-13* plant were bulged. Occasionally, the primary carpels that make up a silique were not properly fused, revealing the internal organs. (F) An *ago10-13 ago1-11/+* gynoecium with internal floral organs (arrow) bursting out of the gynoecium. (G, H) Longitudinal sections of stages 12 *ag-10* and *ag-10 ago10-13* flowers. The floral meristem was not visible in most *ag-10* flowers (G), whereas it was still active in *ag-10 ago10-13* flowers to result in extra whorls of organs inside the fourth whorl carpels (H). (I) A scanning electron micrograph of an *ago1-11 ago10-13*/+ flower. The severe floral determinacy defects were reflected by the presence of numerous floral organs inside unfused primary carpels (indicated by arrows). (J-L) *ago1-11* enhanced the floral determinacy defects of *hua1 hua2* and *ag-10*. (J) An *ago1-11* flower. (K) A *hua1 hua2 ago1-11* flower with bulged gynoecia and petaloid stamens. (L) A representative *ag-10 ago1-11* flower with a severely bulged gynoecium. In (A), (B), (C), and (J), some outer whorl floral organs were removed to expose the gynoecia. Scale bars, 50 μm in (G) and (H), 500 μm in (I), and 1 mm in all other panels.

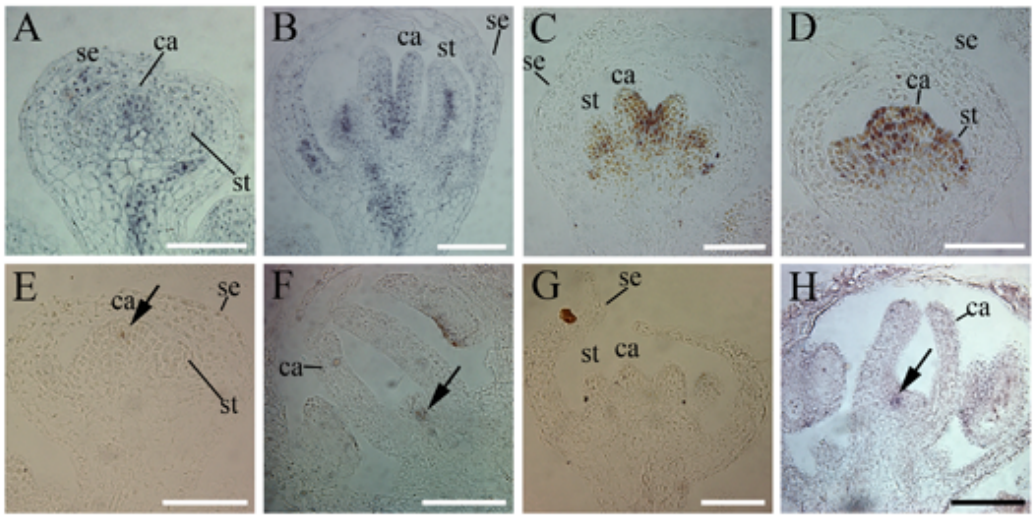

Figure 2.3 Expression patterns of AGO10, AG and WUS in floral meristems
(A, B) Immunolocalization of AGO10 protein using anti-GFP antibodies in pZLL::YFP-ZLL flowers. The grey signals represent AGO10. Before floral stage 6, AGO10 was predominantly localized at the floral meristem and in provascular tissue (A); AGO10 was adaxialized in carpels beyond stage 6 (B). (C, D) The *ago10-13* mutation did not alter the spatial patterns of *AG* expression in developing flowers. *AG* mRNA was similarly present in the inner two whorls of an *ag-10* (C) and an *ag-10 ago10-13* (D) flower at stages 6-7. (E-H) *ago10* mutations led to prolonged *WUS* expression. In *hua1 hua2*, the latest stage when *WUS* mRNA could be detected was stage 6 (E). *WUS* expression persisted to stage 8 or 9 in *hua1 hua2 ago10-12* flowers (F). *WUS* expression was diminished by stage 7 in *ag-10* (G). In *ag-10 ago10-13*, *WUS* expression could be observed in stages 8-9 flowers (H). Scale bars, 50 μm. ca, carpel; se, sepal; st, stamen.

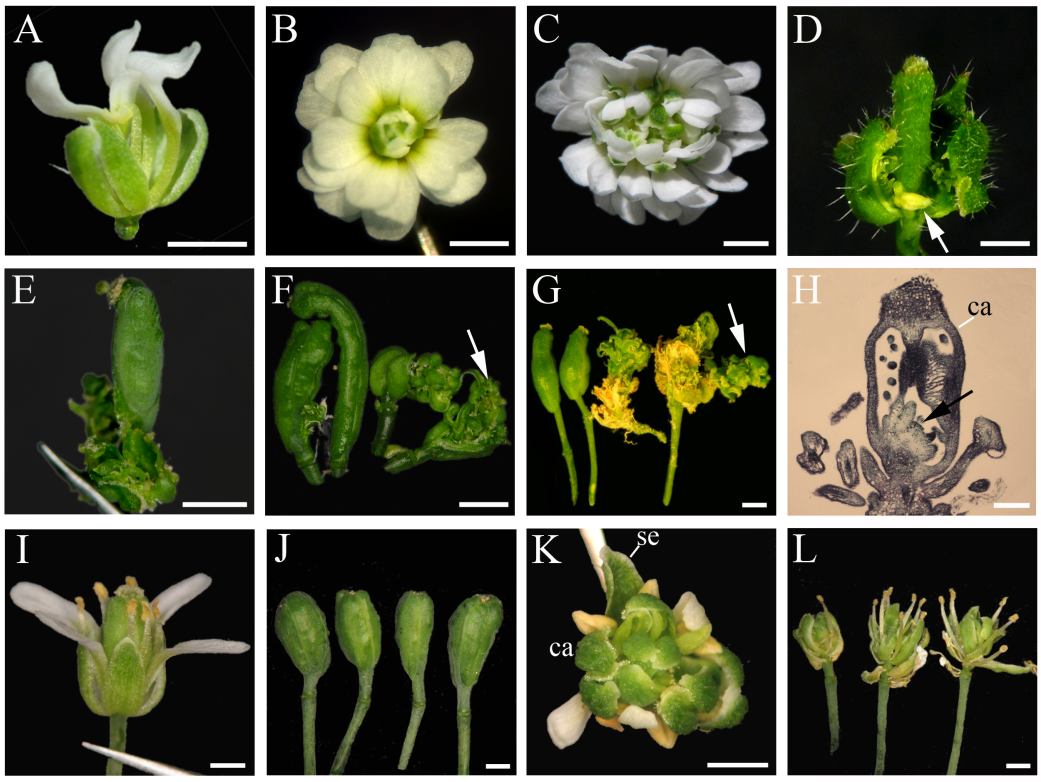

Figure 2.4 Genetic interactions between AGO10 and meristem regulators

(A) A *hua1 hua2 ago10-12 wus-1* flower. *wus-1* was completely epistatic to *hua1 hua2 ago10-12* in floral determinacy such that the quadruple mutant flower had an incomplete set of floral organs as in a *wus-1* flower. (B) An *ag-1* flower. (C) An *ag-1 pnh-1* flower that had apparently more floral organs than an *ag-1* flower and showed signs of fasciation. (D,E) *ap2-2* partially suppressed the floral determinacy defects of *hua1 hua2 ago10-12* and *ag-10 ago10-13*. (D) A representative of the non-bulged gynoecia of some *hua1 hua2 ago10-12 ap2-2* flowers. The petaloid stamens in *hua1 hua2 ago10-12* were rescued back to stamens (arrow) by the *ap2-2* mutation. (E) A representative of *ag-10 ago10-13 ap2-2* gynoecia, which are longer than *ag-10 ago10-13* gynoecia (Fig. 2E). (F-H) *phb-1d* and *phv-5d* each enhanced the determinacy defects of *ag-10*. (F) *ag-10 phb-1d/+* siliques. Ectopic floral organs, indicated by the arrows, were found in the siliques of most *ag-10 phb-1d/+* flowers. (G) *ag-10 phv-5d* siliques, which

were bulged or contained ectopic floral organs, as indicated by the arrow. (H) A longitudinal section of an *ag-10 phb-1d/+* gynoecium. An ectopic floral meristem (indicated by the arrow) could be observed inside the carpels. (I-L) *ag-10* plants harboring transgenic amiR165/166 exhibited loss of floral determinacy. (I-J) Weaker determinacy defects of some *ag-10* amiR165/166 plants. The gynoecia were bulged as in *ag-10 ago10-13*. (K-L) Stronger determinacy defects of some *ag-10* amiR165/166 plants. The gynoecia were replaced by an internal flower. Scale bars, 50 μm in (H), and 1mm in all other panels.

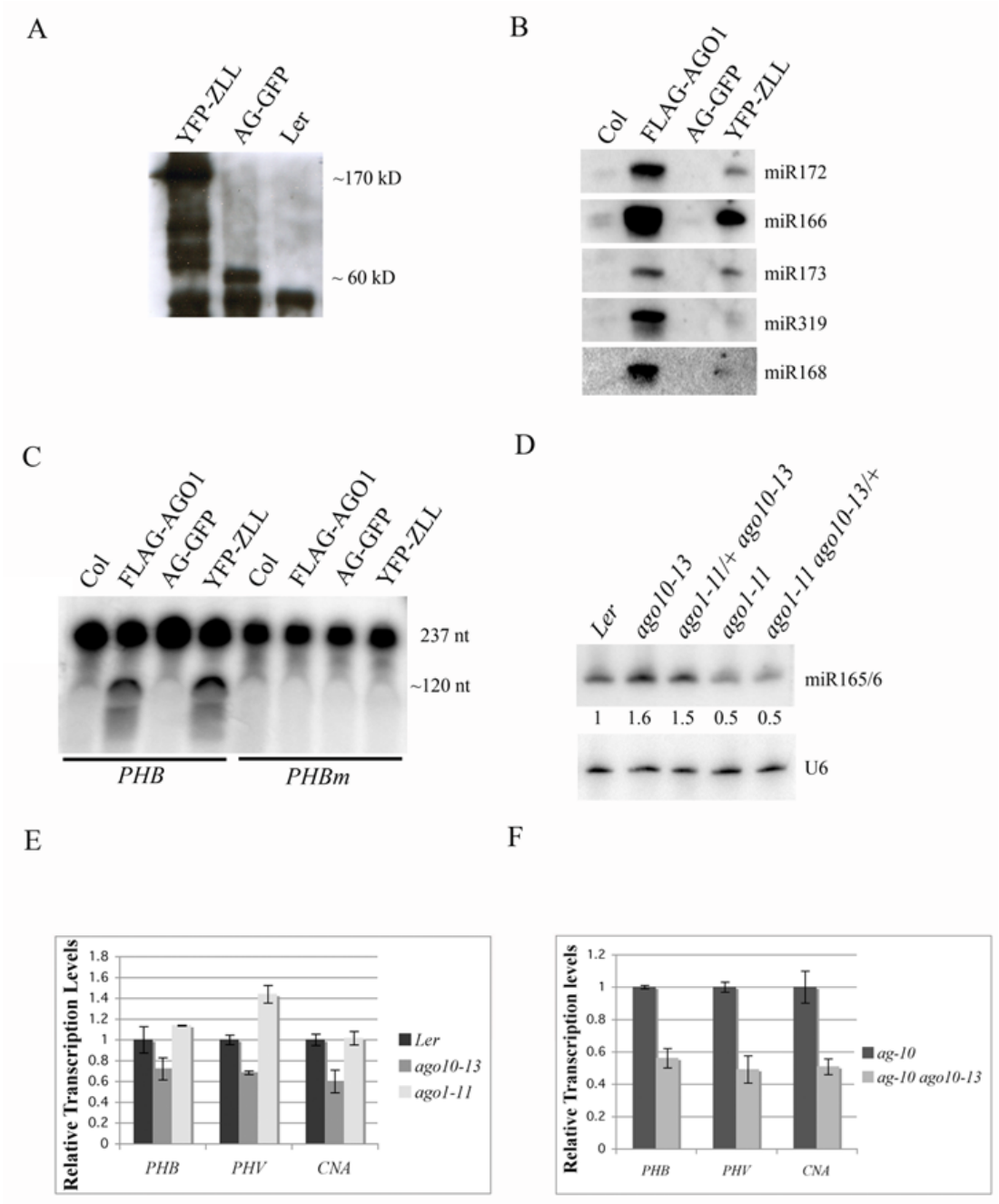

Figure 2.5 AGO10 is associated with miRNAs in vivo and is catalytically active as a "slicer" in vitro

(A) Immunoprecipitation (IP) followed by western blotting using anti-GFP antibodies from three genotypes as indicated. The immunoprecipitated YFP-ZLL

fusion protein could be detected as a band of the expected size (~170 kD). AG-GFP (~60 kD) and L*er* served as a positive and a negative control for the IP, respectively. (B) Detection of miRNAs by northern blotting from FLAG-AGO1 and YFP-ZLL IP. Col and AG-GFP served as negative controls for FLAG-AGO1 and YFP-ZLL, respectively. (C) An *in vitro* “slicer” assay. Both FLAG-AGO1 and YFP-ZLL immune complexes cleaved the *PHB* wild-type probe, but not the miR165/166-resistant probe. The full-length probes were 237 nt, and the 5’ and 3' cleavage fragments were 112 nt and 125 nt, respectively, and were not separated in the gel (represented by the band of approximately 120 nt). (D) Northern blot for miR165/166 in the genotypes as indicated. The numbers below the gel image indicate the relative abundance of miR165/166. (E) Expression of the HD-Zip genes *PHB*, *PHV* and *CNA* in wild type (L*er*), *ago10-13*, and *ago1-11* inflorescences as examined by real-time RT-PCR. (F) Real-time RT-PCR to determine the levels of *PHB*, *PHV*, and *CNA* mRNAs in *ag-10* and *ag-10 ago10-13* inflorescences.

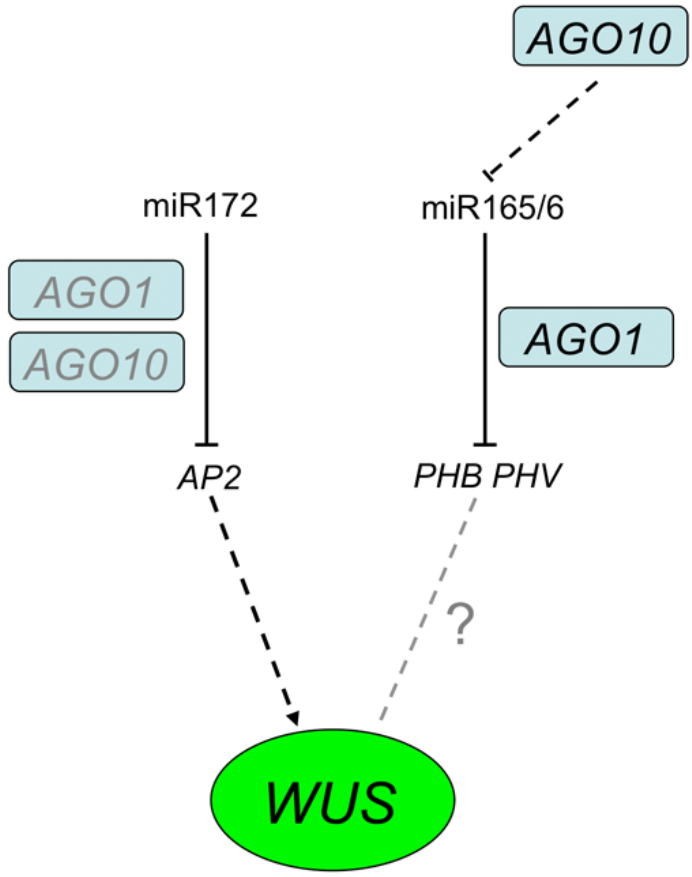

Figure 2.6 A model of AGO1 and AGO10 in floral stem cell regulation
miR172 promotes floral stem cell termination by repressing the expression of *AP2*, which promotes *WUS* expression. Both AGO1 and AGO10 are associated with miR172 *in vivo* and genetic evidence supports a role of AGO10 in mediating the activities of miR172. miR165/166-mediated repression of *PHB* and *PHV* is also necessary for floral stem cell termination. *AGO1* and *AGO10* exert opposite effects on miR165/166. While *AGO1* mediates the activities of miR165/166, *AGO10* represses the expression of miR165/166. The relationship between PHB/*PHV* and *WUS* is unknown. Interactions that are potentially indirect are represented by dotted arrows.

Supplemental Materials

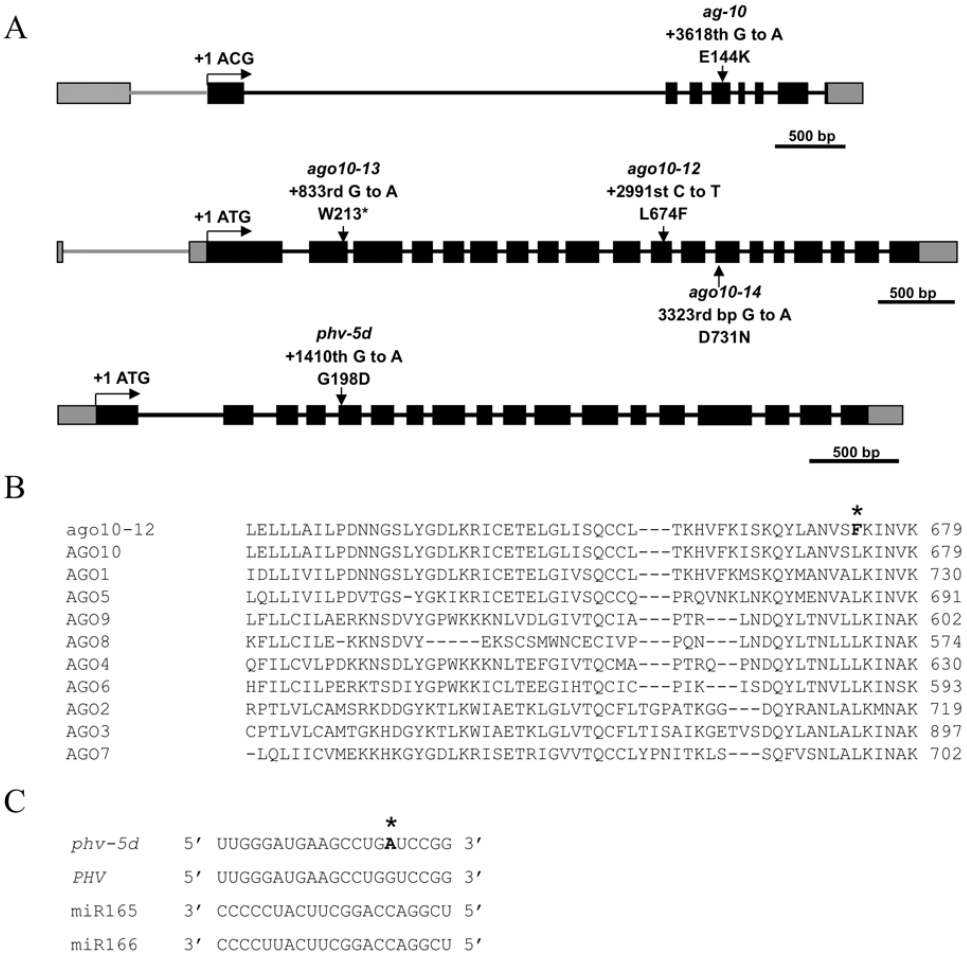

Figure 2.7 Diagrams of AG, AGO10 and PHV genes and multiple sequence alignments of Arabidopsis AGO proteins

(A) Diagrams of *AG*, *AGO10*, and *PHV*. In *ag-10*, the replacement of the guanine at nucleotide 3618 (position 1 being the “A” in the ACG start codon) by adenine causes an E-to-K substitution. *ago10-12* has a C-to-T transition at nucleotide 2991 (position 1 being the “A” in the ATG start codon), which results in an L-to-F substitution at amino acid 674 in the protein. *ago10-13* has a G-to-A transition at nucleotide 833, which introduces a premature stop codon in the second exon. *ago10-14* is a G-to-A mutation at nucleotide 3323 causing a D-to-N substitution.

phv-5d contains a G-to-A transition at nucleotide 1410 (position 1 being the “A” in the ATG start codon), causing an G-to-D substitution. (B) Multiple sequence alignment of all *Arabidopsis* AGO proteins indicates that 674 L is conserved. (C) A diagram showing that the *phv-5d* mutation disrupts the binding site for miR165/166.

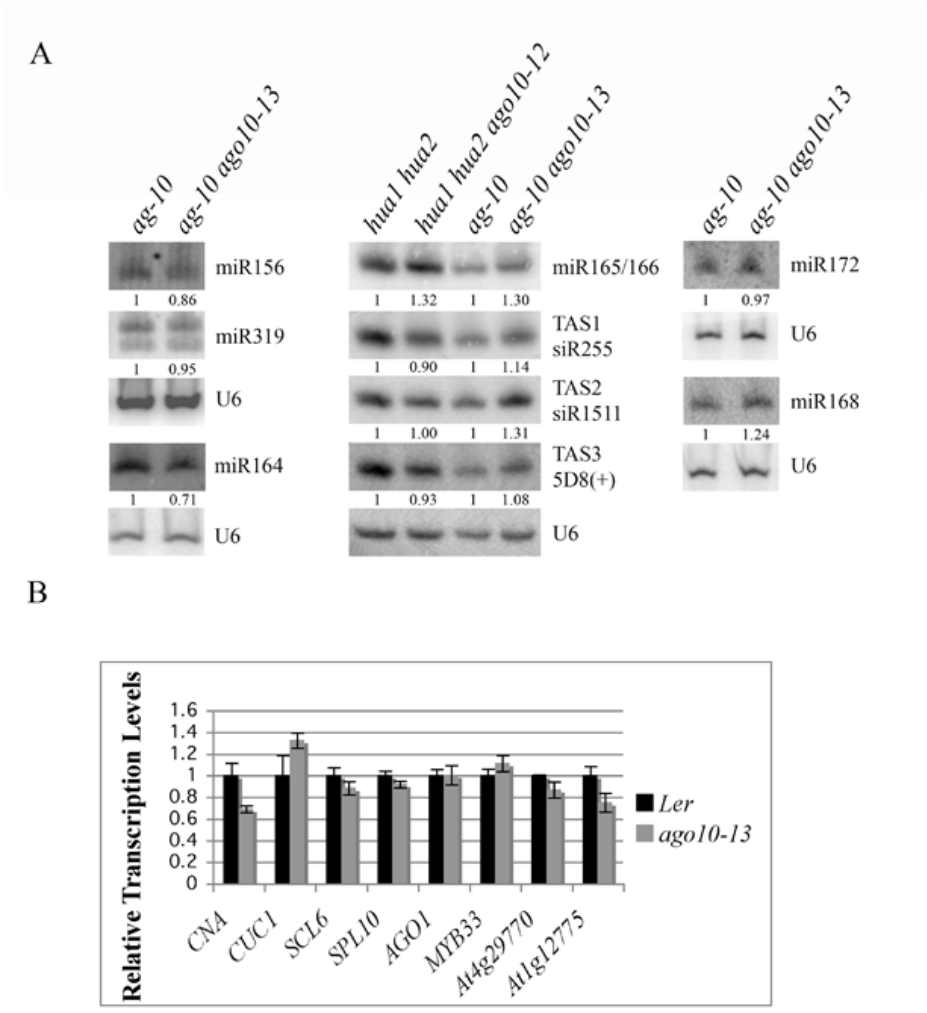

Figure 2.8 The accumulation of miRNAs, ta-siRNAs and their target mRNAs in ago10 mutants

(A) Northern blotting to detect six miRNAs and three ta-siRNAs. The *ago10-13* mutation resulted in slightly elevated levels of miR165/166 and slightly reduced levels of miR164. The other examined miRNAs were not obviously affected. The levels of siR255 (from *TAS1*), siR1511 (from *TAS2*), and 5D8(+) (from *TAS3*), were not affected by *ago10* mutations. The U6 blots served as loading controls for the overlying small RNA blots. The numbers below the small RNA blots indicate the relative abundance of the small RNAs. (B) Real-time RT-PCR to determine the levels of miRNA- and siRNA-targeted mRNAs. Most of the

examined mRNAs were not significantly different between *ago10-13* and L*er* inflorescences. A small elevation was observed for *CUC1* mRNA targeted by miR164. Bars represent standard deviation of three technical replicates. Three biological replicates yielded similar results.

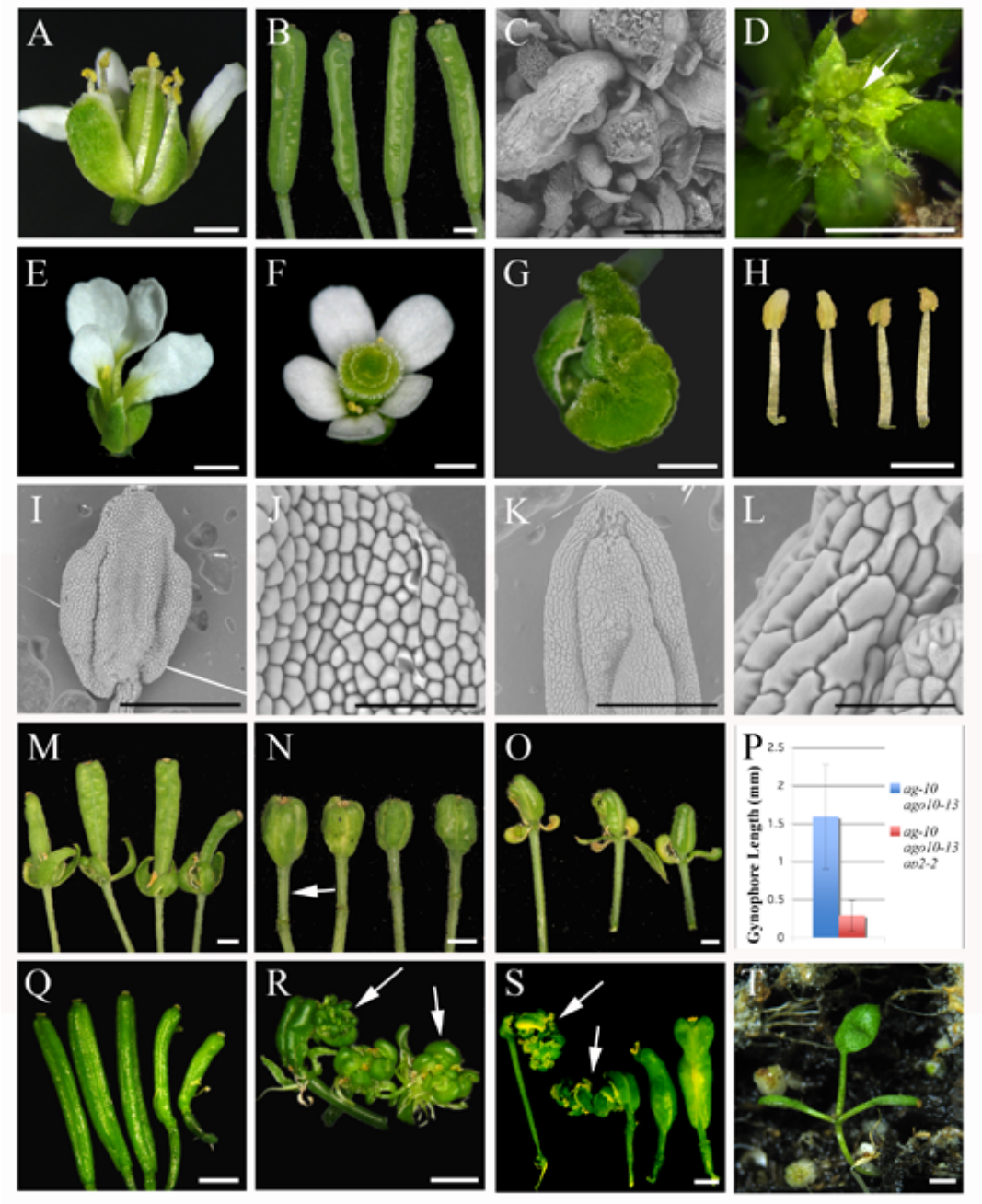

Figure 2.9 Floral phenotypes of various genotypes

(A) An *ago10-13* flower; *ago10-13* flowers resembled wild-type flowers except for the narrower petals. (B) Siliques from *ago10-13* plants. *ago10-13* siliques were shorter and wider than those of wild-type plants. (C) An SEM image of an *ago1-11* flower. (D) An *ago1-11 ago10-13/+* inflorescence with obviously enlarged

floral meristems (arrow). (E) A *wus-1* flower. (F, G) *hua1 hua2 ago10-12* and *clv3-1* exhibited synergistic effects in terms of floral determinacy. (F) A *hua1 hua2 ago10-12 clv3-1* flower with an enlarged gynoecium. (G) A *hua1 hua2 ago10-12 clv3-1* silique with a massive amount of internal stigma tissue bursting out of the primary gynoecium. (H) Third whorl organs in *hua1 hua2 ago10-12* flowers. Some had petaloid features (the two on the left) while others resembled stamens. (I-L) SEM images of anthers and anther epidermal cells in *hua1 hua2 ago10-12* (I and J) and *hua1 hua2 ago10-12 ap2-2* (K and L). (M) Siliques of *ag-10 ap2-2* plants. (N) Siliques of *ag-10 ago10-13* plants. Note the elongated gynophore (arrow). (O) Siliques of *ag-10 ago10-13 ap2-2* plants. (P) Quantification of gynophore length in the two genotypes. (Q) Siliques of *phb-1d*/+ plants. (R) *ag-10 ago10-13/+ phb-1d/+* siliques showing gynoecia enlargement and the presence of ectopic organs (indicated by the arrows). (S) Bulged siliques and ectopic floral organs, indicated by the arrows, were found in *ag-10 phv-5d*/+ plants. (T) An *ag-10* amiR165/166 plant showing SAM defects reminiscent of *ago10* mutants. Scale bar, 500 μm in (C), 300 μm in (I), (K), 50 μm in (J), (L), and 1 mm in the rest of the panels.

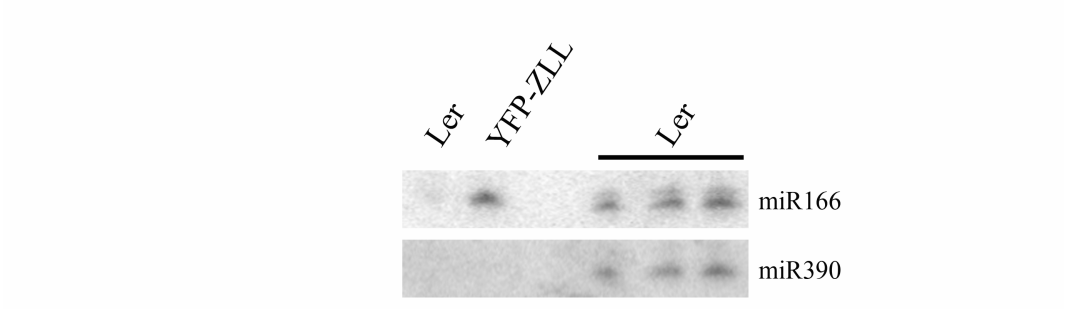

Figure 2.10 AGO10 does not bind miR390

Northern blots for miR166 and miR390 were performed for total RNAs from wild type (L*er*; the three lanes on the right) and immunoprecipitated samples (the first two lanes from the left) using anti-GFP antibodies from L*er* (a negative control) and the *YFP-ZLL* transgenic line. YFP-ZLL was associated with miR166 but not miR390 *in vivo*.

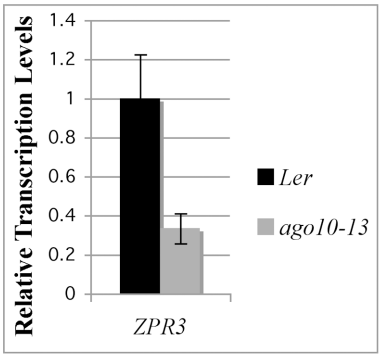

Figure 2.11 The expression of ZPR3 in wild type (Ler) and ago10-13 as determined by real-time RT-PCR

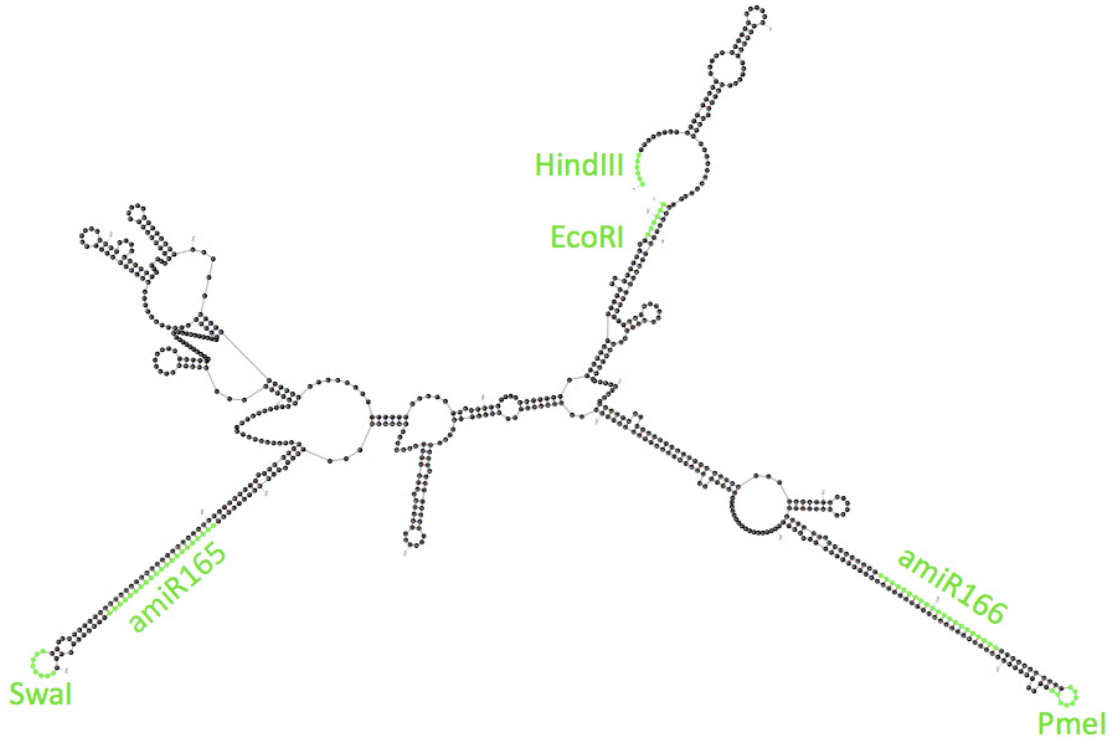

Figure 2.12 A diagram of amiR165/166

A modified, partial pri-miR168 is highlighted in black. The amiR165 and amiR166 sequences (in green) were introduced into the pri-miR168 backbone through two rounds of PCR cloning using the *Swa*I and *Pme*I sites, respectively. The whole structure was inserted between a 2X35S promoter and a 35S terminator through the restriction sites *Hin*dIII and *Eco*RI.

Table 2.1 Floral organ counts in various genotypes

1.	Sepal	Petal	Stamen	Carpel[a, c]	Carpel[b, c]	Inner organ[a] (%)	Inner organ[b] (%)	N[a]	N[b]
L*er*	4.0 ± 0	4.0 ± 0	5.6 ± 0.6	2.0 ± 0	2.0 ± 0	0	0	40	40
pnh-1	4.0 ± 0	4.1 ± 0.3	5.5 ± 0.7	2.8 ± 0.8	2.6 ± 0.6	0	0	24	68
ago10-13	4.0 ± 0.1	4.2 ± 0.3	5.3 ± 0.8	3.2 ± 0.4	2.9 ± 0.4	0	0	27	53
hua1 hua2	4.0 ± 0	4.0 ± 0	5.5 ± 0.7	2.0 ± 0.1	2.3 ± 0.5	0	0	45	15
hua1 hua2 ago10-12[d]	4.0 ± 0.2	4 ± 0.2	5.3 ± 0.6	3.5 ± 0.6	3.5 ± 0.5	44.4	91.1	45	45
ag-10	4.0 ± 0	4.1 ± 0.3	6.0 ± 0.2	2.6 ± 0.6	2.5 ± 0.5	15.4	34.9	26	43
ag-10 ago10-13	4.0 ± 0.2	4.1 ± 0.4	5.5 ± 0.6	3.1 ± 0.7	3.1 ± 0.6	100	100	35	55
hua1 ag-10	4.0 ± 0	4.0 ± 0.2	5.6 ± 0.5	3.0 ± 0.6	2.8 ± 0.5	96.7	100	29	41
hua1 hua2 ago10-12 ap2-2	N/A	N/A	N/A	N/A	3.01 ± 0.82	N/A	40.8	0	76
ag-10 ago10-13 ap2-2	N/A	N/A	N/A	N/A	3.26 ± 0.67	N/A	86.3	0	73

P.S.
a. The carpel number and the percentage for the presence of inner organ of opening flowers (at positions of 12 to 21 on a single inflorescence). From the same flowers, the sepals, petals and stamens are counted.
b. The carpel number and inner organ presence percentage of siliques (at positions of 2 to 11 on a single inflorescence).
c. Some gynoecia of *ag-10 ago10-13* are not fused at flower stage (8.57%) and silique stage (49.09%).
d. The petaloid stamens in the 3rd whorl of *hua1 hua2 ago10-12* were counted as stamens in this analysis.
e. Errors are indicated by standard deviation.

Table 2.2 Sequences of oligos used in the study

Oligo Name	Sequence	Note
PHB_real-timeF2	GAGGAGGCCCTAGCAGAGTT	Real-time RT-PCR
PHB_real-timeR2	CGTTTCCAGCAGGTATCACA	
PHV_real-timeF	GTTAACAACCCAGCTAATCTTC	Real-time RT-PCR; *phv-5d* sequencing
PHV_real-timeR	GAAACAGCTACGATACCAATAG	
CNAF	ATCCTCAGAGAGATGCTAGTCCT	Real-time RT-PCR
CNAR	TTGTAGGCTCAAGACCCACTAG	
AGO1F	TGGACCACCGCAGAGACAAT	Real-time RT-PCR
AGO1R	CATCATACGCTGGAAGACGACT	
CUC1F	AGTTGTTGTATCCTGGGTGTAGCA	Real-time RT-PCR
CUC1R	CCGTTGGTGGTGGTGGAGAC	
MYB33F	AGTTGTTGTATCCTGGGTGTAGCA	Real-time RT-PCR
MYB33R	CCGTTGGTGGTGGTGGAGAC	
SPL10F	TGAGACAAAGCCTACACAGATGGA	Real-time RT-PCR
SPL10R	GATGATGCAACCCGACTTTTTTATG	
SCL6F	GAGGTCATAGAGAGCGACAC	Real-time RT-PCR
SCL6R	GGAATAAGGGTTTAGGGTTT	
AT4G29770F1	CCGTCAGGTAATGAAACAC	Real-time RT-PCR
AT4G29770R1	TGGGATACAGAAGTCAACAA	
AT1G12775F1	GCTTTTTCTACTATGGGGAAG	Real-time RT-PCR
AT1G12775R1	ATGAGAGTGGGTTTATGTCC	
ARF3F	GGTGGCCTGGTTCAAAATGGAG	Real-time RT-PCR
ARF3R	CGGAAGAGGGTGATGATGATAC	
AG_RTF2	TTCTTTGTGATGCTGAAGTC	Real-time RT-PCR
AG_RTR2	ATGCTGATTATTTGTTGACG	
pinheadp13	ACCTGATAACAACGGTTCACTTTA	*ago10-12* genotyping
pinheadp10	TATAAGTTCTTGCCTGTGAGCTTG	
pinheadp3	TTGCAGGTTACAATTACTCCTGAA	

pinheadp2	TACCAGCTAGAAACTCGCCTAAGT	*ago10-13* genotyping
pnh-1F	GTATCCCTTAAAATCCTCGTAAAG	*pnh-1* genotyping
pinheadp11	ACTAGACAATCCACATTCACCGGCG GAAA	*pPZP211-PNHp11/p18* cloning
pinheadp18	GGCCGAGTATATTGCAATTGACGAC AAAA	
ag-10_geno_F	CAGCATACAAAACTCCAACAGGT	*ag-10* genotyping
ag-10_geno_R	ATCGGATTCGGGTAATACTTCTCT	
AG_F	CACCTCTTCTATATTATTAGGATC	*pAG::AG-GFP* cloning
AG_R	CCTACAAAACAGCATAAAG	
AGO10_G_DONRF	GGGGACAAGTTTGTACAAAAAAGCA GGCTTCAATTGATCATATTAAACTA TT	*pAGO10::AGO10-FLAG* cloning
AGO10_G_DONRR	GGGGACCACTTTGTACAAGAAAGCT GGGTCGCAGTAGAACATTACTCTCT TC	
PHBprobeF	CCAAGGCTACAGGAACTGCTGTTG	*PHB* probe cloning
PHBprobeR	CAAAGATCGTCCATCTTGGC	
miR172_LNA[a]	AT+GCA+GCA+TCA+TCA+AGA+TT C+T	
miR166_LNA[a]	GG+GGA+ATG+AAG+CCT+GGT+CC G+T	
miR173_LNA[a]	GT+GAT+TTC+TCT+CTG+TAA+GCG +AA	
miR319_LNA[a]	GGG+AGC+TCC+CTT+CAG+TCC+AA	
miR390_LNA[a]	GG+CGC+TAT+CCC+TCC+TGA+GCT +T	
miR168_LNA[a]	TT+CCC+GAC+CTG+CAC+CAA+GCG +A	
miR156	GTGCTCACTCTCTTCTGTCA	
miR164	TGCACGTGCCCTGCTTCTCCA	
TAS1 siR255	TACGCTATGTTGGACTTAGAA	
TAS2 siR1511	AAGTATCATCATTCGCTTGGA	
TAS3 5D8(+)	AAAGGCCTTACAAGGTCAAGA	

P.S.
a. LNA modified nucleotides are followed by a plus sign.
b. miR166, miR168, miR172, miR319 DNA probes have the same sequences with the corresponding LNA probes. They are not listed separately.

References

1. Sablowski R (2007) Flowering and determinacy in *Arabidopsis*. J Exp Bot 58: 899-907.

2. Laux T, Mayer KF, Berger J, Jurgens G (1996) The *WUSCHEL* gene is required for shoot and floral meristem integrity in *Arabidopsis*. Development 122: 87-96.

3. Smyth DR, Bowman JL, Meyerowitz EM (1990) Early flower development in *Arabidopsis*. Plant Cell 2: 755-767.

4. Schoof H, Lenhard M, Haecker A, Mayer KF, Jurgens G, et al. (2000) The stem cell population of *Arabidopsis* shoot meristems in maintained by a regulatory loop between the *CLAVATA* and *WUSCHEL* genes. Cell 100: 635-644.

5. Irish VF (2010) The flowering of *Arabidopsis* flower development. Plant J 61: 1014-1028.

6. Lenhard M, Bohnert A, Jurgens G, Laux T (2001) Termination of stem cell maintenance in *Arabidopsis* floral meristems by interactions between *WUSCHEL* and *AGAMOUS*. Cell 105: 805-814.

7. Lohmann JU, Hong RL, Hobe M, Busch MA, Parcy F, et al. (2001) A molecular link between stem cell regulation and floral patterning in *Arabidopsis*. Cell 105: 793-803.

8. Bowman JL, Smyth DR, Meyerowitz EM (1989) Genes directing flower development in *Arabidopsis*. Plant Cell 1: 37-52.

9. Jofuku KD, den Boer BG, Van Montagu M, Okamuro JK (1994) Control of *Arabidopsis* flower and seed development by the homeotic gene *APETALA2*. Plant Cell 6: 1211-1225.

10. Aukerman MJ, Sakai H (2003) Regulation of flowering time and floral organ identity by a microRNA and its *APETALA2*-like target genes. Plant Cell 15: 2730-2741.

11. Chen X (2004) A microRNA as a translational repressor of *APETALA2* in *Arabidopsis* flower development. Science 303: 2022-2025.

12. Zhao L, Kim Y, Dinh TT, Chen X (2007) miR172 regulates stem cell fate and defines the inner boundary of APETALA3 and PISTILLATA expression domain in Arabidopsis floral meristems. Plant J 51: 840-849.

13. Drews GN, Bowman JL, Meyerowitz EM (1991) Negative regulation of the *Arabidopsis* homeotic gene *AGAMOUS* by *APETALA2* product. Cell 65: 991-1002.

14. Chen X (2009) Small RNAs and their roles in plant development. Annu Rev Cell Dev Biol 25: 21-44.

15. Hock J, Meister G (2008) The Argonaute protein family. Genome Biol 9: 210.

16. Havecker ER, Wallbridge LM, Hardcastle TJ, Bush MS, Kelly KA, et al. (2010) The *Arabidopsis* RNA-directed DNA methylation argonautes functionally diverge based on their expression and interaction with target loci. Plant Cell 22: 321-334.

17. Mi S, Cai T, Hu Y, Chen Y, Hodges E, et al. (2008) Sorting of small RNAs into *Arabidopsis* argonaute complexes is directed by the 5' terminal nucleotide. Cell 133: 116-127.

18. Montgomery TA, Howell MD, Cuperus JT, Li D, Hansen JE, et al. (2008) Specificity of ARGONAUTE7-miR390 interaction and dual functionality in *TAS3* trans-acting siRNA formation. Cell 133: 128-141.

19. Zheng X, Zhu J, Kapoor A, Zhu JK (2007) Role of Arabidopsis AGO6 in siRNA accumulation, DNA methylation and transcriptional gene silencing. EMBO J 26: 1691-1701.

20. Baumberger N, Baulcombe DC (2005) *Arabidopsis* ARGONAUTE1 is an RNA Slicer that selectively recruits microRNAs and short interfering RNAs. Proc Natl Acad Sci U S A 102: 11928-11933.

21. Vaucheret H (2008) Plant ARGONAUTES. Trends Plant Sci 13: 350-358.

22. Bohmert K, Camus I, Bellini C, Bouchez D, Caboche M, et al. (1998) *AGO1* defines a novel locus of *Arabidopsis* controlling leaf development. EMBO J 17: 170-180.

23. Lynn K, Fernandez A, Aida M, Sedbrook J, Tasaka M, et al. (1999) The *PINHEAD*/*ZWILLE* gene acts pleiotropically in *Arabidopsis* development and has overlapping functions with the *ARGONAUTE1* gene. Development 126: 469-481.

24. Moussian B, Schoof H, Haecker A, Jurgens G, Laux T (1998) Role of the *ZWILLE* gene in the regulation of central shoot meristem cell fate during *Arabidopsis* embryogenesis. EMBO J 17: 1799-1809.

25. McConnell JR, Barton MK (1995) Effect of mutations in the *PINHEAD* gene of *Arabidopsis* on the formation of shoot apical meristems. Dev Genet 16: 358-366.

26. Brodersen P, Sakvarelidze-Achard L, Bruun-Rasmussen M, Dunoyer P, Yamamoto YY, et al. (2008) Widespread translational inhibition by plant miRNAs and siRNAs. Science 320: 1185-1190.

27. Mallory AC, Hinze A, Tucker MR, Bouche N, Gasciolli V, et al. (2009) Redundant and specific roles of the ARGONAUTE proteins AGO1 and ZLL in development and small RNA-directed gene silencing. PLoS Genet 5: e1000646.

28. Cheng Y, Kato N, Wang W, Li J, Chen X (2003) Two RNA binding proteins, HEN4 and HUA1, act in the processing of *AGAMOUS* pre-mRNA in *Arabidopsis thaliana*. Dev Cell 4: 53-66.

29. Chen X, Meyerowitz EM (1999) *HUA1* and *HUA2* are two members of the floral homeotic *AGAMOUS* pathway. Mol Cell 3: 349-360.

30. Chen X, Liu J, Cheng Y, Jia D (2002) *HEN1* functions pleiotropically in *Arabidopsis* development and acts in C function in the flower. Development 129: 1085-1094.

31. Li J, Chen X (2003) PAUSED, a putative exportin-t, acts pleiotropically in *Arabidopsis* development but is dispensable for viability. Plant Physiol 132: 1913-1924.

32. Wang W, Chen X (2004) HUA ENHANCER3 reveals a role for a cyclin-dependent protein kinase in the specification of floral organ identity in Arabidopsis. Development 131: 3147-3156.

33. Western TL, Cheng Y, Liu J, Chen X (2002) HUA ENHANCER2, a putative DExH-box RNA helicase, maintains homeotic B and C gene expression in Arabidopsis. Development 129: 1569-1581.

34. Mayer KF, Schoof H, Haecker A, Lenhard M, Jurgens G, et al. (1998) Role of WUSCHEL in regulating stem cell fate in the Arabidopsis shoot meristem. Cell 95: 805-815.

35. Clark SE, Running MP, Meyerowitz EM (1995) *CLAVATA3* is a specific regulator of shoot and floral meristem development affecting the same processes as *CLAVATA1*. Development 121: 2057-2067.

36. Kidner CA, Martienssen RA (2005) The role of *ARGONAUTE1* (*AGO1*) in meristem formation and identity. Dev Biol 280: 504-517.

37. Park W, Li J, Song R, Messing J, Chen X (2002) CARPEL FACTORY, a Dicer homolog, and HEN1, a novel protein, act in microRNA metabolism in *Arabidopsis thaliana*. Curr Biol 12: 1484-1495.

38. Tucker MR, Hinze A, Tucker EJ, Takada S, Jurgens G, et al. (2008) Vascular signalling mediated by *ZWILLE* potentiates *WUSCHEL* function during shoot meristem stem cell development in the *Arabidopsis* embryo. Development 135: 2839-2843.

39. Baker CC, Sieber P, Wellmer F, Meyerowitz EM (2005) The *early extra petals1* mutant uncovers a role for microRNA miR164c in regulating petal number in *Arabidopsis*. Curr Biol 15: 303-315.

40. Emery JF, Floyd SK, Alvarez J, Eshed Y, Hawker NP, et al. (2003) Radial patterning of *Arabidopsis* shoots by class III HD-ZIP and *KANADI* genes. Curr Biol 13: 1768-1774.

41. Mallory AC, Reinhart BJ, Jones-Rhoades MW, Tang G, Zamore PD, et al. (2004) MicroRNA control of *PHABULOSA* in leaf development: importance of pairing to the microRNA 5' region. EMBO J 23: 3356-3364.

42. Liu Q, Yao X, Pi L, Wang H, Cui X, et al. (2008) The *ARGONAUTE10* gene modulates shoot apical meristem maintenance and leaf polarity establishment by repressing miR165/166 in *Arabidopsis*. Plant J 58(1): 27-40

43. Wenkel S, Emery J, Hou BH, Evans MM, Barton MK (2007) A feedback regulatory module formed by LITTLE ZIPPER and HD-ZIPIII genes. Plant Cell 19: 3379-3390.

44. Qi Y, He X, Wang XJ, Kohany O, Jurka J, et al. (2006) Distinct catalytic and non-catalytic roles of ARGONAUTE4 in RNA-directed DNA methylation. Nature 443: 1008-1012.

45. Vaucheret H, Vazquez F, Crete P, Bartel DP (2004) The action of ARGONAUTE1 in the miRNA pathway and its regulation by the miRNA pathway are crucial for plant development. Genes Dev 18: 1187-1197.

46. Sun B, Xu Y, Ng KH, Ito T (2009) A timing mechanism for stem cell maintenance and differentiation in the *Arabidopsis* floral meristem. Genes Dev 23: 1791-1804.

47. Prigge MJ, Otsuga D, Alonso JM, Ecker JR, Drews GN, et al. (2005) Class III homeodomain-leucine zipper gene family members have overlapping, antagonistic, and distinct roles in *Arabidopsis* development. Plant Cell 17: 61-76.

48. Bowman JL, Smyth DR, Meyerowitz EM (1991) Genetic interactions among floral homeotic genes of *Arabidopsis*. Development 112: 1-20.

49. McConnell JR, Barton MK (1998) Leaf polarity and meristem formation in *Arabidopsis*. Development 125: 2935-2942.

50. Pall GS, Codony-Servat C, Byrne J, Ritchie L, Hamilton A (2007) Carbodiimide-mediated cross-linking of RNA to nylon membranes improves the detection of siRNA, miRNA and piRNA by northern blot. Nucleic Acids Res 35: e60.

3. Chapter II: ARGONAUTE10 accelerates the decay rate of associated miR165/166

Abstract

Arabidopsis ARGONAUTE10 regulates the activities of Shoot Apical Meristems (SAMs) and Floral Meristems (FMs) through specifically sequestering miR165/166 and repressing the levels of miR165/166, a conserved family of miRNAs targeting type III *HD-Zip* genes through AGO1. Here, we report that AGO10 represses the accumulation of miR165/166 at the mature miRNA level by enhancing their decay. Moreover, our results indicate that the enhanced decay is most likely realized through increased dislodging of miR165/166 from the AGO10-miR165/166 complex. Biochemical assays are currently employed to monitor the release and degradation of miR165/166 when they are bound by AGO1 or AGO10. Studies in other organisms show that target regulation enhances the turnover of small RNAs, whether the decay of miR165/166 depends on target regulation in Arabidopsis will be investigated in this study. Our work will demonstrate a novel property for argonaute proteins, and shed light on the diversification and specification of closely related argonaute proteins in many organisms. It will establish a new mechanism for the regulation of miRNA homeostasis.

Introduction

Arabidopsis *AGO10* is an important regulator for the activity of stem cells in Shoot Apical Meristems (SAMs) and Floral meristems (FMs) [1,2]. Our previous study and two other reports show that the functions of AGO10 in both SAMs and FMs require the repression of miR165/166 accumulation and activity [3-5]. miR165/166 is a conserved miRNA family encoded by two *MIR165* loci and seven *MIR166* loci in the Arabidopsis genome [6]. While the different *MIR165/166* genes have distinct and dynamic expression patterns, the mature miR165/166 from these loci all act through AGO1 to down-regulate the *HD-Zip III* genes, which are involved in diverse developmental processes, such as meristem regulation, lateral organ polarity establishment and vascular tissue development [7-9]. We demonstrated that AGO10 promotes *HD-Zip III* expression by reducing the level of miR165/166 in FMs [3]. Liu *et al.* reported that *AGO10* reduces the level of miR165/166 in the SAM and in leaf primordia [4]. Moreover, the levels of miR165/166 in other tissues, such as aerial parts of seedlings, stems, and inflorescences, were also elevated in *ago10* mutants [4]. However, the mechanisms by which AGO10 represses the levels of miR165/166 is currently unknown. An intriguing finding was that AGO10 preferentially associates with miR166/165 *in vivo* such that this miRNA accounts for about 90% of all AGO10-bound miRNAs [5]. AGO10 competes with AGO1 for binding to miR165/166. Deficient loading of miR165/166 into AGO10 underlies the SAM defects of *ago10* mutants [5].

We are aiming to understand the mechanisms underlying the repression of miR165/166 levels by AGO10. The steady-state accumulation of miRNAs is determined by the rates of their biogenesis and turnover. AGO10 could possibly downregulate the levels of miR165/166 by repressing the transcription of the *MIR165/166* genes or the processing of miR165/166 precursors, or by increasing the degradation of mature miR165/166. However, the first two possibilities have been ruled out after the levels of pri-miR165/166 and pre-miR166a were determined in *ago10* mutants. Our results support that AGO10 downregulates the accumulation of miR165/166 at the mature miRNA level, which is possibly an outcome of faster release of miR165/166 from the AGO10-miR165/166 complex.

Results

AGO10 doesn't affect *MIR165/166* transcription or pri-miR165/166 processing

The transcription of *MIR* genes is spatially and temporally regulated similarly to that of many protein-coding genes (reviewed in [10]). Individual *MIR166* genes have unique expression profiles in maize, as revealed by Laser Capture Microdissection combined with RT-PCR [11]. Interestingly, the expression of *MIR166* is regulated by the tasiR-ARF through an as yet unidentified pathway during the establishment of leaf polarity in maize [12]. The expression of *MIR165/166* genes is also differentially regulated in *Arabidopsis* in that *GUS* reporter lines driven by different *MIR165/166* promoters show distinct expression patterns in SAMs and flowers [9].

We first sought to determine whether AGO10 affects the transcription of *MIR165/166* genes, which would be reflected by the accumulation of pri-miR165/166. Using real-time RT-PCR, we determined the levels of several pri-miR165/166 species from the nine *MIR165/166* loci in the genome, including pri-miR165a, pri-miR166a, pri-miR166b, pri-miR166c, and pri-miR166e. The levels of the tested pri-miR165/166s were not altered in *pnh-2* seedlings (Figure 3.1A) or *ago10-13* inflorescences (Figure 3.7A). Therefore, *AGO10* doesn't regulate the transcription of *MIR165/166*.

During miRNA biogenesis, pri-miRNAs are processed into pre-miRNAs, which are further processed into a duplex of miRNA/miRNA*. miRNA biogenesis is subjected to regulation as indicated by several examples in animals (reviewed in[13]). To determine whether *AGO10* affects miR165/66 biogenesis, we examined the levels of pre-miR166a in *pnh-2* seedlings and *ago10-13* inflorescences. cDNAs containing both pri-miRNAs and pre-miR166s were generated by reverse transcription using oligo(dT) as well as a gene-specific primer complementary to the mature miR166 sequence (Figure 3.7B). The RT-PCR following reverse transcription with the oligo(dT) primer would detect pri-miR166. The sum of pri-miR166a and pre-miR166a levels would be determined with the pre-miR166a-specific primers in the real-time RT-PCR. The accumulation of pri-miRNA166a or the summed accumulation of pri-miRNA166a and pre-miRNA166a was not changed significantly in *pnh-2* seedlings (Figure 3.1B). Northern blotting also confirmed that the levels of pre-miR166a were not

elevated in *pnh-2* seedlings or *ago10-13* inflorescences (Figure 3.7C). Therefore, we conclude that the levels of pre-mi166a are not affected by *ago10* mutations. The remaining possibilities are that AGO10 affects the processing of pre-miR166 or the stability of mature miR165/166.

Evidence that miR165/166 is prone to degradation

In the course of our studies of mutants lacking the small RNA methyltransferase HEN1, we obtained hints that miR165/166 might be particularly prone to degradation. In plants, miRNAs and all kinds of siRNAs are stabilized by a methyl group deposited on their 3' most nucleotides by HEN1 [14]. In *hen1* mutants, the small RNAs are subjected to 3' truncation by a 3'-5' exonucleolytic activity and 3' tailing with uridine as the predominant nucleotide by a nucleotidyltransferase. 3' truncation and 3' tailing also occur on small RNAs in wild type but at a much lower frequency [15]. Therefore, mutations in HEN1 "amplify" the *in vivo* small RNA degradation processes. Deep sequencing of the small RNAs in *hen1-1* (a null allele in the L*er* ecotype) and *hen1-8* (a weaker allele in the Col ecotype) inflorescence tissues helped us to visualize the small RNA degradation intermediates. A computational pipeline was developed in our collaborator Dr. Blake Meyers' lab to systematically examine 3' truncation and/or tailing that occur on miRNAs. For any non-genome matching sRNA reads, their 3' nucleotides are continuously removed one by one until the remaining 5' sequences can be perfectly mapped back to the genome. Then the longest 5' genome-matched components (5GMC) were compared to the annotated miRNAs

in miRBase [16] for their origin, while the 3' sequences were designated as tail sequences. With all reads processed into the format of 5GMC plus tail, the reads are further classified into full-length miRNAs or 3' truncated miRNAs. In the end, all sRNA reads originated from a miRNA are processed into four classes according to the tailing and truncation at their 3' termini, namely the full-length group, the truncated-only group, the tailed-only group and the truncated-and-tailed group. The proportion of full-length miR165/166 dropped dramatically in both *hen1-1* and *hen1-8* alleles (Figure 3.2A). Even though the full-length proportion of many miRNAs also shows a significant reduction in the null *hen1-1* mutant, miR165/166 is special in that this family shows the most dramatic reduction in *hen1-8* (Figure 3.2A). These results indicate that miR165/166 has a higher decay rate in *hen1* mutants than other miRNAs. Moreover, miR165/166 species are highly tailed and truncated in *hen1* mutants (Figure 3.2B, C). In contrast, the tailing or truncation of miR165* and miR166* is rare in *hen1* mutants (Figure 3.2D, E) unlike several other miRNA*s (Figure 3.8), implying that the 3' extension and trimming happen after miR165/166 duplexes are loaded into RISC. What makes miR165/166 prone to these 3' modification events? One significant difference between miR165/166 and other miRNAs is its specific binding by AGO10 [5]. One implication from these observations is that AGO10 enhances the 3' modifications and perhaps degradation of miR165/166.

3' modifications of miR165/166 in *ago10* mutants

To examine the degradation of miR165/166, we sequenced the small RNAs from seedling tissues of L*er* and *ago10* mutants with Illumina Next Generation Sequencing technology. The results from one biological replicate show that the levels of full-length miR165/166 were 1.3- to 4-fold higher in *pnh-1*, *pnh-2* and *ago10-13* than in L*er* (Figure 3.3A). This trend is consistent with all previous reports [3,4]. The 3' tailing and trimming status of miR165/166 was analyzed. The proportion of "truncated-only" species of miR165/166 is mildly reduced in all *ago10* mutants (Figure 3.3B). However, the proportions of "tailed-only" or "tailed-and-truncated" species were not consistently altered in the *ago10* mutants (Figure 3.3B). The reduced 3' truncation of miR165/166 in *ago10* mutants is consistent with our hypothesis that AGO10 affects the stability of miR165/166. Therefore, we are sequencing two more biological replicates to perform statistical analysis.

3' modifications of miR165/166 in *35S::YFP-AGO10*

To test the hypothesis that association with AGO10 leads to the increased degradation of miR165/166, we introduced YFP-AGO10 driven by the *Cauliflower mosaic virus* (CaMV) *35S* promoter into the Col background. The transgenic plants exhibit upwardly curled and serrated leaves, indicating defects in abaxial-adaxial polarity establishment (Figure 3.4A). These morphological phenotypes were previously observed to be associated with *AGO10* over expression [17]. RT-PCR confirmed that transgenic plants with these obvious phenotypes had

high levels of *AGO10* mRNA (Figure 3.9). The transgene, when introduced into *pnh-2*, complemented the developmental defects of the mutant. The *pnh-2 35S::YFP-AGO10* plants had similar upwardly curled leaves but no SAM or silique defects (data not shown). The leaf phenotypes of *35S::YFP-AGO10* plants were very similar to those of several miRNA mimicry lines, such as MIM159, MIM160 and MIM165/166, in which the functions of miR159, miR160, and miR165/166 were partially inhibited [18], and *hyponastic leaves1* (*hyl1)* mutants in which miRNA biogenesis is impaired [19]. Therefore, we examined the levels of several miRNAs in *35S::YFP-AGO10* transgenic plants. Wild-type plants, *pnh-2* mutant and two *ago1* alleles were included as controls for the northern blotting since the changes in miRNA accumulation in these mutants are known. As expected, many miRNAs were reduced in abundance in the *ago1* mutant. Strikingly, the accumulation of many miRNAs including miR165/166 was also reduced in *35S::YFP-AGO10* (Figure 3.4B).

To determine how 35S::YFP-AGO10 downregulates so many miRNAs simultaneously, we tested two possible scenarios. First, could 35S::YFP-AGO10 destabilize the miRNAs through reducing the levels of AGO1 protein? AGO10 was identified as a negative regulator of AGO1 at the protein level in hypomorphic *ago1* alleles [20]. AGO10 probably mediates the activities of miR168, which regulates AGO1 through translational inhibition [20]. Moreover, as a major effecter of miRNA function, AGO1 is necessary for the stabilization of associated miRNAs [21] (Figure 3.4B). In this scenario, the reduction in

abundance of many miRNAs is a secondary effect of reduced AGO1 levels. Therefore, we examined the levels of AGO1 mRNA and protein in *35S::YFP-AGO10* plants. Real-time RT-PCR showed that the levels of *AGO1* mRNA were reduced by almost 50% in *35S::YFP-AGO10*, while those of *PHB* mRNA were increased in *35S::YFP-AGO10* plants as previously reported (Figure 3.4C) [22]. Consistently, the levels of AGO1 protein were also reduced in *35S::YFP-AGO10* as shown by western blotting (Figure 3.4D). Therefore, 35S::YFP-AGO10 reduced the expression of *AGO1*. In turn, the reduction in AGO1 may contribute to the reduction in abundance of many miRNAs in *35S::YFP-AGO10*. However, how this mechanism contributes to the repression of miR165/166 by *AGO10* in wild-type plants is unknown since no obvious elevation of AGO1 mRNA or protein levels can be detected in *ago10* mutants [20].

A second scenario is that mis- and over-expressed AGO10 protein associates with more miRNAs in addition to miR165/166 and directly leads to their degradation if AGO10 destabilizes the associated miRNAs. The association of AGO10 with more miRNAs is possible since the expression domain of AGO10 is expanded and maybe overlapping with more miRNAs. We examined the miRNAs in AGO1 and AGO10 complexes in *35S::YFP-AGO10* plants. The YFP-AGO10 protein was immunoprecipitated (IPed) with anti-GFP antibodies, while the AGO1 protein was IPed with anti-AGO1 antibodies from the same tissue samples. Then the associated small RNAs were isolated and subjected to deep sequencing. As a control, total small RNAs from Col and *35S::YFP-AGO10*

samples were also subjected to deep sequencing. The miRNA profile of *35S::YFP-AGO10* samples was similar to that of Col. We found that the overall profiles of miRNAs associated with AGO1 or AGO10 in *35S::YFP-AGO10* resembled those in wild type. For example, in *35S::YFP-AGO10*, AGO1 associates with most miRNAs and AGO10 preferentially associates with miR165/166 (Figure 3.5A) as in wild type [5]. miR165/166 reads account for about 90% of AGO10-associated miRNAs in both *35S::YFP-AGO10* (Figure 3.5A) and wild type [5]. Furthermore, for most miRNAs, the degree of association with AGO10 is one to several orders of magnitudes less than that with AGO1 (Figure 3.5A). Therefore, mis- and over-expression of AGO10 did not alter the profile of its associated miRNAs. However, this observation does not rule out the possibility that AGO10 downregulates the levels of other miRNAs through direct association, since there are more AGO10 proteins and less AGO1 proteins in the *35S::YFP-AGO10* samples.

The reduced AGO1 levels in *35S::YFP-AGO10* cannot explain the reduction in miR165/166 levels, since this miRNA is primarily bound by AGO10. In *35S::YFP-AGO10*, the increased levels of AGO10 should compete with AGO1 for miR165/166 binding. To test this possibility, AGO1 was IPed from L*er*, *pnh-2*, Col and *35S::YFP-AGO10* seedling tissues and several associated miRNAs were examined by northern blotting. Even though the analysis was complicated by the low levels of AGO1 proteins recovered from *35S::YFP-AGO10*, miR166 exhibited the largest reduction among the four tested miRNAs (Figure 3.4E). Therefore, the

increased AGO10 levels resulted in further sequestration of miR165/166 from AGO1. The correlation between increased binding by AGO10 and reduced accumulation of miR165/166 in *35S::YFP-AGO10* suggests that miR165/166 is more prone to destabilization through its association with AGO10. We compared the levels of 3' modifications on miR165/166 species between Col and *35S::YFP-AGO10*. Compared to other miRNAs, the proportion of full-length miR166 was reduced most dramatically in *35S::YFP-AGO10* (Figure 3.5B). Furthermore, 3' modified miR165/166 species were increased in *35S::YFP-AGO10* relative to wild type, suggesting that AGO10 leads to the decay of miR165/166 (Figure 3.5B).

AGO10 accelerates the decay of associated miR165/166

We hypothesized that AGO10-associated miR165/166 is more likely to undergo degradation than AGO1-associated miR165/166. How does AGO10 enhance the decay of miR165/166? We envision two possibilities. First, miR165/166 is more susceptible to 3' truncation and tailing when associated with AGO10 than with AGO1: a key assumption is that tailing and truncation happen when the small RNAs are still in RISC. In this scenario, the 3' end of the small RNA would not be as tightly anchored in the PAZ domain in AGO10 as in AGO1 to allow 3' modification enzymes access to the 3' end. Second, miR165/166 is dislodged faster from AGO10 RISC than from AGO1 RISC and the degradation happens after the small RNAs are released from RISC. However, the two hypotheses are not mutually exclusive. It is possible that the initial 3' modification

occurs to miR165/166 while it is in RISC, and the modified forms are released faster from AGO10 RISC than from AGO1 RISC, and they get further modified after being released. Under the first scenario, we would expect AGO10 RISC to contain more 3' modified miR165/166 than AGO1 RISC. Under the second scenario, AGO1 and AGO10 RISCs are not expected to show much difference in the binding to 3' modified species. We examined the 3' tailing and truncation of miR165/166 in the AGO1 and AGO10 complexes. The deep sequencing results demonstrated that the most abundant species of miR165/166 in both AGO1 and AGO10 complexes IPed from *35S::YFP-AGO10* plants were the full-length miRNAs even though miR165/166 species are highly truncated and tailed in *35S::YFP-AGO10* plants (Figure 3.5C, D), indicating that the majority of the degradation intermediates are not associated with the RISCs *in vivo*. However, the AGO10 IP had a slightly lower percentage of full-length miRNAs mainly due to a slight increase in the truncated-only miR166 species (Figure 3.5E). These data are largely consistent with the second scenario, although the first cannot be ruled out.

Currently, I am employing biochemical assays to determine the release and degradation rates of miR165/166 from AGO1 and AGO10 complexes. As a start, I monitored the remaining miR165/166 in AGO1 RISCs after a time course incubation with SDN1, which is an exoribonuclease degrading small RNAs in Arabidopsis [23]. The levels of miR165/166 in AGO1 RISCs were not significantly altered over time, while AGO10-associated miR165/166 decreased in abundance

during the course of incubation with SDN1 (Figure 3.6A). Therefore, it could be concluded that AGO10 enhances the decay of miR165/166 by SDN1. I will next determine whether AGO10 has a greater tendency to release miR165/166 as compared to AGO1, which could be the underlying mechanism for enhanced decay of AGO10-associated miR165/166. To observe miRNA release from AGO RISCs, AGO1 and AGO10 IPs will be incubated with buffer without SDN1 in a time course, and both AGO-bound and free miR165/166 in the supernatant will be isolated and quantified by northern blotting. If miR165/166 is dislodged more easily from AGO10 RISC than from AGO1 RISC, there will be increased free miR165/166 in the supernatant and less bound miR165/166 left over time for AGO10 RISC.

It has been implicated that the decay of miRNAs may be induced by the presence of target mRNAs in animals [24]. Therefore, I plan to set up a time course degradation assay for both AGO1 and AGO10 RISCs as described before except that an *in vitro* transcript corresponding to a portion of *PHB* mRNA containing the miR165/166 binding site will also be included. RNAs will be separately extracted from the supernatant, which contains the released small RNAs, and the beads, which contain the AGO proteins and the associated small RNAs. The levels of miR166 in the two fractions will be examined by northern blotting. Since the *in vitro* system may be too simplified to mimic the situation *in vivo*, I also plan to make use of wheat germ extracts (WGE) to set up a semi-*in vitro* system to test the degradation of AGO-associated miR166. It has been

demonstrated that the wheat germ extract contains various miRISCs [25]. To avoid the interference from the wheat endogenous miR165/166, Arabidopsis AGO IPs will first be loaded with an *in vitro* synthesized miR166 oligonucleotide containing the 3' methyl modification and a 5' phosphate group labeled with P^{32}, using conditions that I have established. Then the levels of the full-length miR166 and any degradation products, if detectable, will be examined after a time course incubation of the IP complexes in the wheat germ extract with or without the supplement of *PHB* transcripts. The assay is under optimization currently to minimize variations (Figure 3.6B). By comparing the amounts of the full-length miR166 over time, we hope to demonstrate the influence of the AGOs and the target transcripts (*PHB*) on the stability of miR165/166.

Identify the pathway required for AGO10-associated miR165/166 degradation

Our knowledge of small RNA turnover in plants is very limited in that only SDNs in *Arabidopsis* and MUT68 in algae were identified to function in small RNA turnover [23,26]. If either SND or MUT68 is responsible for the degradation of AGO10-associated miR165/166, the morphological or molecular phenotypes of *35S::YFP-AGO10* may be suppressed by mutations in *SDN*s or *MUT68* homologs in Arabidopsis. Initially, we tested the genetic interactions between *35S::YFP-AGO10* and the *sdn1-1 sdn2-1* double mutant. Unfortunately, the *35S::YFP-AGO10* transgene became silenced when it was crossed into *sdn1-1 sdn2-1*, which has the *35S* promoter from the inserted T-DNAs. In both the F1 and F2 generation plants lost the typical *35S::YFP-AGO10* morphological

phenotypes. To circumvent the silencing problem, I am in the process of generating a large number of primary transformants of *35S::YFP-AGO10* in both *sdn1-1 sdn2-1* and Col and will perform statistic analysis on their phenotypic severity. An Arabidopsis homolog of MUT68, which was identified and named Nucleotidyltransferase4 (NTP4) by my colleagues, probably functions in the uridylation of unmethylated small RNAs in the absence of HEN1 activity. I tested the genetic interaction between *35S::YFP-AGO10* and the *ntp4* mutation. Although *35S::YFP-AGO10* was also silenced in some plants in the F2 generation, the analysis of the F2 population of *35S::YFP-AGO10* crossed to *ntp4* was still informative. Out of 18 F2 plants with typical leaf up-curling phenotypes, none of them was *ntp4* homozygous, implying that *ntp4* possibly suppressed the severe phenotypes of *35S::YFP-AGO10*. Obviously, this needs to be confirmed by identifying *35S::YFP-AGO10 ntp4* plants and observing their molecular and morphological phenotypes. I plan to examine the F2 *35S:YFP-AGO10* plants without severe phenotypes for their *ntp4* genotypes and YFP-AGO10 expression level. I am also testing the genetic interactions between *hen1-2* and *pnh-2* to see if *pnh-2* suppresses the preferential degradation of miR165/166 in the *hen1-2* mutant.

Discussion

Argonaute proteins affect small RNA stability differently

Argonaute proteins usually stabilize their associated small RNAs. For example, the accumulation of miRNAs are positively correlated with the cellular

Ago2 levels in humans [27]. However, it is not known whether different argonaute proteins affect the stability of small RNAs equally, since argonaute proteins select their associated small RNAs through different mechanisms in both animals and plants [28,29]. Misloading of small RNAs into wrong AGOs leads to the malfunction of the small RNAs and defects in the biological processes involving the small RNAs [30]. miR165/166 is unique in that it associates with AGO1 to downregulate its target genes, but associates with AGO10 in the meristems for its own inactivation. The abundantly expressed miR165/166, ubiquitously expressed AGO1 and restrictively expressed AGO10 provide us a precious opportunity to learn how different argonaute proteins affect the stability of the same miRNAs. Our work indicated that AGO10-associated miR165/166 has a higher decay rate than AGO1-associated miR165/166, which is most likely due to a faster release of miR165/166 from the AGO10 complex. This mechanism is quite different from how *Drosophila* Ago1 and Ago2 differentially affect the stability of their associated small RNAs when the same miRNAs are loaded into both Ago1 and Ago2 in some rare cases. The difference is largely imparted by the methyl modification on Ago2-associated but not Ago1-associated small RNAs [31]. Therefore, our work will establish a new mechanism for the regulation of miRNA homeostasis. Being two closely related argonaute proteins in the same organism, how do AGO1 and AGO10 achieve the differential effects on the same miRNAs? The answer probably resides in their distinct protein sequences. Interestingly, the PAZ domain, which is responsible for binding the 3’ end of the

small RNA, is interchangeable between AGO1 and AGO10 [20]. This finding suggests that the accessibility of small RNAs to the turnover machinery is not completely determined by the binding affinity for the 3' termini of small RNAs, or that other AGO domains also contribute to the 3' end binding affinity. Target regulation and protein interactions may also play a role in the process. Arabidopsis AGO4, AGO6 and AGO9 are very closely related and have similar preferences for the associated endogenous siRNAs. It will be interesting to know if they affect the stability of the associated small RNAs differently.

Small RNA tailing and truncation happen after RISC loading

In *hen1* mutants, both strands in the small RNA duplexes lack methyl modification on their 3' termini. However, the two strands are not affected equally in terms of 3' truncation and uridylation. For example, miR165/166 species are tailed and/or truncated to a larger extent than the star strands (Figure 3.2B-E). This suggests that 3' tailing and truncation happen after the small RNAs are loaded into RISCs. We noticed that the tailed-only miR165/166 are relative low as compared to the truncated-only species and the truncated-and-tailed species in both *hen1-1* and *hen1-8* libraries. Moreover, many truncated-and-tailed miR165/166 species have the same extent of 3' truncation. This suggests that the 3'-5' exonuclease has higher accessibility to miR165/166 than the tailing enzyme or that truncation precedes tailing during the degradation of unmethylated miRNA165/166. We also note that, in both Col and *35S::YFP-AGO10* plants, some miRNAs have relatively high levels of 3' tailing and/or

truncation. Strikingly, for these miRNAs, the AGO1-bound species also contain higher proportions of 3' tailed and/or truncated species, suggesting that turnover could happen when the small RNAs are still in association with AGO (Figure 3.10). However, the situation is different for miR165/166, in that the majority of the small RNA reads in either AGO1 or AGO10 RISCs were full length even if the levels of 3' truncated and tailed species were relatively high in *35S::YFP-AGO10* plants from which the AGO1 and AGO10 complexes were purified (Figure 3.5C, D). It's likely that decay of this miRNA happens after it is released from AGO10. Alternatively, the initial 3' modification occurs to AGO10-bound miR165/166 and the modified form is rapidly released for further processing and degradation.

I am carrying out additional experiments to test if the degradation of miRNAs is influenced by miRNA target mRNAs in plants. Considering the downregulation of miRNA levels by miRNA target mimics, which can bind miRNAs but cannot be cleaved by them, it appears that unproductive interactions between miRNAs and target mRNAs lead to miRNA degradation [18]. However, whether natural targets influence miRNA stability needs to be confirmed biochemically.

Functional specificity of AGO10 in land plants

The numbers of Ago proteins vary across well-characterized model organisms, indicating different degrees of functional diversification and specification (reviewed in [32]). In addition to the diversified preferences for associated small RNAs, different effects on small RNA stability could be another

parameter for the functional diversification and specification among AGO paralogs in any organism. The specific interaction between AGO10 and miR165/166 is analogous to the specific interaction between AGO7 and miR390 in *Arabidopsis* even though the two miRISCs have different molecular and biological functions [33]. AGO10 sequesters and represses miR166/165 to prevent them from binding to AGO1 and downregulating the target genes. But why would plants evolve such an argonaute protein to downregulate miR165/166 rather than to tune down the transcription of *MIR165/166* in the meristems, which seems to be more energy efficient? Our hypothesis is that AGO10 ensures the elimination of miR165/166 from the domain that expresses AGO10, such as the adaxial side of organ primordia. Because miRNAs can move across a few cell layers, even though the transcription of *MIR165/166* genes can be repressed on the adaxial side, AGO10 is still necessary to clear the molecules that move from the abaxial side.

Given the special partnership between AGO10 and miR165/166 in Arabidopsis, it is intriguing to determine whether the two always co-exist in land plants. miR165/166 and its target genes are conserved (except *CrHB1*) in all lineages of land plants, including bryophytes, lycopods, ferns and seed plants [34,35]. Moreover, the *HD-Zip III* mRNAs from the representatives of each land-plant group are cleaved at the miRNA targeting sequences as in Arabidopsis, indicating that this level of *HD-Zip III* regulation is conserved across land plants [34,35]. However, AGO10 homologs were not identified in *P. patens* and *S.*

moellendorffii genomes where AGO1 homologs were identified (Figure 3.11), indicating that AGO10 function is not needed in bryophytes and lycopods. Consistently, the expression patterns of two *HD-Zip III* homologs from *S. kraussiana,* an early diverging vascular plant*,* indicate an ancestral role of these genes in vascular development and organ initiation but not in organ polarity specification [35]. It's likely that AGO10 is evolved to modify the regulation of *HD-Zip III* genes by miR165/166 in meristems and organ primordia. However, there could be other functions for AGO10 in flowering plants, since AGO10 has been found to act in the repression of target mRNA translation for several miRNAs.

Materials and Methods

Plant Materials

Plants for genetic and phenotypic analysis were grown in soil at 23°C, while seedling tissues were harvested from plants grown on MS plates in the growth chamber. All plants were grown under continuous light. *hen1-8* [36], *sdn1-1 sdn2-1* [23], and *ntp4* (gabi-kat 367H02) are in the Col ecotype. *hen1-1*, *hen1-2*, *pnh-1*, *pnh-2*, *ago10-13*, *ag-10*, *ag-10 ago10-13* are in the L*er* ecotype and are previously described [3,14,36]. The primers used for genotyping are listed in Table 3.1.

Plasmid construction and plant transformation

The full-length *AGO10* gene was amplified using gene specific-primers (AGO10GDONRF and AGO10DONRR(+)) containing sequences for BP reaction.

The AGO10 clone in the Gateway Entry vector was moved into pEarleyGate104 using LR reaction. The clone was sequenced to ensure the lack of mutations. Col plants were transformed with the floral dipping method [37]. The primers used for cloning are listed in Table 3.1.

RNA extraction and analysis

Total RNA was extracted using TRI-reagent (Molecular Research Center, Inc.). For RT-PCR, total RNA was treated with DNase I (Roche) and purified with RNA Clean and Concentrator kit (Zymo Research). RNA was converted to cDNA with ReverseAid (Fermentas) using an oligo(dT) primer or both an oligo(dT) and a pre-miR166 gene-specific primer (listed in Table 3.1). *AGO10* mRNA levels were examined by RT-PCR with gene-specific primers (listed in Table 3.1). pri-miR165/166 and pre-miR166a levels were examined by real-time RT-PCR in triplicates using SYBR Green Supermix (Bio-Rad) in MyiQ Cycler (Bio-Rad) with gene-specific primers (listed in Table 3.1). Values were obtained by normalizing to *UBIQUITIN5*. Northern blotting to detect miRNAs was performed as described [3]. Northern blotting to detect pre-miR166a was performed as described [38]. All probe sequences are listed in Table S1. Small RNA libraries were prepared using the Illumina Tru-Seq kit and sequenced with Illumina's HiSeq2000 platform at the UCR Institute for Integrative Genome Biology (IIGB) genomic core facility.

Protein purification and biochemical analysis

The GST-SDN1 protein was expressed and purified as described [23]. AGO1 and AGO10 complexes were purified from *35S::YFP-AGO10* seedlings

with anti-AGO1 and anti-GFP antibodies, respectively, as described [3]. The IP complexes were resolved in RISC buffer (20 mM Tris HCl pH 7.5, 300 mM NaCl, 5 mM $MgCl_2$, 5 mM DTT, 1% (v/v) protease inhibitor cocktail (Roche)). An *in vitro* miR165/166 degradation assay was performed by incubation of AGO1 and AGO10 IP complexes with purified GST-SDN1 in a time course in RISC buffer containing 1 mM ATP in a 50 ul reaction system at room temperature. Following incubation, the AGO complexes were collected by centrifugation, and the associated RNAs were isolated and subjected to northern blotting. The semi-*in vitro* miR166 degradation assay was performed as follows: A synthesized 3' methylated miR166 RNA oligonucleotide was labeled with P^{32} at the 5' end using T4 PNK (NEB) and purified with G-25 columns (GE Healthcare). The miR166-me probes were incorporated into AGO1 or AGO10 complexes by incubating the miRNA and the AGO IP from plants for two hours at room temperature; then unincorporated miR166-me was removed by SDN1 treatment for one hour; SDN1 was then removed by 4 times of rinses with RISC buffer at room temperature. 20 ul of IP complexes containing the miR166-me were incubated with 8 ul of wheat germ extract (WGE) supplemented with 2 mM ATP. The supernatant and IP complexes were separated, boiled in 2 X small RNA loading buffer (80% Formamide, 0.1% Xylene FF, 0.1% Brophenol Blue), and the RNAs were resolved in 15% 7M urea gels.

Bioinformatic analysis of miRNAs

The libraries were analyzed through a computational pipeline developed at Blake Meyers' laboratory. The normalized abundance (TP2M, transcripts per 2 million) was used to perform the comparison among libraries. The truncation and/or tailing of miRNAs were examined with a newly developed computational pipeline in which the sRNA reads that cannot be perfectly mapped back to genome are mapped back to genome by continuous removal of their 3' nucleotides, one nucleotide at a time. Thus, the non-genome-matched sRNA reads can be divided into two parts: the longest 5' genome-matched component (5GMC), and a 3' "tail"; For the genome-matched sRNA reads, 5GMC will be the same as the read and the tail will be null. The 5GMC of each read was compared to all annotated miRNAs in miRBase [16] for their origin and for the lack of 3' nucleotides, which would indicate 3' truncation.

Phylogenetic analysis

Phylogenetic analysis was performed using the ClustalW2 online tool [39]. The AGO1 and AGO10 homologs were obtained through BLASTp against full-length amino acid sequences of Arabidopsis AGO1 and AGO10 proteins.

Figures

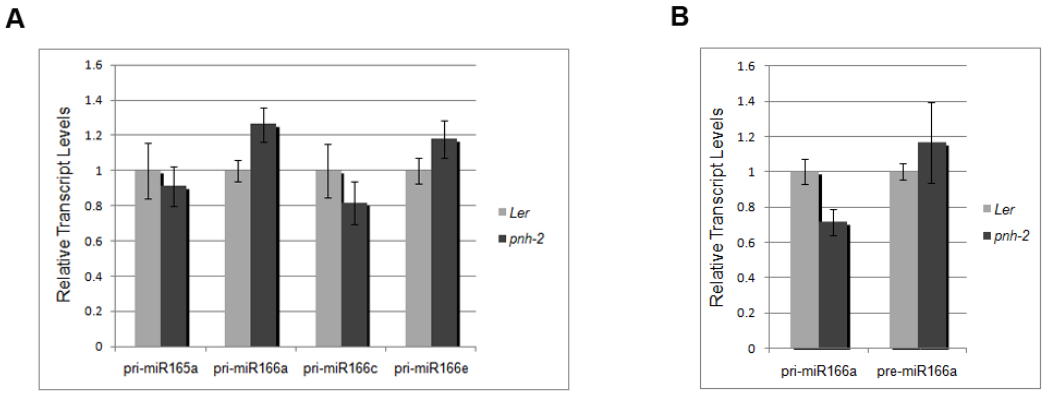

Figure 3.1 Accumulation of pri-/pre-miR165/166 in wild type (Ler) and the pnh-2 mutant

(A) Real-time RT-PCR showing that the levels of pri-miR165/166 are not changed in *pnh-2* seedlings. (B) Real-time RT-PCR showing that the accumulation of pri-miR166a (left) or the summed accumulation of pri-miR166a and pre-miR166a (right) is not changed in *pnh-2* seedlings.

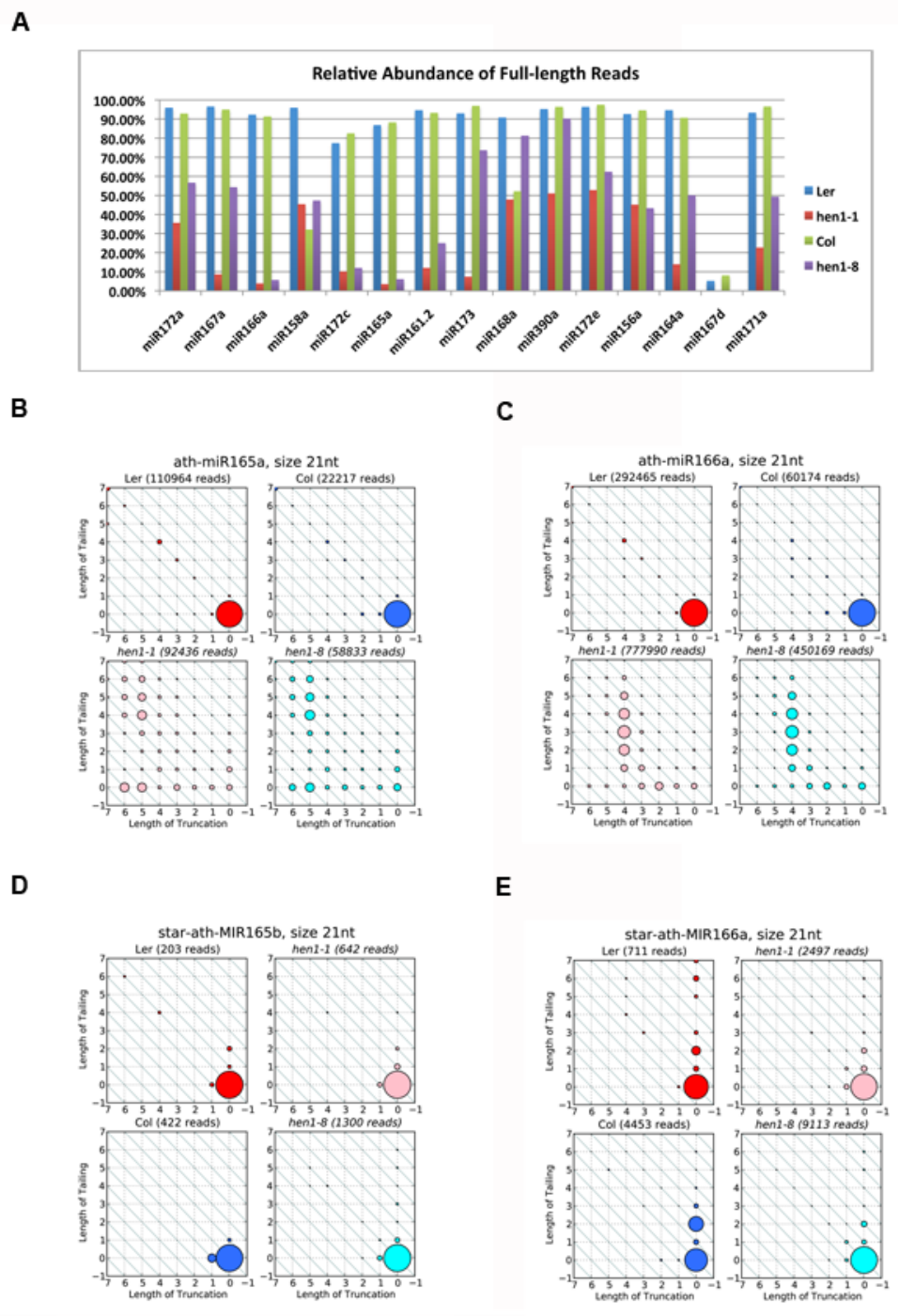

Figure 3.2 miR165/166 is preferentially truncated and tailed in hen1 mutants

(A) Percentage of full-length species of miRNAs in inflorescence tissues of Col, L*er*, *hen1-1* and *hen1-8*. The miRNAs presented are the top 15 in abundance in

L*er*. The proportion of full-length miR165/166 reduced dramatically and consistently in *hen1-1* and *hen1-8* as compared with L*er* and Col. (B, C) Matrices representing the profiles of miR165 (B) or miR166 (C) species with varying 3' ends in L*er* (represented by red circles), Col (represented by blue circles), *hen1-1* (represented by pink circles) and *hen1-8* (represented by cyan circles) genotypes. The X-axis represents the number of 3' truncated nucleotides, while the Y-axis represents the number of 3' added nucleotides. The sizes of the circles are proportional to the relative abundance of the species as determined by high throughput sequencing. The matrices show that miR165/166 species are highly truncated and tailed in both *hen1-1* and *hen1-8*. (D, E) Matrices representing the profiles of miR165b* (D) or miR166a* (E) species with varying 3' ends in L*er*, Col, *hen1-1* and *hen1-8* genotypes. The same color and quantification codes were used as in (B, C). The matrices show that miR165b* and miR166a* are rarely affected by tailing and truncation at their 3' termini in the *hen1* mutants.

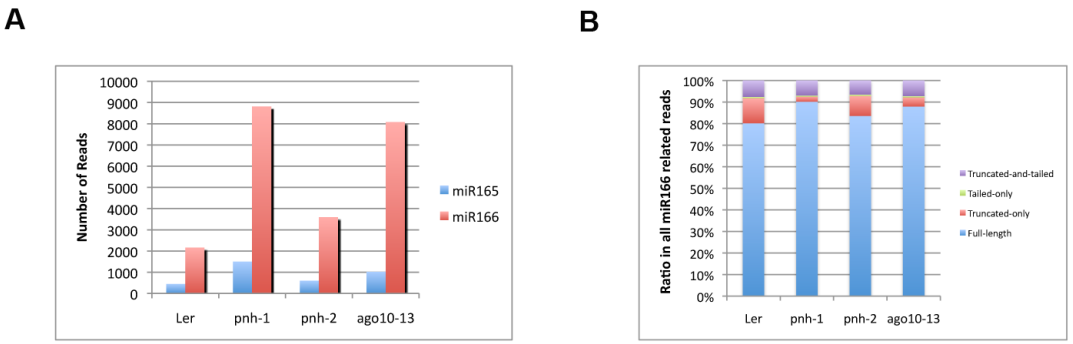

Figure 3.3 Degradation of miR165/166 is reduced in ago10 mutants

(A) Reads of full-length miR165 and miR166 in the sRNA libraries from L*er*, *pnh-1*, *pnh-2* and *ago10-13* seedling tissues. miR166 is represented by more reads than miR165 in the libraries. The levels of miR165 and miR166 are higher in *ago10* mutants. (B) A column diagram showing the proportions of full-length, truncated-only, tailed-only, and truncated-and-tailed miR166 in L*er* and *ago10* mutants. The chart indicates that the proportion of full-length miR166 is mildly increased in *ago10* mutants, while the proportion of truncated-only miR166 is mildly reduced in *ago10* mutants.

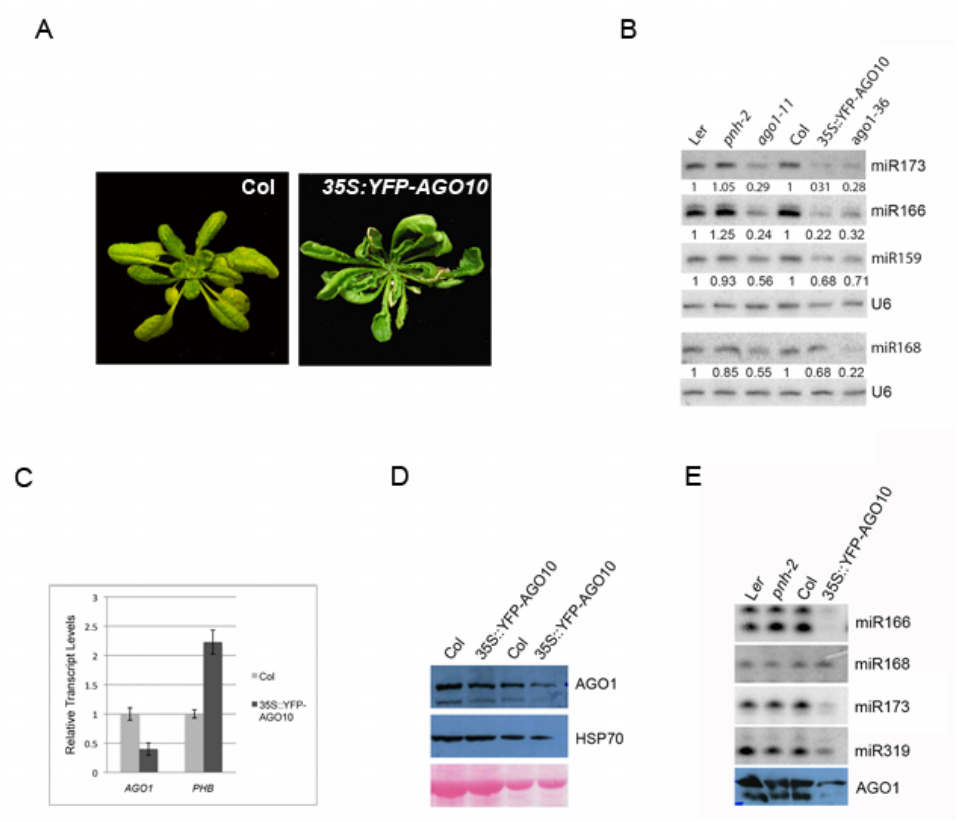

Figure 3.4 Characterization of 35S::YFP-AGO10 plants

(A) Severe morphological phenotypes of *35S::YFP-AGO10* plants, indicated by the upwardly curled and serrated leaves. (B) Northern blotting of miR159, miR166, miR168 and miR173 in L*er*, *pnh-2*, *ago1-11*, Col, *35S::YFP-AGO10* and *ago1-36* seedlings. The levels of these miRNAs are reduced in *35S::YFP-AGO10* and the two *ago1* mutants. (C) Real-time RT-PCR of *AGO1* and *PHB* in Col and *35S::YFP-AGO10* plants. *AGO1* mRNA levels are reduced, while the levels of *PHB* mRNA are increased in *35S::YFP-AGO10* (D) Western blotting to examine AGO1 protein levels in Col and *35S::YFP-AGO10*. Both Heat Shock Protein 70 (HSP70) and the staining of the membrane served to indicate the relative amounts of samples used. The levels of AGO1 are reduced in *35S::YFP-AGO10*

plants. (E) AGO1 protein was immunoprecipitated from L*er*, *pnh-2*, Col and *35S::YFP-AGO10* samples. RNAs and proteins were extracted from the IP complexes at the same time with Tri-reagent and subjected to northern blotting (for various miRNAs) and western blotting (for AGO1 protein), respectively.

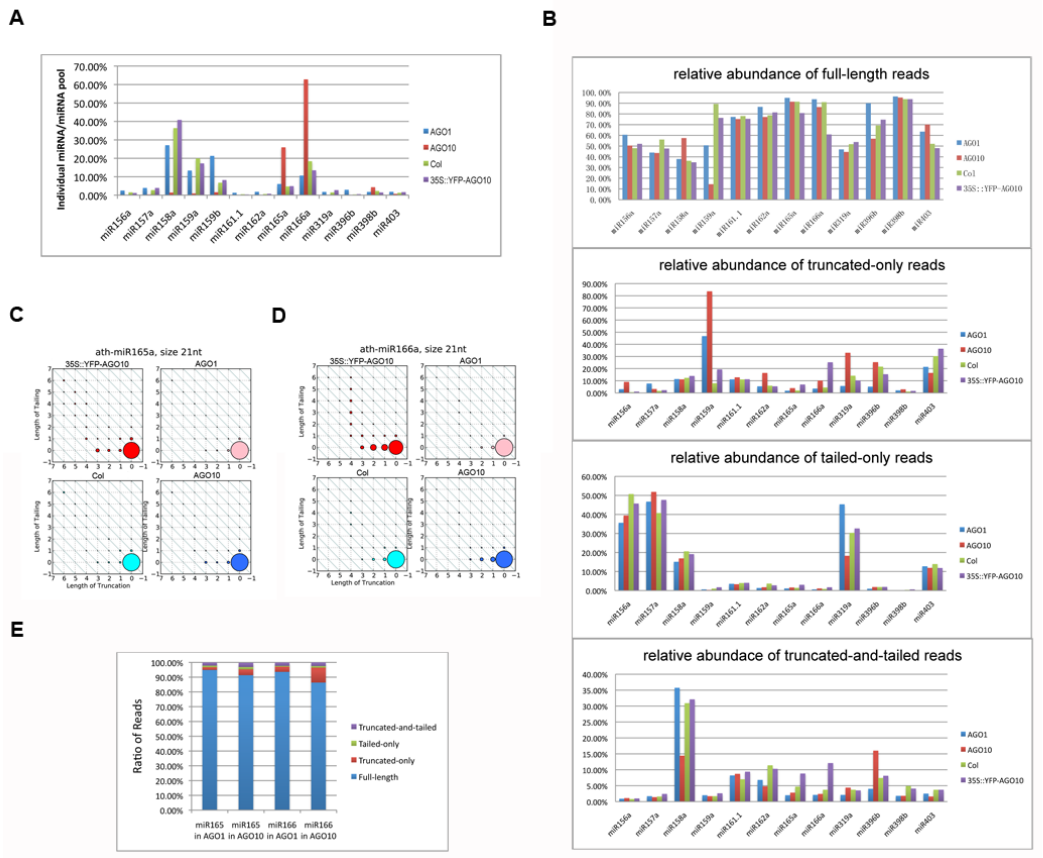

Figure 3.5 Degradation of miR165/166 in 35S::YFP-AGO10

(A) Relative abundance of individual miRNAs in the total miRNA pool in the AGO1 IP (AGO1), AGO10 IP (AGO10), Col, and *35S::YFP-AGO10* sRNA libraries. Only the miRNAs that composed of at least 1.0% of the total miRNA reads in at least one library were shown in the chart for simplicity. miR165/166 is the predominant species among AGO10-associated, but not AGO1-associated miRNAs. (B) Relative abundance of full-length, truncated-only, tailed-only, and truncated-and-tailed miRNA species for each miRNA in AGO1- or AGO10-associated sRNA libraries and Col and *35S::YFP-AGO10* sRNA libraries. The miRNAs included in (A) were selected for consistency. (C, D) Matrices

representing the profiles of miR165 (C) or miR166 (D) species with varying 3' ends in Col (represented by cyan circles), *35S::YFP-AGO10* (represented by red circles), AGO1 IP(represented by pink circles) and AGO10 IP (represented by blue circles). The tailing and truncation of miR165/166 are increased in *35S::YFP-AGO10* relative to Col. However, both AGO1 and AGO10 preferentially associate with full-length miR165/166. (E) Proportions of full-length, truncated-only, tailed-only and truncated-and-tailed miR165 and miR166 in the AGO1 and AGO10 IPs.

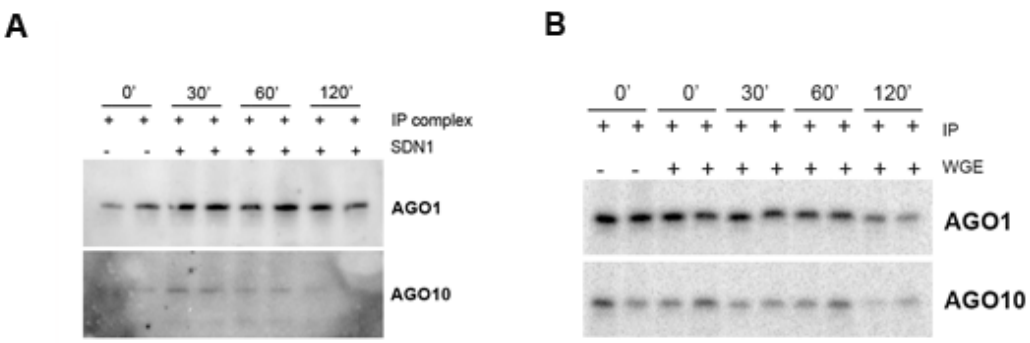

Figure 3.6 Decay of AGO-associated miR165/166

(A) Northern blotting of miR166 after a time course of incubation of AGO1 and AGO10 IP with GST-SDN1. No obvious changes were observed for AGO1-associated miR166, but AGO10-associated miR166 was gradually reduced over time. (B) A degradation assay of AGO1-/AGO10-associated miR166-me in wheat germ extract (WGE). A radiolabeled miR166-me was first incorporated into AGO1 or AGO10 IP and then incubated for the indicated periods of time in WGE. The amount of miR166-me was monitored by gel electrophoresis followed by autoradiography.

Supplemental Materials

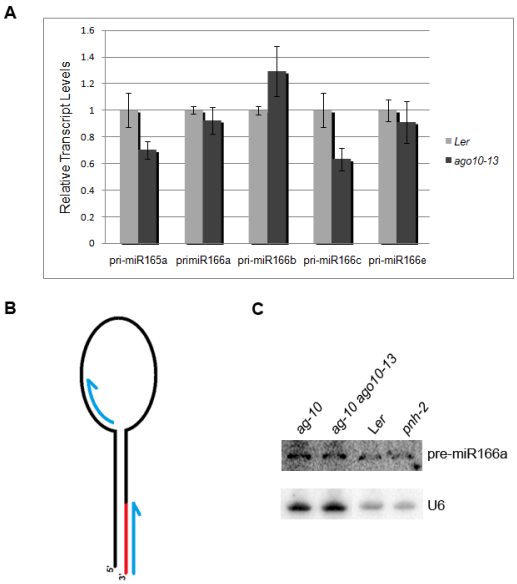

Figure 3.7 Examination of pri-/pre-miR165/166 in ago10 mutants

(A) Real-time RT-PCR showing that the levels of pri-miR165/166 are similar between wild type and the *ago10-13* mutant. (B) A schematic diagram of primers used to examine the levels of the sum of pri-miR166a and pre-miR166a by RT-PCR. The stem-loop structure represents the pre-miR166a with the mature miR166 sequence indicated by the red line. The blue arrows indicate the positions of the gene-specific primers used for the reverse transcription and real-time RT-PCR. The one matching to the 3' end was used in reverse transcription. (C) Northern blotting showing that the levels of pre-miR166a is not changed in the *ago10* mutants relative to wild type.

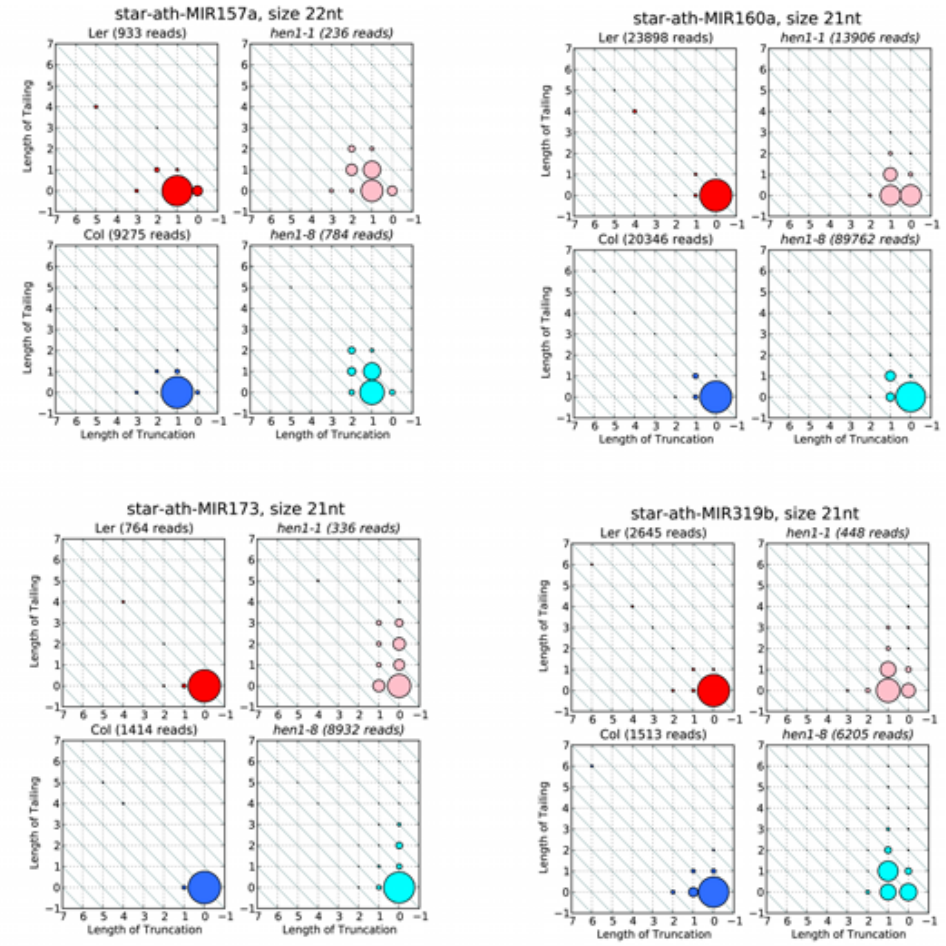

Figure 3.8 Tailing and truncation of several miRNA strands in hen1 mutants*
Matrices representing the profiles of sRNA species with varying 3' ends from miR157a*, miR160a*, miR173* and miR319b* in L*er* (represented by red circles), Col (represented by blue circles), *hen1-1* (represented by pink circles) and *hen1-8* (represented by cyan circles). The X-axis represents the number of 3' truncated nucleotides, while the Y-axis represents the number of 3' added nucleotides.

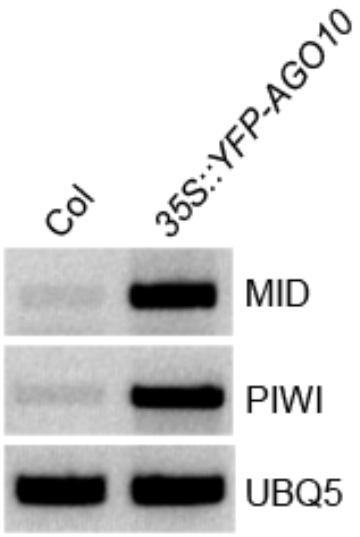

Figure 3.9 RT-PCR examining the levels of AGO10 mRNA in Col and 35S::YFP-AGO10 plants

AGO10 plants. The gene specific primers amplify the AGO10 MID domain and PIWI domain, respectively. In *35S::YFP-AGO10*, the endogenous *AGO10* gene and the transgene were simultaneously detected.

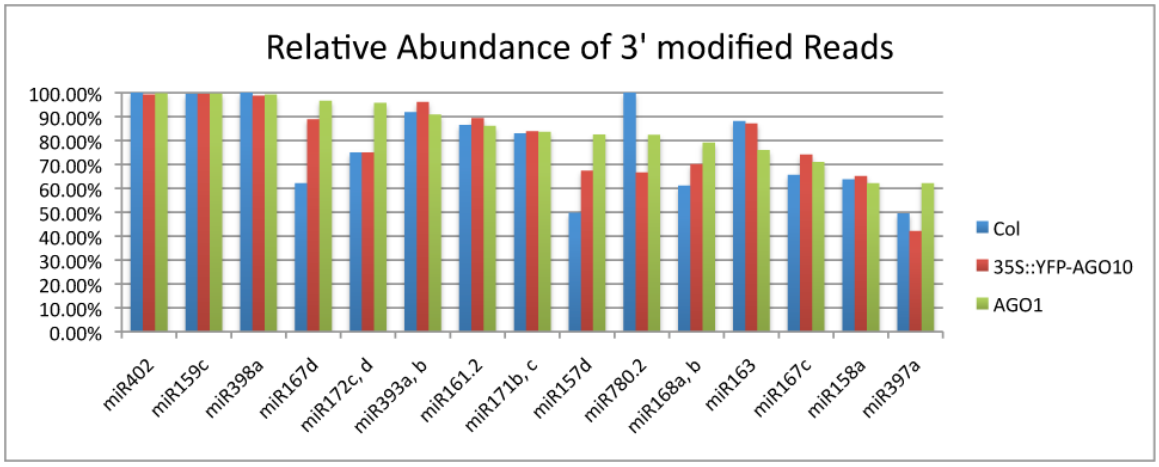

Figure 3.10 Relative abundance of non-intact species of miRNAs in Col, 35S::YFP-AGO10 and IP

The proportion of non-intact species, including truncated-only, tailed-only and truncated-and-tailed species of miRNAs in Col, *35S::YFP-AGO10* and AGO1 IP complex. The top 15 miRNAs with highest frequeces of 3' modification are presented.

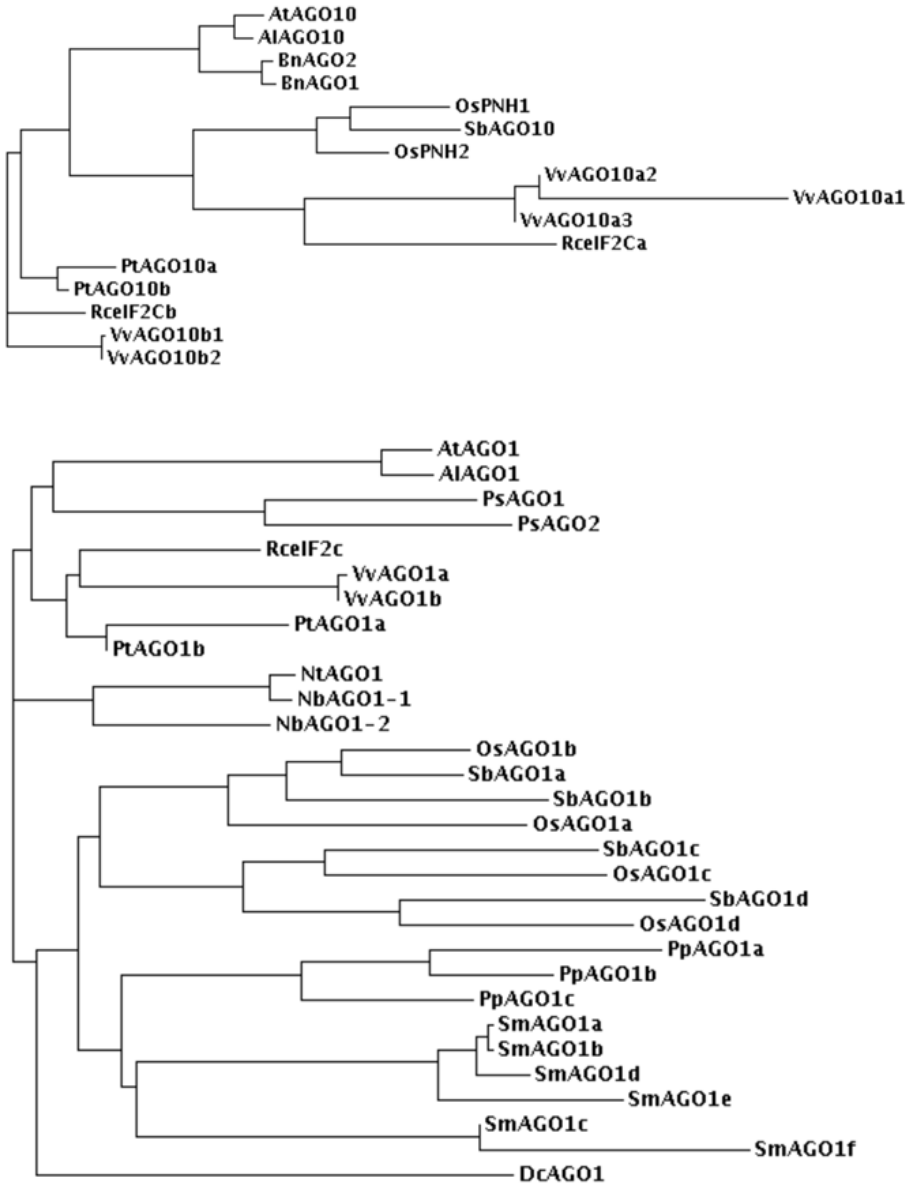

Figure 3.11 Phylogeny of AGO1 and AGO10 in land plants

Phylogenetic trees of AGO1 and AGO10 orthologs in plant species.

Abbreviations: At: *Arabidopsis thaliana*; Al: *Arabidopsis lyrata*; Bn: *Brassica napus*; Os: *Oryza sativa*; Sb: *Sorgum bicolor*; Vv: *Vitis vinifera*; Rc: *Ricinus*

communis; Pt: *Populus trichocarpa*; Nb: *Nicotiana benthamiana*; Nt: *Nicotiana tabaum*; Ps: *Pisum sativum*; Dc: *Daucus carota*; Pp: *Physcomitrella patens*; Sm: *Selaginella moesllendorffii*

Tables

Table 3.1 Sequences of oligos used in the study

Oligo Name	Sequence	Usage
pnh-2F	CTACCTTTGTAGCCATGCGGGAATT	pnh-2 genotyping
pnh-2R	CTCGTCCCAAAGAACATGGTA	
sdn1-1-GF	CACAATTTAAGCATACAATATA	sdn1-1 genotyping
sdn1-1-GR	CAACATCGGATACAAACCAGTC	
sdn2-1-GF	AGCTTGCTTGTTCAACA TCTC	sdn2-1 genotyping
snd2-1-GR	AGTAAGAAAAGCCACCAAATC	
GK367 GT-F	CTGGTTCTGTGATTGTTAGGTG	ntp4 genotyping
GK367 GT-R	GAGACCAACAGCTCCGAGA	
AGO10GDONRF	ggggacaagtttgtaacaaaaaagcaggcttcAATTGAT TGCCGAATTGCATT	35S::YFP-AGO10 cloning
AGO10DONRR(+)	ggggaccactttgtacaagaaagctgggtcTTAGCAGT AGAACATTACTCTC	
AGO10_MID_XhoI_F	CCGctcgagGAGGGACAACGGTACACGAAA	AGO10 MID domain
AGO10_MID_SpeI_R	GGactagtAAGCTCTAACTCTTTGCCTTTG	
AGO10_PIWI_SpeI_F	GGactagtCTGCTGGCAATATTACCTGATA	AGO10 PIWI domain
AGO10_PIWI_SalI_R	ACGCgtcgacTTAGCAGTAGAACATTACTCT CT	
primiR165a-F	tggtgatcagaggcaataaca	pri-miR165a real-time
primiR165a-R	ccatcatcaccattcaccaa	
pri-miR166a_rt_f2	ctttctcttttgaGGGGACTGTT	pri-miR166a real-time
pri-miR166a_rt_r2	aatatggagtaaacagggagcaa	
primiR166b-F	ATC ATT CTC TTC ATC ATC ACC A	pri-miR166b real-time
primiR166b-R	CCC TCT TTA AAT CCT CTT CTT CT	
primiR166c-F	ACA TAC CTT TCT TTC TCT TCT TCT	pri-miR166c real-time
primiR166c-R	CAA GAC TAG AAC CAC GTT ATC A	
primiR166e-F	tcaaagaaggaaagatcgaagc	pri-miR166e real-time
primiR166e-R	ttcagtgaagcttttccttttg	
pre-miR166a_loop-F	TGT TGG ATC TCT TTC GAT CTA	Pre-miR166a real-time
pre-miR166a_stem-r	GGG GAA TGA AGC CTG GTC CGA	

References

1. Moussian B, Schoof H, Haecker A, Jurgens G, Laux T (1998) Role of the ZWILLE gene in the regulation of central shoot meristem cell fate during Arabidopsis embryogenesis. EMBO J 17: 1799-1809.

2. Lynn K, Fernandez A, Aida M, Sedbrook J, Tasaka M, et al. (1999) The PINHEAD/ZWILLE gene acts pleiotropically in Arabidopsis development and has overlapping functions with the ARGONAUTE1 gene. Development 126: 469-481.

3. Ji L, Liu X, Yan J, Wang W, Yumul RE, et al. (2011) ARGONAUTE10 and ARGONAUTE1 regulate the termination of floral stem cells through two microRNAs in Arabidopsis. PLoS Genet 7: e1001358.

4. Liu Q, Yao X, Pi L, Wang H, Cui X, et al. (2008) The ARGONAUTE10 gene modulates shoot apical meristem maintenance and leaf polarity establishment by repressing miR165/166 in Arabidopsis. Plant J.

5. Zhu H, Hu F, Wang R, Zhou X, Sze SH, et al. (2011) Arabidopsis Argonaute10 specifically sequesters miR166/165 to regulate shoot apical meristem development. Cell 145: 242-256.

6. Reinhart BJ, Weinstein EG, Rhoades MW, Bartel B, Bartel DP (2002) MicroRNAs in plants. Genes Dev 16: 1616-1626.

7. Kidner CA, Martienssen RA (2004) Spatially restricted microRNA directs leaf polarity through ARGONAUTE1. Nature 428: 81-84.

8. Kim J, Jung JH, Reyes JL, Kim YS, Kim SY, et al. (2005) microRNA-directed cleavage of ATHB15 mRNA regulates vascular development in Arabidopsis inflorescence stems. Plant J 42: 84-94.

9. Jung JH, Park CM (2007) MIR166/165 genes exhibit dynamic expression patterns in regulating shoot apical meristem and floral development in Arabidopsis. Planta 225: 1327-1338.

10. Xie Z, Khanna K, Ruan S (2010) Expression of microRNAs and its regulation in plants. Semin Cell Dev Biol 21: 790-797.

11. Nogueira FT, Chitwood DH, Madi S, Ohtsu K, Schnable PS, et al. (2009) Regulation of small RNA accumulation in the maize shoot apex. PLoS Genet 5: e1000320.

12. Nogueira FT, Madi S, Chitwood DH, Juarez MT, Timmermans MC (2007) Two small regulatory RNAs establish opposing fates of a developmental axis. Genes Dev 21: 750-755.

13. Schmittgen TD (2008) Regulation of microRNA processing in development, differentiation and cancer. J Cell Mol Med 12: 1811-1819.

14. Yu B, Yang Z, Li J, Minakhina S, Yang M, et al. (2005) Methylation as a crucial step in plant microRNA biogenesis. Science 307: 932-935.

15. Li J, Yang Z, Yu B, Liu J, Chen X (2005) Methylation protects miRNAs and siRNAs from a 3'-end uridylation activity in Arabidopsis. Curr Biol 15: 1501-1507.

16. Kozomara A, Griffiths-Jones S (2011) miRBase: integrating microRNA annotation and deep-sequencing data. Nucleic Acids Res 39: D152-157.

17. Newman KL, Fernandez AG, Barton MK (2002) Regulation of axis determinacy by the Arabidopsis PINHEAD gene. Plant Cell 14: 3029-3042.

18. Todesco M, Rubio-Somoza I, Paz-Ares J, Weigel D (2010) A collection of target mimics for comprehensive analysis of microRNA function in Arabidopsis thaliana. PLoS Genet 6: e1001031.

19. Liu Z, Jia L, Wang H, He Y (2011) HYL1 regulates the balance between adaxial and abaxial identity for leaf flattening via miRNA-mediated pathways. J Exp Bot 62: 4367-4381.

20. Mallory AC, Hinze A, Tucker MR, Bouche N, Gasciolli V, et al. (2009) Redundant and specific roles of the ARGONAUTE proteins AGO1 and ZLL in development and small RNA-directed gene silencing. PLoS Genet 5: e1000646.

21. Vaucheret H, Mallory AC, Bartel DP (2006) AGO1 homeostasis entails coexpression of MIR168 and AGO1 and preferential stabilization of miR168 by AGO1. Mol Cell 22: 129-136.

22. Liu Q, Zhang YC, Wang CY, Luo YC, Huang QJ, et al. (2009) Expression analysis of phytohormone-regulated microRNAs in rice, implying their regulation roles in plant hormone signaling. FEBS Lett 583: 723-728.

23. Ramachandran V, Chen X (2008) Degradation of microRNAs by a family of exoribonucleases in Arabidopsis. Science 321: 1490-1492.

24. Baccarini A, Chauhan H, Gardner TJ, Jayaprakash AD, Sachidanandam R, et al. (2011) Kinetic analysis reveals the fate of a microRNA following target regulation in mammalian cells. Curr Biol 21: 369-376.

25. Tang G, Reinhart BJ, Bartel DP, Zamore PD (2003) A biochemical framework for RNA silencing in plants. Genes Dev 17: 49-63.

26. Ibrahim F, Rymarquis LA, Kim EJ, Becker J, Balassa E, et al. (2010) Uridylation of mature miRNAs and siRNAs by the MUT68 nucleotidyltransferase promotes their degradation in Chlamydomonas. Proc Natl Acad Sci U S A 107: 3906-3911.

27. Diederichs S, Haber DA (2007) Dual role for argonautes in microRNA processing and posttranscriptional regulation of microRNA expression. Cell 131: 1097-1108.

28. Tomari Y, Du T, Zamore PD (2007) Sorting of Drosophila small silencing RNAs. Cell 130: 299-308.

29. Mi S, Cai T, Hu Y, Chen Y, Hodges E, et al. (2008) Sorting of small RNAs into Arabidopsis argonaute complexes is directed by the 5' terminal nucleotide. Cell 133: 116-127.

30. van Wolfswinkel JC, Claycomb JM, Batista PJ, Mello CC, Berezikov E, et al. (2009) CDE-1 affects chromosome segregation through uridylation of CSR-1-bound siRNAs. Cell 139: 135-148.

31. Ameres SL, Horwich MD, Hung JH, Xu J, Ghildiyal M, et al. (2010) Target RNA-directed trimming and tailing of small silencing RNAs. Science 328: 1534-1539.

32. Hutvagner G, Simard MJ (2008) Argonaute proteins: key players in RNA silencing. Nat Rev Mol Cell Biol 9: 22-32.

33. Montgomery TA, Howell MD, Cuperus JT, Li D, Hansen JE, et al. (2008) Specificity of ARGONAUTE7-miR390 interaction and dual functionality in TAS3 trans-acting siRNA formation. Cell 133: 128-141.

34. Floyd SK, Bowman JL (2004) Gene regulation: ancient microRNA target sequences in plants. Nature 428: 485-486.

35. Prigge MJ, Clark SE (2006) Evolution of the class III HD-Zip gene family in land plants. Evol Dev 8: 350-361.

36. Yu B, Bi L, Zhai J, Agarwal M, Li S, et al. (2010) siRNAs compete with miRNAs for methylation by HEN1 in Arabidopsis. Nucleic Acids Res 38: 5844-5850.

37. Clough SJ, Bent AF (1998) Floral dip: a simplified method for Agrobacterium-mediated transformation of Arabidopsis thaliana. Plant J 16: 735-743.

38. Kurihara Y, Takashi Y, Watanabe Y (2006) The interaction between DCL1 and HYL1 is important for efficient and precise processing of pri-miRNA in plant microRNA biogenesis. RNA 12: 206-212.

39. Goujon M, McWilliam H, Li W, Valentin F, Squizzato S, et al. (2010) A new bioinformatics analysis tools framework at EMBL-EBI. Nucleic Acids Res 38: W695-699.

4. Conclusions and Perspectives

The research in my dissertation has furthered our knowledge on the functions of argonaute proteins. Arabidopsis AGO10 is unique in its mode of action in that it represses the activities and levels of miR165/166 through specific interaction with and destabilization of this miRNA. So far, the functions of most Arabidopsis argonaute proteins, except AGO3 and AGO5, have been characterized (reviewed in [1]). It has been elucidated how they act in gene expression regulation, plant immunity, RNA-directed DNA methylation and ta-siRNA biogenesis (reviewed in [1]). However, many aspects of argonaute functions still deserve extensive investigation. There are several major open questions.

First, Arabidopsis miRNAs, in complex with argonaute proteins, could downregulate their targets through both mRNA cleavage and translational repression. Moreover, the level of mRNA cleavage and translational repression varies in individual miRNA–target interactions. For example, translational repression is dominant in the regulation by miR172 and miR156/7 [2-4]. In animals, target RNA degradation often co-exists with translational repression, even though the two events could be uncoupled [5]. It's not very clear if Arabidopsis AGO1 can reduce the stability of miRNA target RNAs without causing their cleavage. Moreover, the relative contribution of mRNA cleavage and translational repression to the function of AGO1-miRNA RISC hasn't been

determined in plants. It's not yet known to what extent the endonuclease activity is required for the functions of other argonaute proteins either. Therefore, the characterization of slicer-defective AGO proteins would be necessary to dissect the roles of sequence-specific cleavage, translation repression and RNA degradation in target gene regulation. These studies may reveal a broader scope of activities of small RNAs and argonaute proteins. If slicer-defective argonaute proteins are able to regulate target transcripts, we may need to revise the way to identify small RNA targets in plants. Could RNA transcripts containing target sites with lower complementary to small RNAs also serve as targets in plants? The interactions between target RNAs and RISCs should be subjected to systemic investigation to achieve a comprehensive understanding of the scope of actions of RISCs to lay the foundation for a full appreciation of the functions of small RNAs in various biological processes.

Second, the activities of argonaute proteins are regulated in the context of different small RNA pathways. For example, AGO10 possesses endonuclease activity *in vitro* and is able to repress the translation of miRNA targets in planta. However, the downregulation of *HD-Zip III* genes by AGO10 is inhibited by as yet unknown factors. One major attempt in the future is to uncover the mechanisms that regulate the activities of argonaute proteins *in vivo*. For example, what are the factors that determine the level of RNA cleavage and translational repression activities of individual AGO-miRNA RISCs? What determines the ability of miRNAs of 22 nt to trigger the initiation of ta-siRNA biogenesis? It will be

essential to identify the partners of argonaute proteins (i.e. associated small RNAs and interacting proteins) and to understand how the specificities are realized in various tissue and developmental contexts. In addition, the protein factors bound to the target RNAs could influence the outcomes of the interactions between RISCs and target RNAs. Furthermore, identification of post-translational modifications would be of great help to understand the functional diversification and specification of argonaute proteins. In mammals, hydroxylation, phosphorylation and ubiquitylation have been found on argonaute proteins (reviewed in [6]), indicating argonaute proteins are embedded in complex cellular signaling networks. A detailed structural characterization of argonaute proteins in conjunction with their associated small RNAs will enable us to understand the underlying mechanisms regulating the functions of argonaute proteins.

Third, how are the dynamics of AGO-small RNA complexes regulated? Many important and exciting findings have been reported for small RNA turnover and its regulation even though this area only became a main focus in RNA silencing very recently. Many novel mechanisms are still awaiting discovery in this field. Additional questions include but are not limited to: What's the fate of argonaute protein following the turnover of associated-small RNAs? Are the components of RISC recycled or degraded afterwards? How do the associated small RNAs affect the stability of AGO proteins? In plants, miRNAs could diffuse across several cell layers, while siRNAs could traffic systemically. Do AGO proteins play any role in the trafficking of small RNAs?

References

1. Mallory A, Vaucheret H (2010) Form, function, and regulation of ARGONAUTE proteins. Plant Cell 22: 3879-3889.

2. Aukerman MJ, Sakai H (2003) Regulation of flowering time and floral organ identity by a MicroRNA and its APETALA2-like target genes. Plant Cell 15: 2730-2741.

3. Chen X (2004) A microRNA as a translational repressor of APETALA2 in Arabidopsis flower development. Science 303: 2022-2025.

4. Gandikota M, Birkenbihl RP, Hohmann S, Cardon GH, Saedler H, et al. (2007) The miRNA156/157 recognition element in the 3' UTR of the Arabidopsis SBP box gene SPL3 prevents early flowering by translational inhibition in seedlings. Plant J 49: 683-693.

5. Huntzinger E, Izaurralde E (2011) Gene silencing by microRNAs: contributions of translational repression and mRNA decay. Nat Rev Genet 12: 99-110.

6. Johnston M, Hutvagner G (2011) Posttranslational modification of Argonautes and their role in small RNA-mediated gene regulation. Silence 2: 5 doi:10.1186/1758-907X-2-5.

5. Appendix A: Side projects and constructs

In plants, the subcellular compartmentalization of small RNA duplexes and their 3' modification by HEN1 are not very clear. Sequence analysis indicated that HEN1 contains three putative Nuclear Localization Signals (NLSs) and one putative Nuclear Export Signal (NES) (Figure 5.1). To determine the subcellular location where the small RNA duplexes are methylated *in vivo*, a former colleague, Manu Agarwal, generated a series of plant expression plasmids containing YFP-HEN1 and derivatives with mutations in the localization signals. The NLSs were mutated individually or in combination (Table 5.1, 5.3). An additional series of plant expression vectors was also generated to incorporate an exogenous NLS or NES or their mutation versions to YFP-HEN1 (Table 5.4, 5.5). YFP-HEN1 and the mutants were driven by CaMV *35S* promoter in one set of constructs, and by the endogenous *HEN1* promoter in another set of constructs.

I introduced most of the transgenes into *hen1-1* plants. The morphological phenotypes of the transgenic plants indicated that HEN1 might largely function in the nuclei, since when two of the NLS were simultaneously mutated or an exogenous NES was incorporated, the constructs couldn't completely rescue *hen1-1* defects. Namely, HEN1pr::YFP-HEN1, HEN1pr::YFP-HEN1(NLS3), HEN1pr::YFP-mNES-HEN1, HEN1pr::YFP-mNLS-HEN1, 35S::YFP-HEN1, 35S::YFP-HEN1(NLS1), 35S::YFP-HEN1(NLS3) rescued *hen1-1* defects; while HEN1pr::YFP-HEN1(NLS3NLS2), HEN1pr:: YFP-HEN1(NLS3NLS1), 35S::YFP-

HEN1(NLS3NLS2), 35S::YFP-HEN1(NLS3NLS1) and 35S::YFP-NES-HEN1 couldn't completely rescue *hen1-1* defects. However, the YFP signals couldn't be detected under the microscope for the transgenes driven by HEN1 endogenous promoter, even though they could be detected with western blotting. Moreover, immunolocalization with GFP antibody showed that the transgenes driven by the *35S* promoter weren't expressed constitutively. Therefore, we couldn't obtain a very conclusive result about the localization of HEN1 function and I didn't pursue this project further.

Later, some studies on the plant virus RNA silencing suppressor proteins showed that siRNAs derived from cytoplasmically replicating cr-TMV were partially methylated in wild type Arabidopsis, suggesting that HEN1 is also active in the cytoplasm. Moreover, viral siRNAs from the CIRV19stop virus were also completely 3' methylated, while TEV-derived siRNAs have unmethylated 3′-termini. However, TEV infection showed varied effects on the methylation of different miRNAs and miRNA*s in the cytoplasm. The findings suggested that the methylation occurs not only in the nucleus, but also in the cytoplasm.

Putative Nuclear Import-Export signals in HEN1 and mutations

MAGGGKHTPTPKAIIHQKFGAKASYTVEEVHDSSQSGCLGLAIPQKGPCLYRCHLQLPEFSVVSNVF**KKKK**DSEQSA

AELALDKLGIRPQNDDLTVDEARDEIVGRIKYIFSDEFLSAEHPLGAHLRAALRRDGERCGSVPVSVIATVDAKINSRCK

IINPSVESDPFLAISYVMKAAAKLADYIVASPHGL**RRK**NAYPSEIVEALATHVSDSLHSREVAAVYIPCIDEEVVELDTLYI

SSNRHYLDSIAERLGLKDGNQVMISRMFGKASCGSECRLYSEIPKKYLDNSSDASGTSNEDSSHIVKSRNARASYICG

QDIHGDAILASVGYRWKSDDLDYDDVTVNSFYRICCGMSPNGIYKISRQAVIAAQLPFAFTTKSNWRGPLPREILGLFC

HQHRLAEPILSSSTAPVKSLSDIFRSHKKLKVSGVDDANENLSRQKEDTPGLGHGFRCEVKIFTKSQDLVLECSPRKF

YEKENDAIQNASLKALLWFSKFFADLDVDGEQSCDTDDDQDTKSSSPNVFAAPPILQKEHSSESKNTNVLSAEKRVQ

SITNGSVVSICYSLSLAVDPEYSSDGESPREDNESNEEMESEYSANCESSVELIESNEEIEFEVGTGSMNPHIESEVTQ

MTVGEYASFRMTPPDAAEALILAVGSDTVRIRSLLSERPCLNYNI**LLLGVKG**PSEERMEAAFFKPPLSKQRVEYALKHI

RESSASTLVDFGCGSGSLLDSLLDYPTSLQTIIGVDISPKGLARAAKMLHVKLNKEACNVKSATLYDGSILEFDSRLHDV

DIGTCLEVIEHMEEDQACEFGEKVLSLFHPKLLIVSTPNYEFNTILQRSTPETQEENNSEPQLPKFRNHDHKFEWTRE

QFNQWASKLGKRHNYSVEFSGVGGSGEVEPGFASQIAIFRREASSVENVAESSMQPYKVIWEW**KK**EDVE**KKK**TDL

NLS1 mutation KKKK to EEEE
NLS2 mutation RRK to EEE
NLS3 mutation KKEDVEKKKTDL to EEEDVEEEETDL

Figure 5.1 Arabidopsis HEN1 sequence and predicted NLS, NES

Table 5.1

Vector Name	pEarleyGate104-HEN1(NLSx)	Other Name	35S::YFP-HEN1(NLSx)	Construction Time	
Owner	Manu Agarwal	Selection	Kan/Basta	Storage	-80°C

HEN1 CDS was amplified with gene specific primers (Hen1EntryF and Hen1EntryR) and cloned in pENTR/D-topo as per the manufacturer's instruction, the resulting plasmid was named pTOPO-HEN1.

The NLS1 and NLS2 of HEN1 were mutated by site directed mutagenesis using inverse primer pairs (NLS1F/NLS1R and NLS2F/NSL2R) on the pTOPO-HEN1 plasmid.

The NLS3, which is at the very C-terminus of HEN1, was incorporated using

reverse primer (Hen1NLS3R(+)) containing the mutations. The PCR product of Hen1EntryF and Hen1NLS3R(+) was cloned into pENTR/D-topo.

The NLS3NLS1 mutant was made by mutating NLS1 using site directed mutagenesis on pTopo-HEN1(NLS3). The NLS3NLS2 mutant was created in a similar manner. To create the NLS3NLS2NLS1 mutant, NLS2 was mutated using site directed mutagenesis on pTOPO-HEN1(NLS3NLS1).

The pTOPO-HEN1, pTOPO-HEN1(NLS1), pTOPO-HEN1(NLS2), pTOPO-HEN1(NLS3), pTOPO-HEN1(NLS3NLS1), pTOPO-HEN1(NLS3NLS2), and pTOPO-HEN1(NLS3NLS2NLS1) plasmids were sequenced, linearized, and recombined with pEarleyGate104 by LR reaction.

Hen1EntryF: caccATGGCCGGTGGTGGGAAGC

Hen1EntryR: TCAAAGATCAGTCTTTTTC

NLS1F: GAGGAGGAGGAGGATTCTGAACAATCTGCTGCTG

NLS1R: CTCCTCCTCCTCGAAGACATTTGACACAACAGA

NLS2F: CTCGAGGAGGAGAATGCATACCCTTCAGAAATCGTG

NLS2R: GCATTCTCCTCCTCGAGTCCATGCGGAGATGCAACA

Hen1NLS3R(+):

TCAAAGATCAGTCTCCTCCTCTTCTACATCTTCCTCCTCCCACTCCCA

Transgenic plants in the *hen1-1* background were generated for all pEarleyGate104-HEN1(NLSx) plasmids except for pEG104-HEN1NLS3NLS2NLS1.

Reference	Earley, Keith, Jeremy R. Haag, Olga Pontes, Kristen Opper, Tom Juehne, Keming Song, and Craig S. Pikaard (2006). Gateway-compatible vectors for plant functional genomics and proteomics. *The Plant J.* 45:616-629.

Table 5.2

Vector Name	pCambia3300-Hen1prCasANos and derivatives	Other Name		Construction Time	
Owner	Manu Agarwal	Selection	Kan	Storage	-80°C
HEN1 promoter was amplified with HEN1prECOF and HEN1prSACR. The PCR product was cloned into the pGEM-T Easy vector. The promoter was cloned into pCambia3300 by EcoRI/SacI digestion and ligation. Gateway cassette A was cloned into the SmaI site in pCambia3300-Hen1pr vector. Then, Nos terminator was inserted in the HindIII site to give rise to the pCAM3300-Hen1prCasANos plasmid. HEN1prECOF: CCGgaattcACAATTGTCTCATGGATTCGTG (EcoRI) HEN1prSACR: CTAGgagctcCACAAACACAATGTAGCTTCTTT (SacI) NosterminatorHindF: CCCaagcttTCGTTCAAACATTTGGCAATAA (HindIII) NosterminatorHindR: CCCaagcttGAATTCGATCTAGTAACATAG (HindIII)					
Reference	http://www.cambia.org/daisy/cambia/2070.html				

Table 5.3

Vector Name	Hen1pr::YFP-HEN1(NLSx)	Other Name	pCambia-HEN1(NLSx)	Construction Time	
Owner	Manu Agarwal	Selection	Kan/Basta	Storage	-80°C
YFP-HEN1 and the NLS mutant forms in pEarleyGate104 were amplified using a forward primer against YFP and a reverse primer against HEN1. The PCR products were cloned into pENTR1A with KpnI/NotI digestion and ligation. The resulting pENTR1A clones were sequenced, linearized, followed by LR reaction with pCambia3300-Hen1prCasANos.					

YFPKpnF: GGggtaccGAATGGGCAAGGGCGAGGAGCTGTTC (KpnI)

SV40NNotR: ATAAGAATgcggccgcGATCAAAGATCAGTCTTTTTC (NotI)

NLS3(+)NotRnew: ATAAGAATgcggccgcTCAAAGATCAGTCTCCTCCTCTTC (NotI)

hen1-1 transgenic plants had been generated for all the constructs except for Hen1pr::YFP-HEN1(NLS3NLS2NLS1).

Table 5.4

Vector Name	pEarleyGate104-(m)NLS/NES-HEN1	Other Name		Construction Time	
Owner	Manu Agarwal	Selection	Kan	Storage	-80° C

A 2-step PCR approach was used to incorporate the sequences of exogenous NLS, NES and their mutant versions into HEN1. In the first PCR, sequences for partial NLS /mNLS/NES/mNES were designed into the forward primer. The first PCR products were used as templates for the second PCR with primers in which the remaining sequences of the NLS/mNLS/NES/mNES were included. KpnI site was included in the secondary forward primers and NotI in the reverse primer (SV40NNotR). The PCR products were cloned into pENTR1A by restriction digestion and ligation.

NLSCHORYDIF1: AGAAGCGCAAGGTGGAGGACGCCGGTGGTGGGAAGCATACTCC

NLSCHORYDIF2: GGggtaccGAATGCCGGAGCCTCCTAAAAAGAAGCGCAAGGTGGA (KpnI)

mNLSCHORYDIF1:

CGACGCGCAAGGTGGAGGACGCCGGTGGTGGGAAGCATACTCC

mNLSCHORYDIF2:

GGggtaccGAATGCCGGAGCCTCCTAAAACGACGCGCAAGGTGGAG (KpnI)

NESDIF1:

AAAAAGCTGGAAGAGCTCGAACTTGATGAGCAACAGGCCGGTGGTGGGAAGCATACTCC NESDIF2: GGggtaccGACCGAACCTAGTAGATCTTCAGAAAAAGCTGGAAGAGCTCGAA (KpnI) mNESDIF1: AAAAAGGCCGAAGAGCTCGAACTTGATGAGCAACAGGCCGGTGGTGGGAAGCATACTCC mNESDIF2: GGggtaccGACCGAACCTAGTAGATGCCCAGAAAAAGGCCGAAGAGCTCGAA (KpnI) SV40NNotR: ATAAGAATgcggccgcGATCAAAGATCAGTCTTTTTC (NotI) NLS-HEN1, NES-HEN1, mNLS-HEN1 and mNES-HEN1 were amplified from pENTR1A-HEN1 vectors using phosphorylated forward and reverse primers and the PCR products were cloned into pEarleyGate104 with SmaI digestion and ligation. NESDIF2_BLUNT_PO4: AGGACCGAACCTAGTAGATCTTCAGAAAAAGCTGGAAGAGCTCGAA mNESDIF2_BLUNT_PO4: AGGACCGAACCTAGTAGATGCCCAGAAAAAGGCCGAAGAGCTCGAA NLSCHORY_BLUNT_PO4: AGGAATGCCGGAGCCTCCTAAAAAGAAGCGC mNLSCHORY_BLUNT_PO4: AGGAATGCCGGAGCCTCCTAAAACGACGCGC HEN1_ENTRY_RPO4: TCAAAGATCAGTCTTTTTC Hen1-1 35S::YPF-(m)NLS/NES-HEN1 transgenic plants have been generated.	
Reference	Gregory Vert and Joanne Chory. (2006) Downstream nuclear events in brassinosteroid signaling. Nature. Vol 441|4

Table 5.5

Vector Name	HEN1pr::(m)NLS/ NES-HEN1	Other Name		Construction Time	
Owner	Manu Agarwal	Selection	Kan	Storage	-80°C

YFP-(m)NLS/NES-HEN1OCS were amplified from pEarleyGate104-(m)NLS/NES-HEN1 series using forward a primer against YFP and a reverse primer against the OCS terminator. Both primers had XmaI site at their ends. The PCR products were cloned in the XmaI site of the pCambia3300-Hen1pr plasmid.

YFPXmaF: TCCCcccgggATGGGCAAGGGCGAGGAGCTGTTC (XmaI)

OCSXmaR: TCCCcccgggGTTGTCGCAAAATTCGCCCTGGACC (XmaI)

hen1-1 Hen1pr::YFP-(m)NLS/NES-Hen1 transgenic plants have been generated.

Table 5.6

Vector Name	pEarleyGate301/ 302-AGO(x)	Other Name	AGO(x)-HA/FLAG	Construction Time	
Owner	Manu Agarwal	Selection	Kan	Storage	-80°C

Full-length Argonaute genes were amplified using gene specific primers containing sequences for BP reaction. The clones generated after BP recombination were sequenced and moved into either pEarleyGate301 or pEarleyGate302 using LR reaction.

AGO1_DONRF: ggggacaagtttgtacaaaaaagcaggctACCTCTATACTATAATCATTC

AGO1_DONRR: ggggaccactttgtacaagaaagctgggtcTAAAGAAAGGATCAAAGTCTGTT

AGO2_DONRF: ggggacaagtttgtacaaaaaagcaggcttcTAATTAATCTTGTAAGCTTAATAT

AGO2_DONRR: ggggaccactttgtacaagaaagctgggtcGACGAAGAACATAACATTCTCAAG

AGO3_DONRF: ggggacaagtttgtacaaaaaagcaggcttcCAGAACATGACTATTACTGACTGA

AGO3_DONRR: ggggaccactttgtacaagaaagctgggtcGACAAAGAACATAAAGTTCTCGAT

AGO6G_DONRF: ggggacaagtttgtacaaaaaagcaggcttcTTTGCTTTCAAAAGATTTCTTC

AGO6G_DONRR: ggggaccactttgtacaagaaagctgggtcGCAGAAGAACATGTTGCCTTCG

AGO7G_DONRF: ggggacaagtttgtacaaaaaagcaggcttcTCCTCTTCTATACAACTTTACC

AGO7G_DONRR: ggggaccactttgtacaagaaagctgggtcGCAGTAAAACATGAGATTCTTG

AGO9G_DONRF: ggggacaagtttgtacaaaaaagcaggcttcTTACCATTCATCAATTATAGTC

AGO9G_DONRR: ggggaccactttgtacaagaaagctgggtcACAGAAGAACATGGAGGTTGAA

AGO10G_DONRF: ggggacaagtttgtacaaaaaagcaggcttcAATTGATCATATTAAACTATT

AGO10G_DONRR: ggggaccactttgtacaagaaagctgggtcGCAGTAGAACATTACTCTCTTC

AGO10-FLAG/HA transgenic plants have been generated.

At the early stage of my Ph.D study, I generated the following constructs to investigate the specificity of miR172 regulation on their target genes.

Table 5.7

Vector Name	pMDC107-/ pEG301-/ pEG302-TOE2	Other Name	TOE2-GFP TOE2-HA/FLAG	Construction Time	Fall 2006
Owner	Lijuan Ji	Selection	Kan	Storage	-20°C

TOE2 genomic DNA including the endogenous promoter (about 3.8 kb upstream of ATG) was amplified with TOE2F1b and TOE2R1b. The PCR product was cloned into pENTR-D/TOPO, and then the insert was moved into pMDC107, pEarlyGate301 and pEarleyGate302 with LR reaction.

TOE2F1b: caccTTTTGGAGTGCGACGGAGATAG

TOE2R1b: TGGTGGTGGTTGTGGGCGGTT

Transgenic plants have been generated.

Reference	LJ note #1

Table 5.8

Vector Name	pPZP100A-Kan	Other Name	PZPcas	Construction Time	Dec 2006
Owner	Lijuan Ji	Selection	Cmr	Storage	-20°C
The NPTII gene from Salk lines was amplified with casF and casR primers containing a BamHI site. The PCR product was cloned into the pGEM-T vector by TA cloning, and then inserted into the MCS of pPZP100A with BamHI digestion and ligation. The original MCS was separated into two smaller MCSs by the BamHI site. casF: ATggatccCAGAGCCGCCACCCTCAGAA (BamHI) casR: ATggatccGATCATGAGCGGAGAATTAAGG (BamHI)					
Reference	LJ note #1				

Table 5.9

Vector Name	pPZP100A-kan-miR172b2/b1	Other Name	PZPcas-b2/b1	Construction Time	Jan 2007
Owner	Lijuan Ji	Selection	Cmr	Storage	-20°C
Upstream genomic sequences of miR172b2 and miR172 b1 were amplified with B2UF/B2UR and B1UF/B1UR; downstream genomic sequences were amplified with B2DF/B2DR and B1DF/B1DR. The PCR products were first cloned into the pGEM-T vector by TA cloning. Then they were cloned into pPZP100A-Kan by restriction digestion and ligation into the two MCSs with designed restriction sites in the primers. B2UF: ATAAAAgagctcCGTACGAGGAGGAGTAGTAGGCTCT (SacI) B2UR: AGGGcccgggATTAGGGAAACAGTTGCACATCGTA (SmaI)					

B2DF: TGTGtctagaCATATTTGTGGACAAAACGATG (Xba I)

B2DR: AGGCaagcttGCAAATCTAAACTCTCactgacctt (Hind III)

B1UF: AAAATAgagctcGGAGTGGGAGAGAGATAACGCG (Sac I)

B1UR: ATATcccgggCGATAAAGAAGAGCCTATTTGGTGT (SmaI)

B1DF: TTTTgtcgacCTCAAATGATCTTAGCTTTCCGAAA (Sal I)

B1DR: CTCGaagcttACGATGGAACGGTGTCGTACTTGT (Hind III)

The constructs were designed to use homologous recombination in plants to knock out miR172b2 and miR172b1 genes. Transgenic plants were generated for pPZP100A-Kan-miR172b2, but no HR plants were isolated.

Reference	LJ note #1

The following constructs were generated to study the functionality of miR165/166 and *HD-Zip III* genes in floral determinacy.

Table 5.10

Vector Name	pCambia99-IPS1 /MIM165/MIM166	Other Name		Construction Time	Oct 2008
Owner	Lijuan Ji	Selection	Chl	Storage	-20°C

IPS1 full length cDNA was amplified with gene specific primers containing restriction sites. IPS1 cDNAs containing complementary sites (with mismatch bulge in the center) for miR165 and miR166 were generated using 2-step PCR. The PCR products were cloned into pGEM-T by TA cloning, and then moved into pCambia99-1 (a derivative of pCambia2000) with restriction digestion and ligation.

IPS1-SacI-F: GTgagctcAAGAAAAATGGCCATCCCCTAGC (SacI)

IPS1-BamHI-R: GTggatccGAGGAATTCACTATAAAGAGAATCG (BamHI)

MIM165-P1: CTtcggaccaggTAGAttcatcccaaTTTCTAGAGGGAGATAA

MIM165-P2: AAttgggatgaaTCTAcctggtccgaAGCTTCGGTTCCCCTCG

MIM166-P1: CTtcggaccaggTAGAttcattccaaTTTCTAGAGGGAGATAA

MIM166-P2: AAttggaatgaaTCTAcctggtccgaAGCTTCGGTTCCCCTCG

The pCambia-MIM165/MIM166 constructs were designed to down regulate the activities of miR165 and miR166 in transgenic plants. However, no obvious phenotypes were observed in the transformants.

Reference	LJ note #6; http://www.cambia.org/daisy/bioforge_legacy/3725.html

Table 5.11

Vector Name	pMDC164-HD-Zip III	Other Name	FLAG-HD-Zip III	Construction Time	Nov 2008
Owner	Lijuan Ji	Selection	Kan	Storage	-20°C

PHV/REV/CNA full length CDS with 3'UTR was amplified with gene specific primers (the forward primers containing 1XFLAG sequence). The PCR products were cloned into pENTR/D-TOPO (pTOPO-PHV #16, pTOPO-REV #1 and pTOPO-CNA were sequenced). PHV/REV/CNA promoters (including 5' UTR) were amplified with promoter specific primers and cloned into the pGEM-T Easy vector by TA cloning. Then the promoters were moved into pTOPO-FLAG-PHV/REV/CNA with NotI digestion and ligation respectively. pPHV::FLAG-PHV, pREV::FLAG-REV and pCNA::FLAG-CNA were moved into pMDC164 with LR reaction.

FLAG-PHV-F:

caccATGGACTACAAGGACGACGATGACAAGATGATGGCTCATCACTCCATGGA

PHV-R: AAAACGAAACAAGTCCAAAACATA

pPHV-1268F: AAGAACAATGACAGAATCCGTG

pPHV-R: ATCTTCCAAACAGGTCAGTAGAAAT FLAG-REV-F: caccATGGACTACAAGGACGACGATGACAAGATGGAGATGGCGGTGGCTAAC REV-R: GAAAATGAAACTGTCAAATGCGATA pREV-F: GATGTTAGGAGGGGACAAAGTG pREV-R: TTTAGCTCGACCCTCAAAAAAAGT FLAG-CNA-F: caccATGGACTACAAGGACGACGATGACAAGATGGCAATGTCTTGCAAGGA CNA-R: CAAGAAAAGAAAAAGATCATCATTAT pCNA-250F: CTGCTCTAAACAAAAACACAGAACC pCNA-R: TACTCCTCAGCAAAACTCTTCTTA Transgenic plants were generated, but expression level of the transgenes is low. FLAG signal couldn't be detected with western blotting.	
Reference	LJ note #5 Mark Curtis and Ueli Grossniklaus (2003) A Gateway TM cloning vector set for high-throughput functional analysis of genes in planta. *Plant Physiology* 133:462-469

Table 5.12

Vector Name	pMDC164-HDZip IIIpr	Other Name	HDZip IIIpr ::GUS	Construction Time	Nov 2008
Owner	Lijuan Ji	Selection	Kan	Storage	-20°C
PHV/REV/CNA promoter sequences were amplified with promoter specific primers. The PCR products were first cloned into pENTR/D-TOPO, and then the inserts					

were moved into pMDC164 with LR reaction. cacc-pPHV-F : caccAAGAACAATGACAGAATCCGTG pPHV-R: ATCTTCCAAACAGGTCAGTAGAAAT cacc-pREV-F: caccGATGTTAGGAGGGGACAAAGTG pREV-R: TTTAGCTCGACCCTCAAAAAAAGT cacc-pCNA-F: caccCTGCTCTAAACAAAAACACAGAACC pCNA-R: TACTCCTCAGCAAAACTCTTCTTA Transgenic plants have not been made.

Reference	LJ note #5

Table 5.13

Vector Name	pER8-PHB(d)	Other Name		Construction Time	Aug 2008
Owner	Lijuan Ji	Selection	Spe	Storage	-20°C

PHB and PHB (G202G) full length CDSs were amplified with gene specific primers with designed restriction sites. The PCR products were initially cloned into pGEM-T by TA cloning, and then the inserts were moved into pER8 by restriction digestion and ligation.

PHB-F-ApaI: TTTgggcccATGATGATGGTCCATTCGATGAGCA (ApaI)

PHB-R-SpeI: TTTactagtTCAAACGAACGACCAATTCACGA (SpeI)

Transgenic plants were generated.

Reference	LJ note #5

Table 5.14

Vector	pEG100-	Other	AmiR-ARF	Construction	Dec

Name	AmiR-ARF	Name		Time	2008
Owner	Lijuan Ji	Selection	Kan	Storage	-20°C
Artificial miRNA targeting ARF2, ARF3, ARF4 was generated by PCR using the pRS300 vector (containing pre-miR319) as a template, following the protocol by Rebecca Schwab (2005). The final PCR product was cloned into pENTR/D-TOPO, and then moved into pEarleyGate100 by LR reaction. ARF I miR-s: gaTTCTTGACCTTGCAAGACCGTtctctcttttgtattcc ARF II miR-a: aACGGTCTTGCAAGGTCAAGAAtcaaagagaatcaatga ARF III miR*s: aACAGTCTTGCAAGCTCAAGATtcacaggtcgtgatatg ARF IV miR*a: gaATCTTGAGCTTGCAAGACTGTtctacatatatattcct Plant transformants were generated.					
Reference	LJ note #6; http://wmd3.weigelworld.org/cgi-bin/webapp.cgi				

To study the function and biochemical activity of AGO10, I generated a series of vectors expressing recombinant proteins with the N/PAZ domain, MID domain and PIWI domain swapped between AGO1 and AGO10. Moreover, constructs for “slicer” defective AGO10 expression in plants were also generated to test the contribution of the cleavage activity to the function of AGO10 in plant development and small RNA pathways.

Table 5.15

Vector Name	pEG101/104-AGO10	Other Name		Construction Time	May 2007
Owner	Lijuan Ji	Selection	Kan	Storage	-20°C
For cloning into pEarleyGate101, AGO10 genomic DNA without stop codon was					

amplified with AGO10GDONRF and AGO10DONRR(-). For cloning into pEarleyGate104, AGO10 genomic DNA with stop codon was amplified with AGO10GDONRF and AGO10DONRR(+). The PCR products were cloned into pDONR207 with BD reaction, and then cloned into pEarleyGate101 and pEarleyGate104, respectively, with LR reaction.

AGO10GDONRF: ggggacaagtttgtaacaaaaaagcaggcttcAATTGATTGCCGAATTGCATT

AGO10DONRR(-): ggggaccactttgtacaagaaagctgggtcGCAGTAGAACATTACTCTCTTC

AGO10DONRR(+): ggggaccactttgtacaagaaagctgggtcTTAGCAGTAGAACATTACTCTC

Transgenic plants have been generated.

Reference	LJ note #2

Table 5.16

Vector Name	pEG104-NPAZ$^{1/10}$MID$^{1/10}$PIWI$^{1/10}$	Other Name		Construction Time	Aug 2010
Owner	Lijuan Ji	Selection	Kan	Storage	-20°C

The four structural domains of AGO1 and AGO10 were separated into three sections, the N- Terminal and PAZ section, the MID section and the PIWI section, for swapping. The recombinant sequences were generated by two-step or three-step of PCR amplification.

The first-step PCR was carried out with the following primers to amplify the individual or contiguous domains (For simplification, the amplified domains were designated by a single letter):

	Forward primer	Reverse primer	Template	Domain
A	Cacc_AGO10F	AGOp1	PS1	10-NPAZ

B	AGOp6	AGO1_R	35S-HA-AGO1	1-MID&PIWI
C	AGOp6	AGOp7	35S-HA-AGO1	1-MID
D	AGOp4	PNH_R	cDNA/ps1	10-PIWI
E	Cacc_AGO10F	AGOp3	Ps1	10-NPAZ&MID
F	AGOp8	AGO1_R	35S-HA-AGO1	1-PIWI
G	Cacc-ago1F	AGOp5	35S-HA-AGO1	1-NPAZ
H	AGOp2	PNH_R	cDNA/ps1	10-MID&PIWI
I	AGOp2	AGOp3	PS1	10-MID
J	Cacc_AGO1F	AGOp7	35S-HA-AGO1	1-NPAZ&MID

The second round of PCR was carried out with the following primers to amplify the final products (AB, EF, GF, JD) and intermediate products (AC, CD, GI and IF).

	Forward primer	Reverse primer	Combination
AB	Cacc_AGO10_F	AGO1_R	10-NPAZ + 1-MID&PIWI
AC	Cacc_ago10-F	AGOp7	10-NPAZ + 1-MID
CD	AGOp6	PNHR	1-MID + 10-PIWI
EF	Cacc-ago10-F	AGO1_R	10-NPAZ&MID + 1-PIWI
GH	Cacc-ago1-F	PNH-R	1-NPAZ + 10-MID&PIWI
GI	Cacc-ago1-F	AGOp3	1-NPAZ + 10-MID
IF	AGOp2	AGO1_R	10-MID + 1 PIWI
JD	Cacc-ago1-F	PNH_R	1-NPAZ&MID + 10-PIWI

The third round of PCR was carried out to generate the following combinations:

	Forward primer	Reverse primer	Combination

ACD	Cacc-ago10-F	PNH-R	10-NPAZ + 1-MID + 10-PIWI
GIF	Cacc-ago1-F	AGO1_R	1-NPAZ + 10-MID + 1-PIWI

The final PCR products were cloned into pENTR-D/TOPO and sequenced to confirm the correct configurations. Then the inserts were moved into pEarleyGate104 with LR reaction.

caccAGO10F: caccATGCCGATTAGGCAAATGAAAGA

PNH-R: TTAGCAGTAGAACATTACTCTCTTCAC

caccAGO1F: caccATGGTGAGAAAGAGAAGAACGGA

AGO1R: TCAGCAGTAGAACATGACACGCT

AGOp1: TTTGGAATACCGCTGGCCTTCgacaattttgcatgcctcca

AGOp2: TGGAGGTATGCAAGATTGTTgagggacaacggtacacgaa

AGOp3: TCGGGCAGAATGACAATAAGaagctctaactctttgccttt

AGOp4: AAGGAAAAGAAATTGATCTGctgctggcaatattacctgata

AGOp5: ttcgtgtaccgttgtccctcAACAATCTTGCATACCTCCA

AGOp6: tggaggcatgcaaaattgtcGAAGGCCAGCGGTATTCCAAA

AGOp7: tatcaggtaatattgccagcagCAGATCAATTTCTTTTCCTT

AGOp8: aaaggcaaagagttagagcttCTTATTGTCATTCTGCCCGA

P.S. uppercase sequences match to AGO1, lowercase sequences match to AGO10.

Transgenic plants for pEG104-ACD show phenotypes similar to pEG104-AGO10, while transgenic plants for pEG104-GIF show phenotypes similar to pEG104-AGO1.

Reference	LJ note #11

Table 5.17

Vector Name	pEG104-AGO10 H747P	Other Name		Construction Time	

Owner	Lijuan Ji	Selection	Kan	Storage	-20°C
Full length CDS of AGO10 was amplified with caccAGO10F and PNHR primers and cloned into pENTR-D/TOPO. H747 was mutated to P747 by site directed mutagenesis with inverted primers. The resulting vectors were linearized, and the insert was moved by LR reaction into the pEarleyGate104 vector. caccAGO10F: caccATGCCGATTAGGCAAATGAAAGA PNH-R: TTAGCAGTAGAACATTACTCTCTTCAC Transgenic plants have been generated.					
Reference	LJ note # 11				

A series of vectors to express two unrelated miRNAs simultaneously in plants were generated to examine suspected miRNA-specific effects with one miRNA as the target of examination, and the other miRNA as the control.

Table 5.18

Vector Name	pEG100-miRNA cluster	Other Name		Construction Time	
Owner	Lijuan Ji	Selection	Kan	Storage	-20°C
Genomic sequences of miR164a, miR166a and miR173 were amplified with gene specific primers containing designed linker sequences or restriction sites for cloning into pJLBlueR. The miRNA clusters (miR173~164a, miR173~166a, miR166a~164a, miR164a~166a, miR164a~173, miR166a~173) were generated by a second of round PCR using combined PCR products of individual miRNA genes as templates. The final forward and reverse primers contain designed restriction sites. The miRNA clusters were cloned into pJLBlueR by restriction digestion and ligation. The					

resulting clones were linearized, and the inserts were moved into by LR reaction into pEarleyGate100. miR166a-SalI-F: agagGTCGACccctagattctataatttcgactg (SalI) miR166a-linker-R: acaacatttcaACTAGTgtgggtttgaacggtaagagatcaaacctttaacaa (SpeI) miR166a-linker-F: *gttcaaacccacACTAGTtgaaatgttgt*ccctagattctataatttcgactg (SpeI) miR166a-EcoRI-R: atatGAATTCggtaagagatcaaacctttaacaa (EcoRI) miR164a-SalI-F: agagGTCGACacaaacctttccataaccaaagt (SalI) miR164a-linker-R: acaacatttcaACTAGTgtgggtttgaacgaagagctagtcaagaacaacga (SpeI) miR164a-linker-F: gttcaaacccacACTAGTtgaaatgttgtacaaacctttccataaccaaagt (SpeI) miR164a-EcoRI-R: atatGAATTCgaagagctagtcaagaacaacga (EcoRI) miR173-SalI-F: agagGTCGACgtaatctcagcccaatacccta (SalI) miR173-linker-R: acaacatttcaACTAGTgtgggtttgaacccctaatgagatactttccagtga (SpeI) miR173-linker-F: gttcaaacccacACTAGTtgaaatgttgtgtaatctcagcccaatacccta (SpeI) miR173-EcoRI-R: atatGAATTCccctaatgagatactttccagtga (EcoRI)	
Reference	LJ note # 14

6. Appendix B: Side projects and protocols

The high-resolution crystal structure of HEN1 indicated that the methyltransferase activity is Mg^{2+} dependent and several residues are potentially critical for its catalytic activity. I performed *in vitro* methyltransferase assays to verify the functional importance of those residues and Mg^{2+}, described in [1].

At the early stage of my Ph.D study, I was involved in the investigation of the function of DAWDLE and SNIP1 during small RNA biogenesis. To prepare the materials needed for studying the function of SNIP1 in humans, I knocked down SNIP1 expression in HeLa cells by RNAi, and expressed the SNIP1, Drosha and Dicer proteins in 293T cells [2]. Later, I cultured two mammalian cell lines to generate antibodies for another colleague's project. In the process of learning these new techniques, the following sites served as good references:

Invitrogen transfection products and protocol (http://www.invitrogen.com/site/us/en/home/Products-and-Services/Applications/Cell-Culture/Transfection.html)

ATCC (http://www.atcc.org/)

Online protocol (http://www.protocol-online.org/)

References

1. Huang Y, Ji L, Huang Q, Vassylyev DG, Chen X, et al. (2009) Structural insights into mechanisms of the small RNA methyltransferase HEN1. Nature 461: 823-827.
2. Yu B, Bi L, Zheng B, Ji L, Chevalier D, et al. (2008) The FHA domain proteins DAWDLE in Arabidopsis and SNIP1 in humans act in small RNA biogenesis. Proc Natl Acad Sci U S A 105: 10073-10078.